

1955

Substituent effect in 1,10-phenanthroline chelation kinetics

Dale William Margerum
Iowa State College

Follow this and additional works at: <https://lib.dr.iastate.edu/rtd>

 Part of the [Analytical Chemistry Commons](#)

Recommended Citation

Margerum, Dale William, "Substituent effect in 1,10-phenanthroline chelation kinetics " (1955). *Retrospective Theses and Dissertations*. 13642.
<https://lib.dr.iastate.edu/rtd/13642>

This Dissertation is brought to you for free and open access by the Iowa State University Capstones, Theses and Dissertations at Iowa State University Digital Repository. It has been accepted for inclusion in Retrospective Theses and Dissertations by an authorized administrator of Iowa State University Digital Repository. For more information, please contact digirep@iastate.edu.

NOTE TO USERS

This reproduction is the best copy available.

UMI[®]

134

SUBSTITUENT EFFECT IN
1,10-PHENANTHROLINE
CHELATION KINETICS

by

Dale William Margerum

A Dissertation Submitted to the
Graduate Faculty in Partial Fulfillment of
The Requirements for the Degree of

DOCTOR OF PHILOSOPHY

Major Subject: Analytical Chemistry

Approved:

Signature was redacted for privacy.

In Charge of Major Work

Signature was redacted for privacy.

Head of Department

Signature was redacted for privacy.

Dean of Graduate College

Iowa State College

1955

UMI Number: DP12831

INFORMATION TO USERS

The quality of this reproduction is dependent upon the quality of the copy submitted. Broken or indistinct print, colored or poor quality illustrations and photographs, print bleed-through, substandard margins, and improper alignment can adversely affect reproduction.

In the unlikely event that the author did not send a complete manuscript and there are missing pages, these will be noted. Also, if unauthorized copyright material had to be removed, a note will indicate the deletion.

UMI[®]

UMI Microform DP12831

Copyright 2005 by ProQuest Information and Learning Company.

All rights reserved. This microform edition is protected against unauthorized copying under Title 17, United States Code.

ProQuest Information and Learning Company
300 North Zeeb Road
P.O. Box 1346
Ann Arbor, MI 48106-1346

QD501
M3365
c.1

1126-34

TABLE OF CONTENTS

	Page
I. INTRODUCTION	1
A. Importance of 1,10-Phenanthroline	1
B. Distinctive Properties of 1,10-Phenanthroline	1
C. Purpose of This Work	3
D. 1,10-Phenanthroline Substituents	4
E. Review and Contradictions of Kinetic Theories	5
II. APPARATUS AND REAGENTS	8
III. NICKEL(II) WITH THE 1,10-PHENANTHROLINES	10
A. Introduction	10
B. The Mono(1,10-phenanthroline)nickel(II) Ion Complexes	13
1. Experimental	13
a. Mono(1,10-phenanthroline)nickel(II) ion	13
(1) Rate of formation	13
(2) Rate of dissociation	52
b. Mono(5-methyl-1,10-phenanthroline)nickel(II) ion	66
(1) Rate of formation	66
(2) Rate of dissociation	66
c. Mono(5-nitro-1,10-phenanthroline)nickel(II) ion	66
(1) Rate of formation	66
(2) Rate of dissociation	81
2. Discussion	81
C. The Bis(1,10-phenanthroline)nickel(II) Complexes	112
1. Experimental	112
2. Discussion	113
D. The Tris(1,10-phenanthroline)nickel(II) Complexes	117
1. Experimental	117
2. Discussion	121
E. Equilibrium Constants	122
F. Summary	127

TABLE OF CONTENTS (continued)

	Page
IV. IRON(II) WITH THE 1,10-PHENANTHROLINES	129
A. Introduction	129
B. Experimental	132
C. Discussion	134
V. VANADIUM(IV) WITH THE 1,10-PHENANTHROLINES	143
A. Introduction	143
B. Experimental	143
C. Discussion	153
VI. ANALYTICAL APPLICATION	156
VII. SUMMARY AND CONCLUSIONS	162
VIII. LITERATURE CITED	166
IX. ACKNOWLEDGMENTS	169
X. APPENDIX - LIST OF ABBREVIATIONS	170

LIST OF TABLES

	Page
Table 1 Acid Dissociation Constants of 5-Substituted 1,10-Phenanthrolines	5
Table 2 Formation Reactions of the Mono(1,10-phenanthroline)-nickel(II) Complex	19
Table 3 Dissociation Reactions of the Mono(1,10-phenanthroline)-nickel(II) Complex	21
Table 4 Spectrophotometric Data and Calculation of Reaction 1	24
Table 5 Spectrophotometric Data and Calculation of Reaction 2	26
Table 6 Spectrophotometric Data and Calculation of Reaction 3	28
Table 7 Spectrophotometric Data and Calculation of Reaction 4	30
Table 8 Spectrophotometric Data and Calculation of Reaction 5	32
Table 9 Spectrophotometric Data and Calculation of Reaction 6	34
Table 10 Spectrophotometric Data and Calculation of Reaction 7	36
Table 11 Spectrophotometric Data and Calculation of Reaction 8	38
Table 12 Spectrophotometric Data and Calculation of Reaction 9	40
Table 13 Spectrophotometric Data and Calculation of Reaction 10	42
Table 14 Spectrophotometric Data and Calculation of Reaction 11	44
Table 15 Spectrophotometric Data and Calculation of Reaction 12	46
Table 16 Spectrophotometric Data and Calculation of Reaction 13	48
Table 17 Spectrophotometric Data and Calculation of Reaction 14	50
Table 18 Spectrophotometric Data and Calculation of Reaction 15	55
Table 19 Spectrophotometric Data and Calculation of Reaction 16	57
Table 20 Spectrophotometric Data and Calculation of Reaction 17	59
Table 21 Spectrophotometric Data and Calculation of Reaction 18	61
Table 22 Spectrophotometric Data and Calculation of Reaction 19	63

LIST OF TABLES (continued)

	Page
Table 23 Formation and Dissociation Reactions of the Mono(5-methyl-1,10-phenanthroline)nickel(II) Complex . . .	65
Table 24 Spectrophotometric Data and Calculation of Reaction 20 . . .	68
Table 25 Spectrophotometric Data and Calculation of Reaction 21 . . .	70
Table 26 Spectrophotometric Data and Calculation of Reaction 22 . . .	72
Table 27 Spectrophotometric Data and Calculation of Reaction 23 . . .	74
Table 28 Spectrophotometric Data and Calculation of Reaction 24 . . .	76
Table 29 Spectrophotometric Data and Calculation of Reaction 25 . . .	78
Table 30 Formation and Dissociation Reactions of the Mono(5-nitro-1,10-phenanthroline)nickel(II) Complex . . .	80
Table 31 Spectrophotometric Data and Calculation of Reaction 26 . . .	82
Table 32 Spectrophotometric Data and Calculation of Reaction 27 . . .	84
Table 33 Spectrophotometric Data and Calculation of Reaction 28 . . .	86
Table 34 Spectrophotometric Data and Calculation of Reaction 29 . . .	88
Table 35 Spectrophotometric Data and Calculation of Reaction 30 . . .	90
Table 36 Spectrophotometric Data and Calculation of Reaction 31 . . .	92
Table 37 Acid Dependence of Rate of Formation of Nickel(II)-1,10-Phenanthrolines	104
Table 38 Spectrophotometric Data and Calculation of Reaction 32 . . .	114
Table 39 Spectrophotometric Data and Calculation of Reaction 33 . . .	118
Table 40 Equilibrium Constants for the Mono(1,10-phenanthroline)-nickel(II) Complexes	123
Table 41 Equilibrium Constants for the Tris(1,10-phenanthroline)nickel(II) Complex	125
Table 42 Spectrophotometric Data and Calculation of Reaction 34 . . .	135
Table 43 Spectrophotometric Data and Calculation of Reaction 35 . . .	136

	Page
Table 44 Spectrophotometric Data for Job's Continuous Variations with Vanadium(IV) and 1,10-Phenanthroline	146
Table 45 Spectrophotometric Data and Calculation of Reaction 36	150
Table 46 Spectrophotometric Data and Calculation of Reaction 37	151
Table 47 Spectrophotometric Data and Calculation of Reaction 38	152

LIST OF FIGURES

	Page
Figure 1 Absorption Spectra of Phenanthroline with Varying Michael in Acid Solution, 220 - 300 m μ	17
Figure 2 Absorption Spectra of Phenanthroline Showing the Reaction with Michael in Acid Solution	18
Figure 3 Absorption Spectra of Phenanthroline with Varying Michael in Acid Solution, 290 - 340 m μ	20
Figure 4 Reaction No. 1	23
Figure 5 Reaction No. 2	25
Figure 6 Reaction No. 3	27
Figure 7 Reaction No. 4	29
Figure 8 Reaction No. 5	31
Figure 9 Reaction No. 6	33
Figure 10 Reaction No. 7	35
Figure 11 Reaction No. 8	37
Figure 12 Reaction No. 9	39
Figure 13 Reaction No. 10	41
Figure 14 Reaction No. 11	43
Figure 15 Reaction No. 12	45
Figure 16 Reaction No. 13	47
Figure 17 Reaction No. 14	49
Figure 18 Reaction No. 15	54
Figure 19 Reaction No. 16	56
Figure 20 Reaction No. 17	58
Figure 21 Reaction No. 18	60
Figure 22 Reaction No. 19	62

LIST OF FIGURES (continued)

	Page
Figure 23 Spectrophotometric Evidence of Mono- and Di- protonated Phenanthroline	64
Figure 24 Reaction No. 20	67
Figure 25 Reaction No. 21	69
Figure 26 Reaction No. 22	71
Figure 27 Reaction No. 23	73
Figure 28 Reaction No. 24	75
Figure 29 Reaction No. 25	77
Figure 30 Absorption Spectra of Nitrophenanthroline with Varying Nickel in Acid Solutions	79
Figure 31 Reaction No. 26	83
Figure 32 Reaction No. 27	85
Figure 33 Reaction No. 28	87
Figure 34 Reaction No. 29	89
Figure 35 Reaction No. 30	91
Figure 36 Reaction No. 31	93
Figure 37 Effect of pH on Mono(phenanthroline)nickel Rate Constant	95
Figure 38 Effect of Acidity on Formation Rate Constant of Nickel Phenanthroline	96
Figure 39 Proposed Mechanism for Reaction between the Phenanthroline Ion and Nickel Ion	98
Figure 40 Proposed Mechanism for Acid Catalysis of Reaction between Phenanthroline and Nickel Ion	100
Figure 41 Acid Dependence of Mono(phenanthroline)nickel Formation Rate	103
Figure 42 Acid Dependence of Mono(methylphenanthroline)nickel Formation Rate	105

LIST OF FIGURES (continued)

	Page
Figure 43 Acid Dependence of Mono(phenanthroline)nickel Dissociation Rate	107
Figure 44 Substituent Effect on Mono(phenanthroline)nickel Rate Constant	111
Figure 45 Reaction No. 32	116
Figure 46 Reaction No. 33	120
Figure 47 Reaction No. 35	137
Figure 48 Substituent Effect on the Formation Rate Constant of the Iron(II) Triphenanthroline Complexes	139
Figure 49 Absorption Spectra of Phenanthroline with Vanadium(IV) for Job's Plot	145
Figure 50 Continuous Variations for Phenanthroline and Vanadium(IV)	147
Figure 51 Continuous Variations for Phenanthroline and Vanadium(IV)	148
Figure 52 Rates of Formation of Vanadium(IV) with the Phenanthrolines	149
Figure 53 Substituent Effect on Mono(phenanthroline)vanadium(IV) Rate Constant	155

I. INTRODUCTION

A. Importance of 1,10-Phenanthroline

Few chelates exceed the scope and strength of the 1,10-phenanthroline complexes. The aromatic -N-C-C-N-C- grouping, which is characteristic of 1,10-phenanthroline and 2,2'-bipyridine, forms chelates with metallic ions from nearly every periodic group (7). The complexes formed are generally of a high order of stability and are comparable to the well-known ethylenediamine complexes.

1,10 phenanthroline has already proved to be a most valuable analytical reagent. Tris(1,10-phenanthroline)iron(II) ion, commonly called ferroin, has enjoyed wide use as an oxidation-reduction indicator (28). Ferroin has also proved to be a useful precipitating agent and has found limited application for the determination of some anions (7). Perhaps the primary use of 1,10-phenanthroline has been as a colorimetric reagent for iron. The intense red color of ferroin has led to the determination of trace quantities of iron in all types and kinds of materials. Phenanthroline-type compounds have also proved useful for the colorimetric determination of copper in which the copper(II) ion forms intensely colored complexes (4). The colorimetric application of 1,10-phenanthroline has also found wide use as a masking agent for several ions in the analysis of other elements (26).

B. Distinctive Properties of 1,10-Phenanthroline

In comparison to ethylenediamine, 1,10-phenanthroline is a relatively weak base and as a weaker nucleophilic reagent might be expected

to form much less stable complexes than it does. Hence, it appears that more is involved in the chelate formation than the simple functional grouping. Unlike the paramagnetic ethylenediamine complexes with iron(II), the formation of the tris(1,10-phenanthroline)iron(II) complex is accompanied by the pairing of the 3d electrons of the iron to form a diamagnetic substance. It has been suggested by Klynkin (6, 28, 29) that the major factor responsible for electron pairing in the iron complex and also for the strong covalent bonding in many of these complexes is the formation of double bonds between the chelate nitrogen and iron. The second bond, a π bond, might be formed through the donation of a pair of electrons by the metal, utilizing a p orbital of the ligand. For this process to occur, resonance structures must be possible which make available a p orbital of the ligand. The aromatic nucleus of 1,10-phenanthroline furnishes the possibility of such resonance structures, while none are possible with ethylenediamine. This type of double bond formation has also been proposed for the porphyrins (27). There is little direct experimental evidence to support the suggestion of double bond formation. However, Klynkin and Short (30) have examined the C=O stretching force constants in Ni(CO)₄, Ni(CO)₂(bipy) and Ni(CO)₂(diacetylene) and conclude that the Ni-C bond in Ni(CO)₄ is best regarded as a double bond and that both the Ni-As and Ni-N bonds in these compounds have considerable double bond character.

The phenanthroline-type chelates are unique in another respect, for unlike most chelates the 1,10-phenanthroline complexes of ions, such as, iron(II), nickel(II) and vanadium(IV), are slow to dissociate and

have a measurable rate of formation. This rather distinctive property of the phenanthroline-type compounds introduces an additional use for these chelates. Their wide variation of reaction rates with transition metal ions makes them useful as reagents for the analytical separation of these ions. It will be seen later in this work that 1,10-phenanthroline can be utilized to separate and determine trace quantities of iron in chromium, vanadium and nickel solutions.

C. Purpose of This Work

The effect of substituents on the 5-position in 1,10-phenanthroline is to alter the nucleophilic character of the ring nitrogens. This offers the opportunity to study the reaction rates of a homologous series of chelates that differ only in their electron donating ability. Since all other variables are constant, it is possible to measure the effect of nucleophilic character on the rate of chelation. A study of the kinetics of formation and dissociation of the 1,10-phenanthroline complexes is of interest not only to extend the usefulness of chelate kinetics for analytical separations, but also in order to help understand the nature of chelation reactions. In this work the kinetics of nickel(II), iron(II) and vanadium(IV) with 1,10-phenanthroline, 5-methyl-1,10-phenanthroline and 5-nitro-1,10-phenanthroline are studied and compared.

Previous work has indicated some unusual effects of hydrogen ion concentration on 2,2'-bipyridine reactions with iron(II) (22, 5). The hydrogen ion effect on the nickel(II)-1,10-phenanthroline system is thoroughly studied and a reaction mechanism is proposed for both the nickel(II) and iron(II) systems. A knowledge of this hydrogen ion effect

is extremely important when adapting chelates for analytical procedures.

D. 1,10-Phenanthroline Substituents

The effect of groups substituted for hydrogen in the 1,10-phenanthroline molecule may be two-fold in regard to the reaction of 1,10-phenanthroline with metallic ions. Substitution of groups in positions immediately adjacent to the bonding nitrogens, as in the 2 and 9 positions, will frequently lead to steric hindrance in its reaction with metallic ions. In this manner greater specificity for ions can occur as with 2,9-dimethyl-1,10 phenanthroline which reacts with copper(II), but iron(II) (34). The other effect of substituents in phenanthroline is to alter the electron donating capacity of the ring nitrogens and hence affect the stability of the 1,10-phenanthroline complexes. Substitution in the 5 position creates no steric effects, being well away from the bonding nitrogens, but can alter the nucleophilic character of the bonding nitrogens. This work is limited to a study of 5-methyl-1,10-phenanthroline, 5-nitro-1,10-phenanthroline and 1,10-phenanthroline, itself. Just as these substituents affect the stability of the complexes with metal ions, they would also be expected to have some effect on the reaction rates of those systems which proceed at measurable rates. In order to compare these rate effects, it is necessary to have some measure of the nucleophilic character of these chelates. The value of the acid dissociation constant of the 1,10-phenanthrolium ion serves as a measuring device of the nucleophilic character of each 1,10-phenanthroline. These values, from the work of Brandt and Gullstrom (8), are given in Table 1.

Table 1

Acid Dissociation Constants of 5-Substituted 1,10-Phenanthrolines

Substituent	pK _a
NO ₂	3.57
Cl	4.26
H	4.96
CH ₃	5.23

where:

$$K_a = \frac{[E^+][Ph]}{[HPh^+]}$$

E. Review and Contradictions of Kinetic Theories

The reactions in solution between metal ions and coordinating groups are substitution reactions with the displacement of water from the aquated metal ion. In considering metal ions of coordination number six, Taube (35) prefers to use the nomenclature of inner orbital and outer orbital complexes rather than covalent and ionic complexes. An inner orbital complex in the first transition series is of the type $3d^2 4s 4p^3$, while an outer orbital complex utilizes the $4s 4p^3 4d^2$ orbitals. Recent calculations (12) of the $4s 4p^3 4d^2$ hybridization lends support to this definition showing these orbitals especially suitable for highly electronegative ligands. The outer orbital complexes, with the exception of central ions of very high charge, such as SF_6 and PF_6^- , react practically instantaneously and are termed labile.

According to Taube the inner orbital complexes have two distinct

nitric oxides, the labile and the inert, or sluggish. The sluggish complexes are those whose formation or dissociation proceeds at measurable rates at room temperature. Taube has pointed to what seems to be a rather sharp discontinuity between those labile and inert inner orbital complexes. It has been observed that if there are three or more lower d orbitals of the central ion occupied, the inner orbital complexes are sluggish and if less than three, they are labile. The explanation has been suggested that during the transition state of such a substitution reaction there are necessarily seven coordinating groups around the central ion and that they require seven orbitals. In order to provide those orbitals when there are more than three electrons in the d level, electron pairing must take place. The energy required in electron pairing represents the transition state energy, an energy barrier which the system must overcome before the substitution reaction proceeds. According to this explanation, reactions with vanadium(III) ($d^3e^1e^0e^0e^0$) proceed rapidly because d orbitals are available for an incoming group. With chromium(III) ($d^3e^2e^1e^0e^0$), the reaction must proceed slowly because one of the 3d electrons must first be paired before substitution can proceed.

However, there are many experimental contradictions to Taube's explanation of sluggish substitution in inorganic complexes. Nickel(II) has the electronic structure, $d^8e^2e^2e^1e^1$, and cannot form inner orbital complexes without promoting two 3d electrons. The energy requirements to promote the two 3d electrons and the paramagnetism of the nickel(II)-1,10-phenanthroline complexes make electron promotion seem unlikely (6, 35), yet nickel(II) does react slowly with 1,10-phenanthroline. Vanadium(IV) has the electronic structure, $d^1e^1e^0e^0e^0$, and yet it reacts

slowly with 1,10-phenanthroline. It is not possible for electron pairing to be the energy requirement for this slow reaction. The exchange of cobalt(II) with bis(2,2',2''-terpyridine)cobalt(II) has been reported to be slow (39). This is a contradiction of Swabe's proposal since cobalt(II) should form an outer orbital complex.

It has been suggested that double bond formation is responsible for the unexpected stability of the 1,10-phenanthroline complexes (6, 29). Such double bonds might be expected to account for slow reaction rates, but neither vanadium(IV) nor chromium(III) have electron pairs available for double bond formation while zinc(II) does. The former two are singlet while the latter is labile.

It is obvious that the present theory concerning these sudden changes in reaction rates with various metal ions and chelates is inadequate. The present study of the effect of the nucleophilic character of 1,10-phenanthroline on the rates of some of these reactions is performed in the hope of presenting additional information that may be useful in distinguishing different kinetic mechanisms.

II. APPARATUS AND MATERIALS

Absorbance measurements were made with a Beckman Model DU quartz spectrophotometer and a Cary Model 12 recording spectrophotometer. A Beckman Model 0 pH meter was used for pH measurements. The kinetic studies were followed with the Beckman spectrophotometer using a photo-multiplier attachment for the ultraviolet and using thermopaper for the cell compartment. A water bath with a circulating pump kept the cell compartment at $25.0 \pm 0.1^\circ$. All glassware used was of class A specification.

All chemicals used were reagent-grade quality. The three 1,10-phenanthroline compounds were obtained from the G. Frederick Smith Chemical Company and were recrystallized from alcohol and from water before use. The following stock solutions were prepared by weighing out the dried 1,10-phenanthroline crystals:

1,10-phenanthroline	6.504 x 10 ⁻³ molar (first stock solution)
	2.506 x 10 ⁻³ molar (second stock solution)
5-methyl-1,10-phenanthroline	5.555 x 10 ⁻³ molar
5-nitro-1,10-phenanthroline	6.986 x 10 ⁻³ molar

The nickel solution used was prepared from high nickel of greater than 99.9% purity which was dissolved in acid and recrystallized as nickel perchlorate. Solutions of two semicarbazone were used, both of which were analyzed with 1,2-cyclohexanediamineoxime (57). The concentrations were 7.65×10^{-1} molar and 3.060×10^{-3} molar.

The iron(II) was prepared by dissolving electrolytic iron wire in perchloric acid. The solution was then diluted and stored in contact with

additional iron wire. The solution was analyzed with cerium(IV) sulfate at the time each aliquot was taken for a kinetic study.

The vanadium(IV) solution was prepared from pure vanadium pentoxide which was dissolved and crystallized as ammonium vanadate, ignited to the oxide again, redissolved in sodium hydroxide and made acid with perchloric acid. This solution was electrolyzed to vanadium(IV) until spectrophotometric tests showed the absence of vanadium(V) or vanadium(III). The solution was stored under nitrogen. The solution was analyzed with cerium(IV) sulfate.

III. NICKEL(II) WITH THE 1,10-PHENANTHROLINES

A. Introduction

Although the complexes between nickel(II) and 1,10-phenanthroline have been known for a long time, no overall study of the kinetics or equilibrium constants of the systems have been made. In 1896, Blau (4) reported the formation of a nickel(II)-1,10-phenanthroline complex and Pfeiffer and Tapperman (32) called attention to the complex again in 1933. Shortly afterwards, Cambi and Cagnasso (11) measured the magnetic susceptibility of the tris(1,10-phenanthroline)nickel(II) complex, finding it to be paramagnetic. Vosburgh and Cooper (36) were able to show the existence of mono-, bis- and tris(1,10-phenanthroline)nickel(II) complexes by the spectrophotometric application of Job's method of continuous variation. In addition to many tris(1,10-phenanthroline)nickel(II) salts (7), there have been a number of reports (31, 32) of the preparation of bis(1,10-phenanthroline)nickel(II) salts, such as $[\text{Ni}(\text{Ph})_2(\text{H}_2\text{O})_2]\text{Cl}_2 \cdot 3\text{H}_2\text{O}$ and $[\text{Ni}(\text{Ph})_2(\text{H}_2\text{O})_2][\text{ClO}_4]_2$. The substance $[\text{NiPh}(\text{H}_2\text{O})_4][\text{ClO}_4]_2$ has also been described but its preparation has been questioned (31). Russell, Vosburgh and Cooper (35) found that all of the 1,10-phenanthroline-nickel(II) complexes are paramagnetic; the magnetic moment decreasing slightly as the coordinating reagent is added. The resolution of the tris(1,10-phenanthroline)nickel(II) complex by Dwyer and Gyarfás (14) illustrated its high stability. Davis and Dwyer (15) reported from a private communication with Dunstone and Mellor that the pK of the tris(1,10-phenanthroline)nickel(II) complex is 18.5, where $K = [\text{Ni}^{++}][\text{Ph}]^3 / [\text{NiPh}_3^{++}]$. This value has been in the literature ever

since with no experimental confirmation. It is seen later in this work that this value of 18.5 is erroneous.

It is known that the dissociation of the tris(1,10-phenanthroline)-nickel(II) complex is not immeasurably fast, but proceeds at a rather slow pace. The kinetics of this dissociation have been studied by Busolo, Hayes and Newman (2). They reported a dissociation rate constant of 5.4×10^{-4} in 2M hydrochloric acid at 25°C and observed no major change in this rate between 2M and 2M hydrochloric acid. However, they did report a hydrogen ion effect on the rate of dissociation of the tris-(2,2'-bipyridine)nickel(II) complex. Margrave and Smith (25) showed that the rate of reaction between nickel(II) and 1,10-phenanthroline is sufficiently slow to allow separation of trace amounts of iron from nickel solutions.

The nickel(II)-1,10-phenanthroline system has attracted considerable theoretical interest by virtue of the slow reaction rates and the paramagnetism of the complexes. Table (5) was unable to fit a slow nickel reaction rate into his classification of rates and suggested that the complex, $[\text{Ni}(\text{bipy})_3]^{4+}$, was of the inner orbital type, where two electrons are promoted to higher energy levels, namely, $d^2 \uparrow \uparrow \uparrow \uparrow \uparrow \uparrow \uparrow \uparrow \uparrow \uparrow$. Significant oversight, is the fact that such an electron promotion would also have to apply to the reaction of just one molecule of 1,10-phenanthroline or 2,2'-bipyridine with nickel(II), since these reactions are also slow. Burstell and Nyholm (6) pointed out that it takes a great deal of energy for electron promotion. They also argued that promoted electrons should pair in the 5s orbital making the resultant compound diamagnetic and not paramagnetic. Furthermore, they reported the preparation of $[\text{Ni}(\text{diacetyne})_3]^-$

$[\text{GlO}_4]_2$, which is diamagnetic, indicating presumably $3d^2 4sp^3$ orbitals with the promotion of an electron pair to the 5s level. The postulated promotion of the two electrons to higher orbitals was supported by the fact that the complex was oxidised by chlorine to a higher oxidation state of nickel.

In the following work it is proved that all of the nickel(II)-1,10-phenanthroline reactions are slow.

The reactions are written with the rate constants designated as shown in Equations [1], [2], and [3].



The mono(1,10-phenanthroline)nickel(II) system is carefully examined with respect to its rate and equilibrium constants. The effect of hydrogen ion concentration on the kinetics is dealt with at length. The mono complexes of 5-methyl-1,10-phenanthroline and 5-nitro-1,10-phenanthroline are also studied and the effect of the nucleophilic character of the nitrogens on the rate of reaction is examined. Estimates are made of the rates of formation of the bis- and tris(1,10-phenanthroline)nickel(II) complexes. Equilibrium constants for all three of the nickel(II)-1,10-phenanthroline complexes are also calculated.

B. The Mono(1,10-phenanthroline)nichel(II) Ion Complexes

1. Experimental

a. Mono(1,10-phenanthroline)nichel(II) ion

(1) Rate of formation. The reaction between 1,10-phenanthroline and nichel(II) ion is so rapid that it would be extremely difficult to measure the progress of the reaction in a neutral solution. However, 1,10-phenanthroline is a weak base and will add one proton readily in slightly acidic solutions to form the 1,10-phenanthrolium ion.



$$K_a = \frac{[\text{Ph}][\text{H}^+]}{[\text{HPH}^+]} = 1.1 \times 10^{-3} \quad [5]$$

The 1,10-phenanthrolium ion is much less reactive towards metal ions than 1,10-phenanthroline. Therefore, in acid solutions the 1,10-phenanthrolium ion serves as a source of reactant while maintaining a sufficiently low concentration of 1,10-phenanthroline so that the rate of formation of the nichel complex can be observed.

The mono(1,10-phenanthroline)nichel(II) formation reaction is pictured, in the most simple form, as a reaction between only the unprotonated phenanthroline molecule and the aquated nichel(II) ion. In acid solutions, a prior equilibrium is established between 1,10-phenanthrolium and 1,10-phenanthroline so as to maintain a quite low concentration of the latter. Then the rate of formation is:

$$\frac{d[\text{HPH}^+]}{dt} = k_1[\text{H}^{++}][\text{Ph}] - k_2[\text{HPH}^+] \quad [6]$$

The reaction rate may be followed in a large excess of nickel(II) provided the solution is sufficiently acidic. The kinetics then become first order.

If $[H^+] \gg K_a$:

$$[Ph] = \frac{K_a}{[H^+]} [NiPh^+] = \frac{K_a}{[H^+]} (Ph_T - [NiPh^{++}]) \quad [7]$$

$$\frac{d[NiPh^{++}]}{dt} = \frac{k_{1f} K_a Ni_T Ph_T}{[H^+]} - \left(\frac{k_{1r} K_a Ni_T + k_{1d}}{[H^+]} \right) [NiPh^{++}] \quad [8]$$

This expression may be integrated between limits $t = 0$ to $t = t$ which gives the following expression where $K_1 = \frac{k_{1d}}{k_{1r}}$:

$$t = \frac{2.3[H^+]}{k_{1f} K_a Ni_T + K_1 [H^+]} \log \frac{1}{1 - \left(\frac{Ni_T K_a + K_1 [H^+]}{Ni_T K_a Ph_T} \right) [NiPh^{++}]} \quad [9]$$

Since K_1 can be measured at equilibrium, the only variables are t and $[NiPh^{++}]$.

In order to observe the formation of mono(1,10-phenanthroline)-nickel(II) at lower acidity it is necessary to reduce the nickel(II) concentration and the rate law obtained is again second order. In this case the mathematical expression becomes too cumbersome if treated as above. Therefore, the reaction rate is observed over a sufficiently small fraction of the total reaction time so that the dissociation of mono(1,10-phenanthroline)nickel(II) may be neglected. The rate expression is then as follows:

$$\begin{aligned} \frac{d[\text{NiPh}^{++}]}{dt} &= k_{1f}[\text{Ni}^{++}][\text{Ph}] \\ &= \frac{k_{1f}K}{[H^+]} (\text{Ni}_T - [\text{NiPh}^{++}])(\text{Ph}_T - [\text{NiPh}^{++}]) \end{aligned} \quad (10)$$

and

$$t = \frac{2.3[H^+]}{k_{1f}K(\text{Ph}_T - \text{Ni}_T)} \log \left[\frac{\text{Ph}_T - [\text{NiPh}^{++}]}{\text{Ni}_T - [\text{NiPh}^{++}]} \cdot \frac{\text{Ni}_T}{\text{Ph}_T} \right] \quad (11)$$

As will be seen later, the reaction mechanism is not just the simple one proposed in Equations (4) and (1). Therefore, the observed rate constant obtained by calculation with the above expressions, is termed k_o instead of k_{1f} , because the rate constant k_{1f} represents only the simple mechanism.

In order to follow the reaction, the concentration of *meso*(1,10-phenanthroline)nickel(II) is measured spectrophotometrically. The 1,10-phenanthroline ion, 1,10-phenanthroline, and *meso*(1,10-phenanthroline)-nickel(II) all absorb throughout the ultraviolet region. The 1,10-phenanthroline concentration can be maintained at an extremely low level due to the 1,10-phenanthroline equilibrium and hence the 1,10-phenanthroline absorbance is negligible. The *meso*(1,10-phenanthroline)nickel(II) concentration is therefore based on the difference in the initial and final absorbance,

$$[\text{NiPh}^{++}] = \frac{c_{\text{NiPh}} \text{Ph}_T - A_o/l}{c_{\text{NiPh}} - c_{\text{NiPh}}} \quad (12)$$

where c is the molar absorptivity of the species indicated by the subscript, l is the cell path and A_o is the observed absorbance corrected for any cell blank.

The ultraviolet absorption spectra of phenanthroline with varying amounts of nickel in acid solutions are seen in Figure 1. Several wavelengths are suitable for observing the change from the 1,10-phenanthroline ion to the nickel(II)-1,10-phenanthroline complex ion. Figure 2 shows the effect of time on the absorption spectra between 200 and 300m μ when 1,10-phenanthroline and nickel(II) are mixed in acid solution. The appearance of seven well-defined isobestic points clearly indicates that there are only two absorbing species present in the solution. In this region, 277.5 m μ is relatively free from interference and is a suitable wavelength for observing a large change in absorbance as the reaction proceeds. Another wavelength which serves this purpose somewhat better is seen in Fig. 3 to be 310 m μ .

The reaction rate between nickel(II) ion and 1,10-phenanthroline was studied under varying conditions from a large excess of nickel(II) perchlorate to a slight excess of 1,10-phenanthroline and from 0.75 molar to 0.005 molar perchloric acid as is seen in Tables 2 and 3. The reaction rate was observed in the ultraviolet region by following a decrease in the absorbance of the 1,10-phenanthroline ion and therefore, it was not possible under ordinary conditions to use a large excess of 1,10-phenanthroline to nickel(II). The rapidity of the reaction prevented the use of a large excess of nickel(II) at low acidities. The visible spectrum is not a suitable region for studying the reaction because the molar absorptivity there is quite small. The insolubility of 1,10-phenanthroline perchlorate and the rapidity of the reaction are also prohibitive.

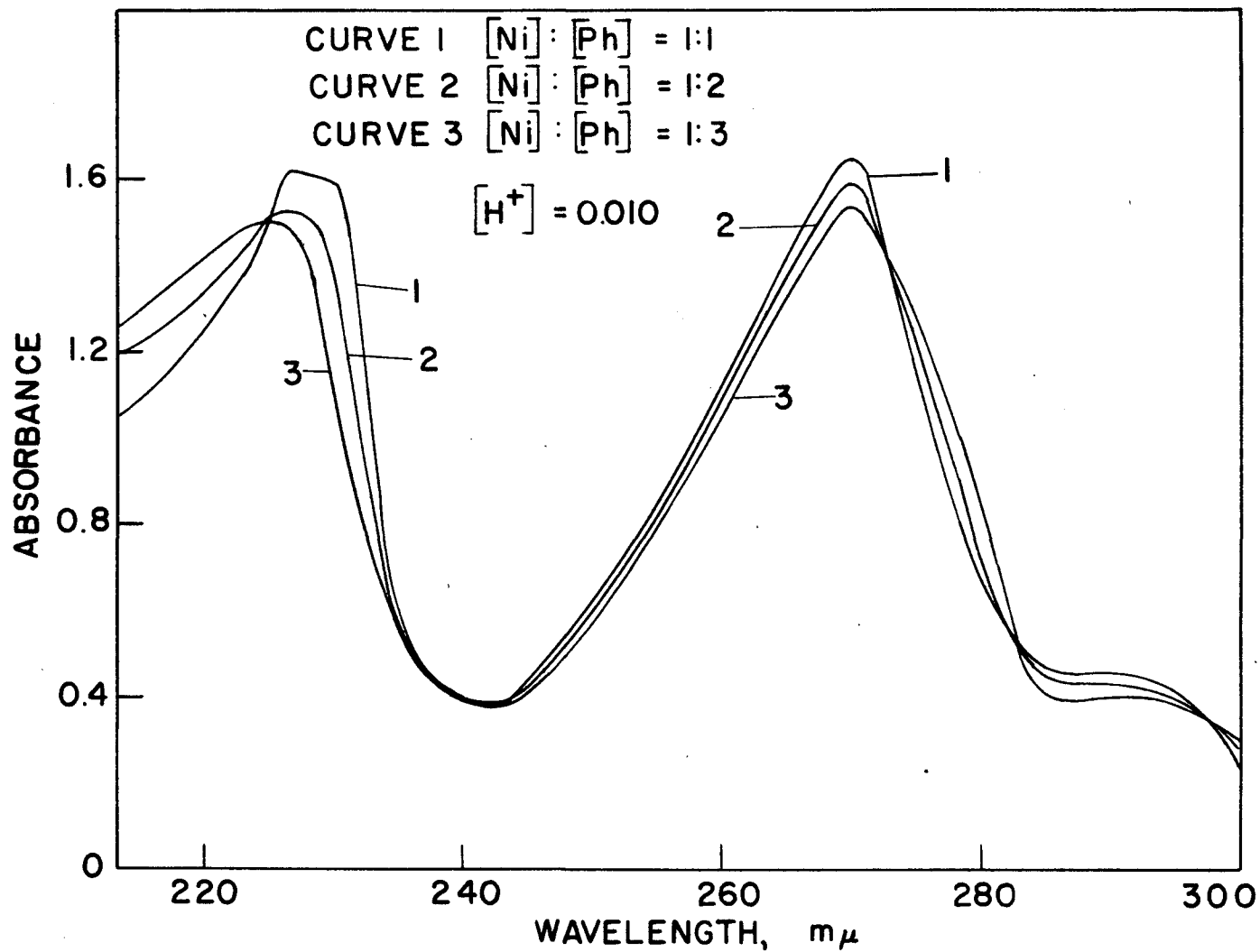


FIGURE 1, ABSORPTION SPECTRA OF PHENANTHROLINE WITH VARYING NICKEL IN ACID SOLUTION, 220-300 mμ

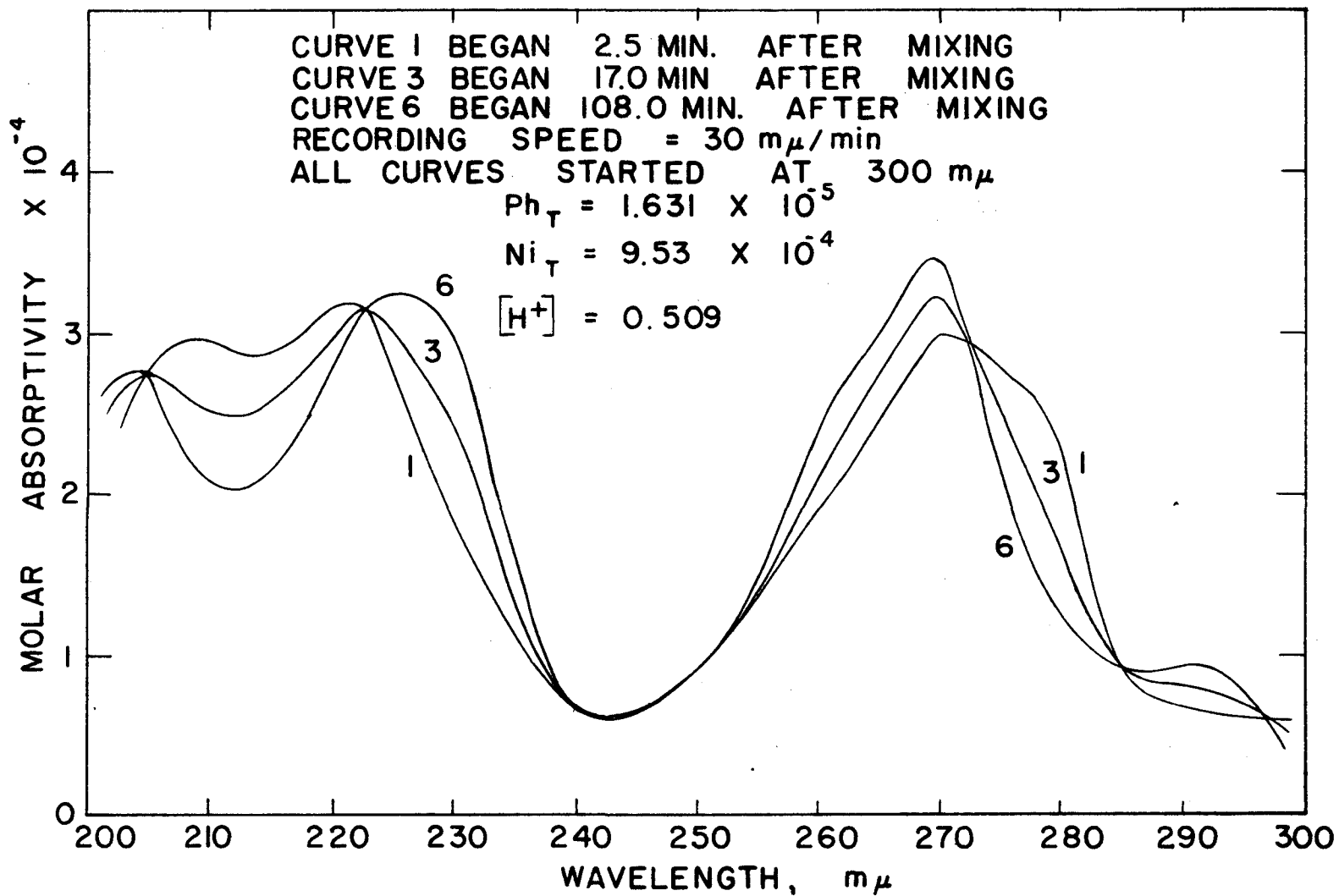


FIGURE 2, ABSORPTION SPECTRA OF PHENANTHROLINE
 SHOWING THE REACTION WITH NICKEL IN ACID SOLUTION

Table 2. Formation Reactions of the Mono(1,10-phenanthroline)nickel(II) Complexes

Reaction No.	λ (m μ)	ϵ_{Mn}	ϵ_{Mn}^2	ϵ_{Mn}^3	cell length	$M_{1/2}$	$M_{1/2}$	χ_0
1	0.767	277.5	2.86×10^4	1.97×10^4	2 cm.	1.304×10^{-5}	3.072×10^{-5}	1.70×10^6
2	0.532	277.5	2.86×10^4	1.55×10^4	2 cm.	1.304×10^{-5}	1.306×10^{-5}	1.89×10^6
3	0.532	277.5	2.86×10^4	1.55×10^4	2 cm.	1.304×10^{-5}	1.306×10^{-5}	2.00×10^6
4	0.535	277.5	2.86×10^4	1.55×10^4	2 cm.	1.304×10^{-5}	3.072×10^{-5}	1.97×10^6
5	0.498	310	5.14×10^3	1.55×10^3	1 cm.	1.153×10^{-4}	6.12×10^{-4}	1.84×10^6
6	0.498	310	5.10×10^3	1.55×10^3	1 cm.	1.153×10^{-4}	7.65×10^{-5}	1.65×10^6
7	0.427	310	5.06×10^3	1.58×10^3	2 cm.	6.52×10^{-5}	3.06×10^{-4}	1.68×10^6
8	0.106	310	5.20×10^3	1.58×10^3	1 cm.	6.52×10^{-5}	4.59×10^{-5}	1.19×10^6
9	0.0686	310	5.10×10^3	1.58×10^3	2 cm.	6.52×10^{-5}	4.59×10^{-5}	1.04×10^6
10	0.0686	310	5.15×10^3	1.58×10^3	1 cm.	6.52×10^{-5}	4.59×10^{-5}	0.96×10^6
11	0.027	310	5.09×10^3	1.58×10^3	1 cm.	6.52×10^{-5}	4.59×10^{-5}	0.52×10^6
12	0.02225	310	4.95×10^3	1.58×10^3	1 cm.	1.304×10^{-4}	4.59×10^{-5}	0.547×10^6
13	0.0207	310	5.20×10^3	1.58×10^3	1 cm.	6.52×10^{-5}	4.59×10^{-5}	0.48×10^6
14	0.0056	310	4.96×10^3	1.58×10^3	1 cm.	6.52×10^{-5}	4.59×10^{-5}	0.36×10^6

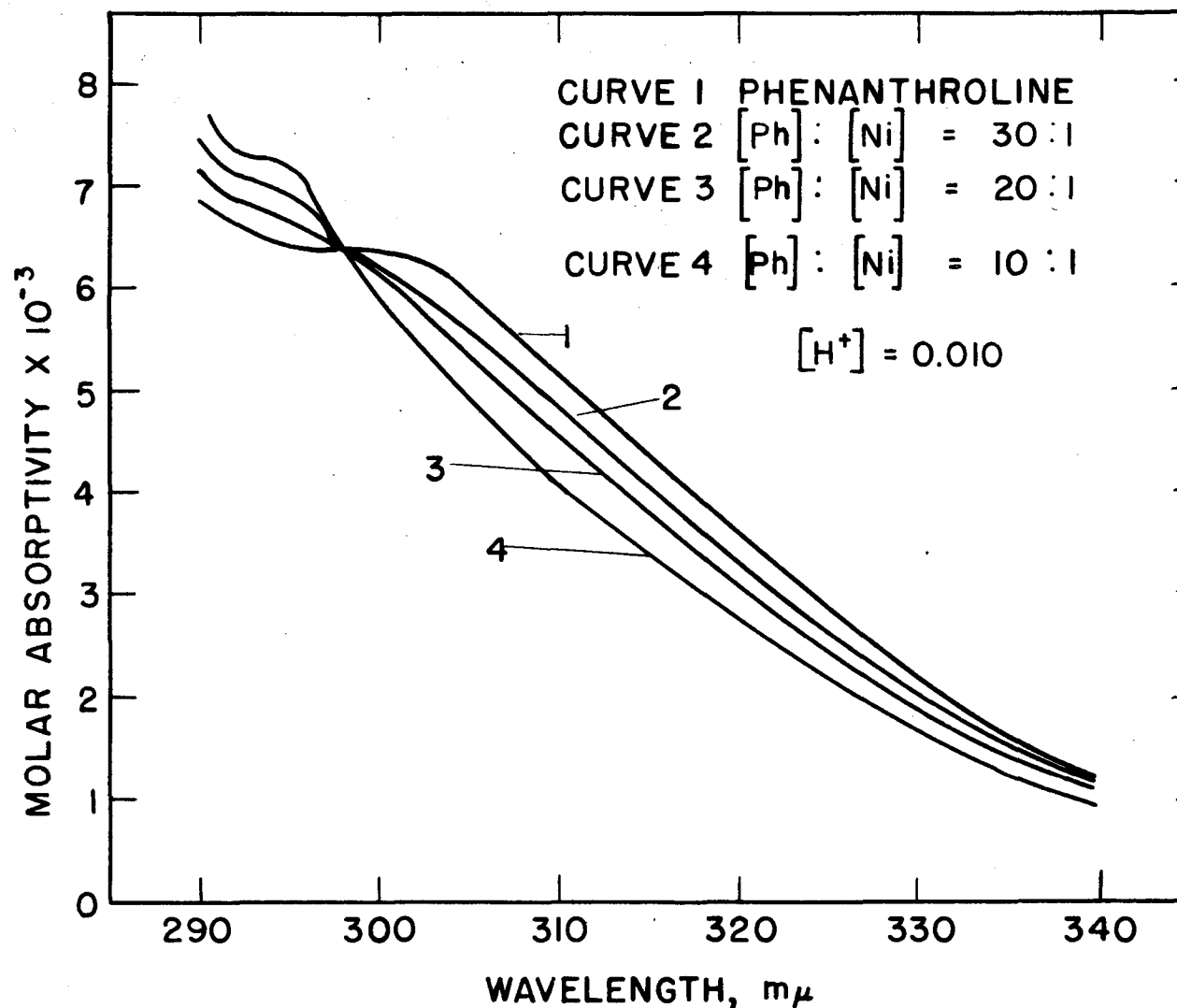


FIGURE 3, ABSORPTION SPECTRA OF PHENANTHROLINE
 WITH VARYING NICKEL IN ACID SOLUTION, 290-340 mμ

Table 3. Dissociation Reactions of the Mono(1,10-phenanthroline)nickel(II) Complex

Reaction No.	$[K']$	λ (m μ)	ϵ_{max}	ϵ_{H^+}	cell length	K_1	K_2	K_3
15	4.5	277.5	3.27×10^4	1.83×10^4	1 cm.	2.306×10^{-3}	1.506×10^{-4}	5.5×10^{-3}
16	1.0	277.5	2.90×10^4	1.60×10^4	1 cm.	1.153×10^{-3}	8.40×10^{-4}	5.9×10^{-3}
17	0.5	310	5.14×10^3	1.36×10^4	3 cm.	5.76×10^{-3}	1.905×10^{-4}	3.98×10^{-3}
18	0.2	310	5.14×10^3	1.36×10^4	3 cm.	5.76×10^{-3}	1.905×10^{-4}	2.37×10^{-3}
19	0.02	310	5.14×10^3	1.34×10^4	3 cm.	5.76×10^{-3}	1.905×10^{-4}	0.81×10^{-3}

Tables 4 through 17 present the data taken with the Beckman DU spectrophotometer, where A_0 is the observed absorbance corrected for any cell blank and nickel absorbance. The substitution of Equation [12] into Equation [9] gives the expression which is used to calculate Reactions 1 through 4. The substitution of Equation [12] into Equation [11] gives the expression which is used to calculate Reactions 5 through 14. Figures 4 through 17 are graphs of these data where $k_0 t$ is plotted against t .

For each kinetic run a 1,10-phenanthroline blank was measured to determine the molar absorptivity of the 1,10-phenanthrolium ion under the particular conditions of that run. The molar absorptivity of the mono-(1,10-phenanthroline)nickel(II) was determined by using a large excess of nickel(II) over 1,10-phenanthroline at low acidity. Table 2 shows that the molar absorptivity of the 1,10-phenanthrolium ion (ϵ_{HPH}) at 310m μ varies considerably more than would be expected from volumetric or instrumental errors. Careful tests indicated that 1,10-phenanthroline was kept in solution as 1,10-phenanthrolium ion throughout the acidity range used in this work. However, 1,10-phenanthroline showed an affinity for silica surfaces and at times slight adsorption on the surface of the silica cells was observed. This factor is believed to account for the variability of the observed molar absorptivities.

Several other peculiarities of the data in Table 2 should be noted. First, a comparison of the molar absorptivities of mono(1,10-phenanthroline)nickel(II) at 277.5m μ shows a very slight increase in the molar absorptivity as the acidity increases. This becomes especially apparent in the dissociation reaction at 4.5 molar hydrogen in Table 3, where the value of the molar absorptivity of the mono(1,10-phenanthroline)-

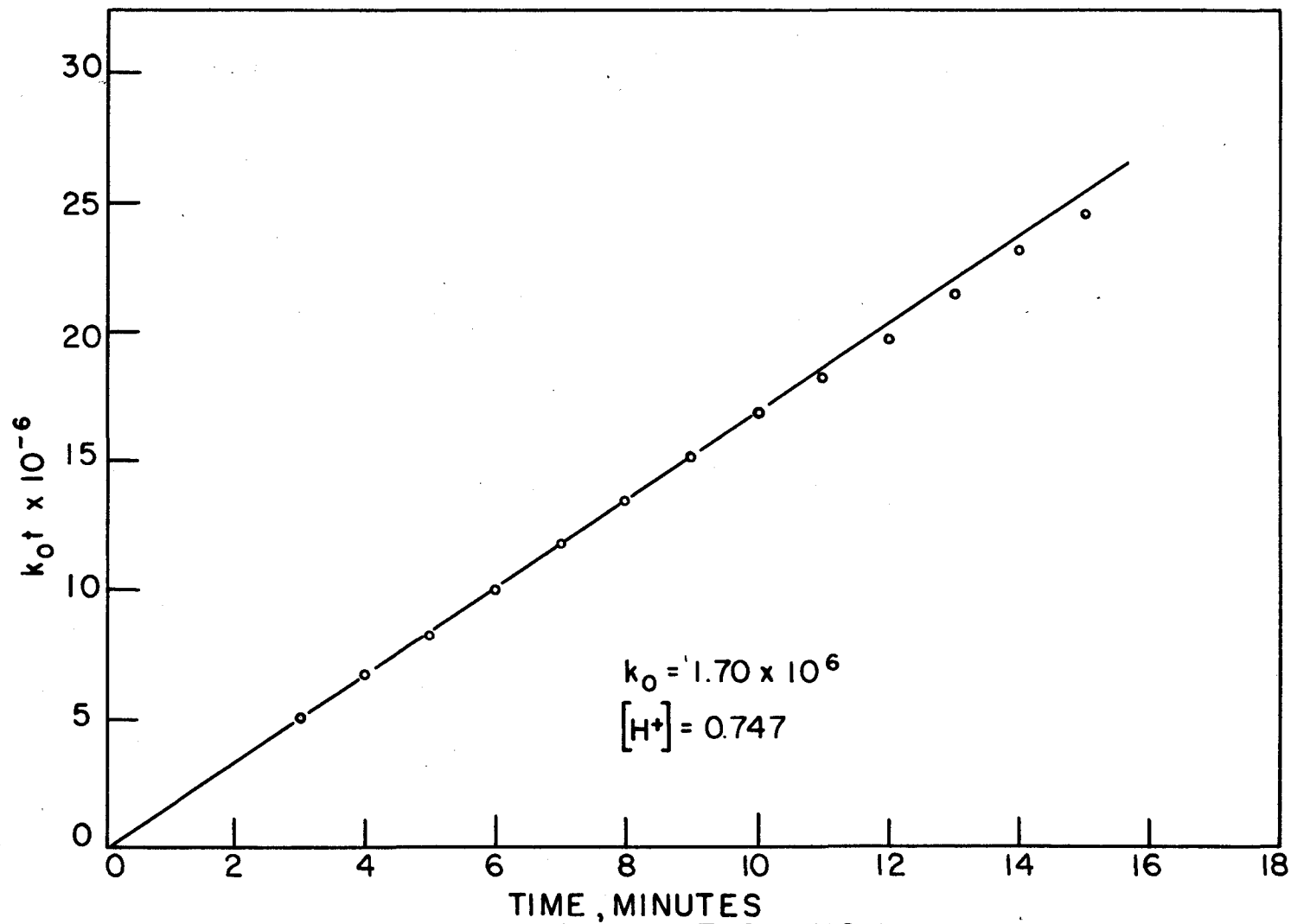


FIGURE 4, REACTION NO. 1

Table 4. Spectrophotometric Data and
Calculation of Reaction 1.

$$k_0 s = 5.12 \times 10^7 \log \frac{1}{1 - 3.06 (.796 - A_0)}$$

Time (min.)	A_0	$\log \frac{1}{1 - 3.06 (.796 - A_0)}$	$k_0 s$
3	0.680	0.098	5.0×10^6
4	0.661	0.131	6.7×10^6
5	0.646	0.159	8.2×10^6
6	0.627	0.196	10.0×10^6
7	0.611	0.232	11.9×10^6
8	0.598	0.262	13.4×10^6
9	0.585	0.295	15.1×10^6
10	0.575	0.328	16.9×10^6
11	0.563	0.357	18.5×10^6
12	0.554	0.385	19.7×10^6
13	0.544	0.418	21.4×10^6
14	0.535	0.451	23.1×10^6
15	0.528	0.479	24.5×10^6

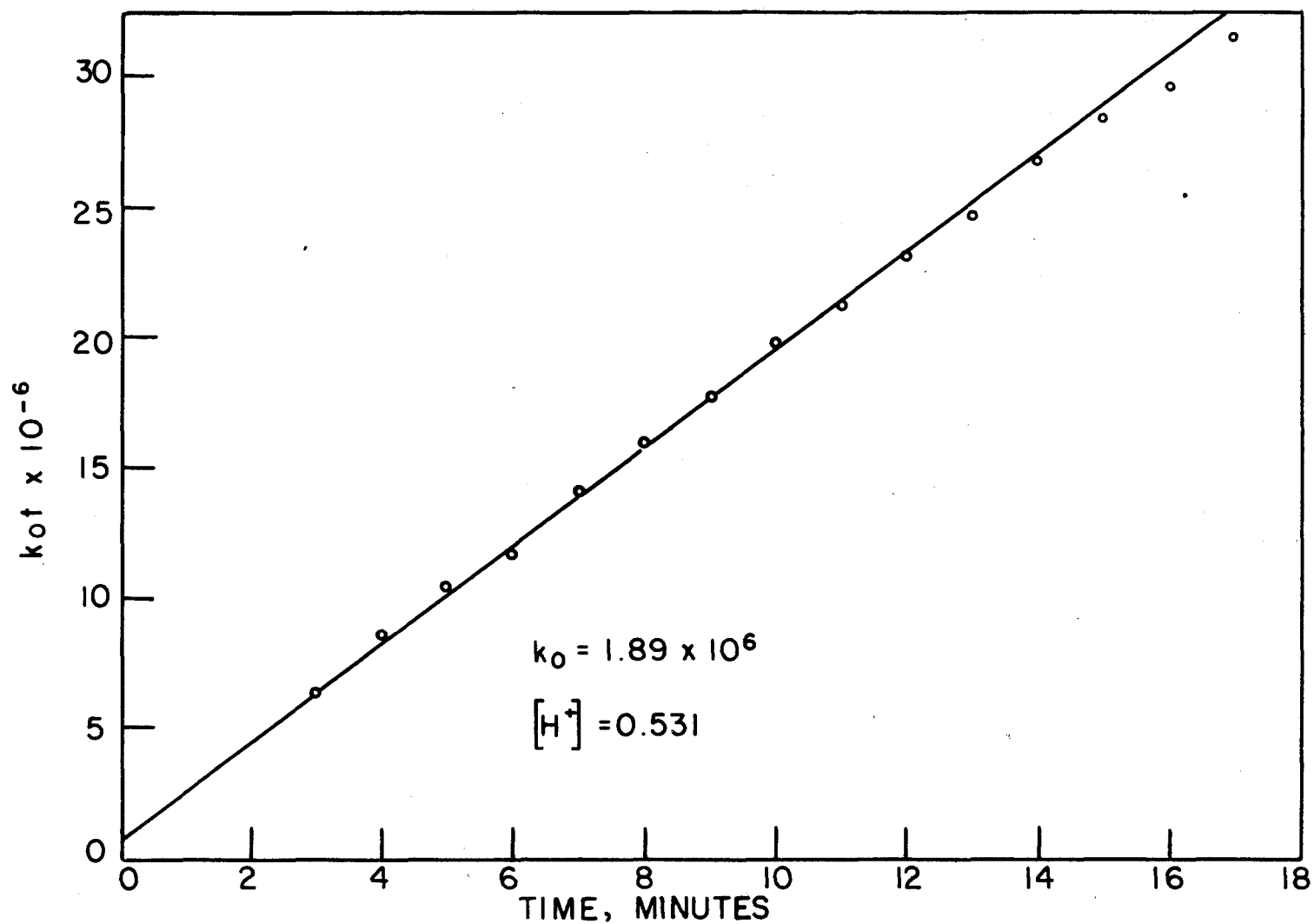


FIGURE 5, REACTION NO. 2

Table 2. Spectrophotometric Data and Calculation of Reaction B

$$k_0^B = 7.87 \times 10^7 \log \frac{1}{1 - 3.25 (A_0 - A_t)}$$

Time (min.)	A_0	$\log \frac{1}{1 - 3.25 (A_0 - A_t)}$	k_0^B
3	0.690	0.088	6.4×10^6
4	0.674	0.118	8.6×10^6
5	0.662	0.143	10.4×10^6
6	0.652	0.161	11.7×10^6
7	0.638	0.192	14.0×10^6
8	0.626	0.221	16.1×10^6
9	0.616	0.245	17.8×10^6
10	0.606	0.272	19.8×10^6
11	0.599	0.291	21.2×10^6
12	0.590	0.317	23.1×10^6
13	0.583	0.339	24.6×10^6
14	0.576	0.362	26.7×10^6
15	0.568	0.389	28.3×10^6
16	0.563	0.407	29.6×10^6
17	0.556	0.433	31.3×10^6
18	0.551	0.453	33.1×10^6
19	0.544	0.483	35.1×10^6
20	0.541	0.496	36.1×10^6

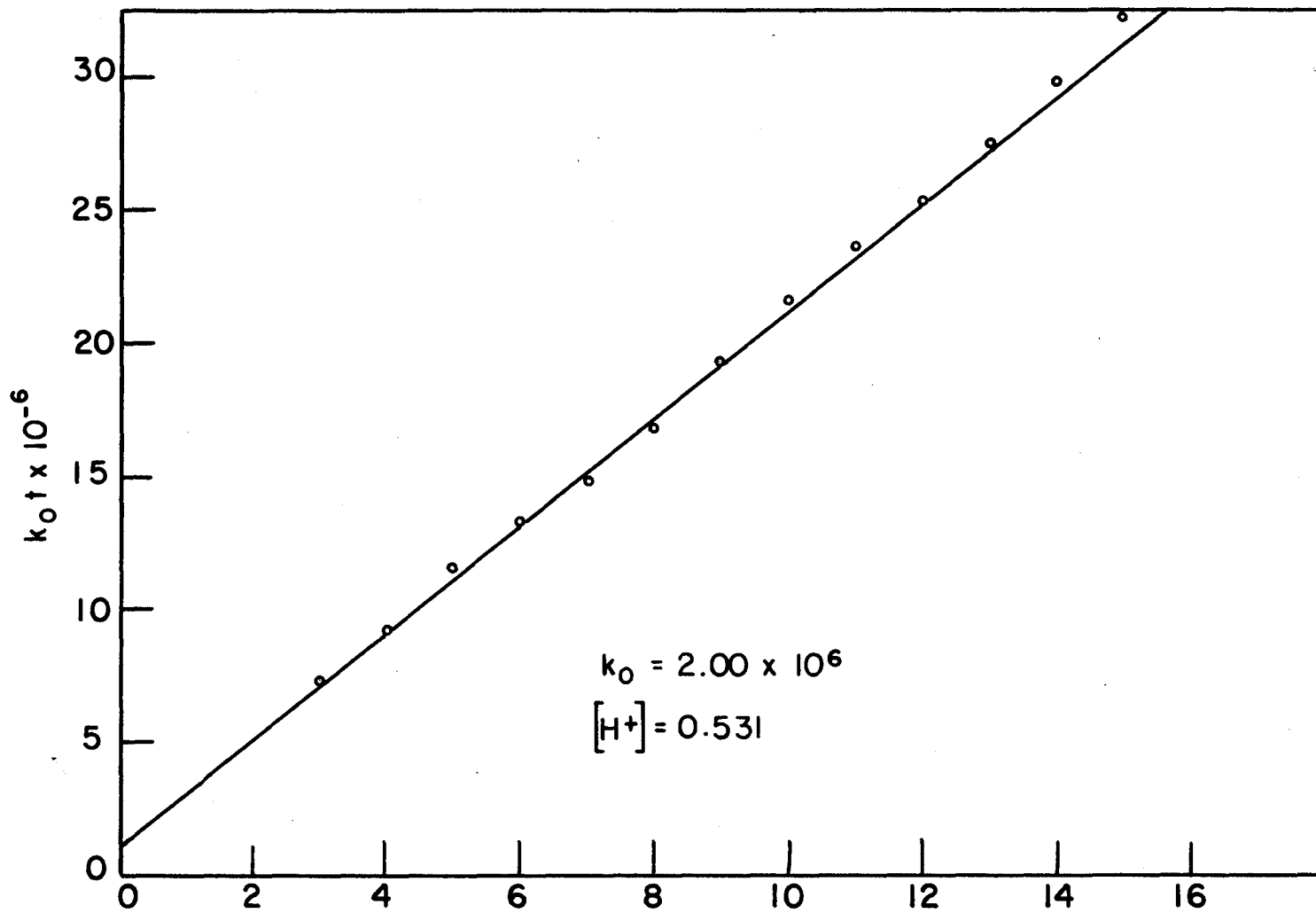


FIGURE 6, REACTION NO. 3

Table 6. Spectrophotometric Data
and Calculation of Reaction 3

$$k_0 t = 7.27 \times 10^7 \log \frac{1}{1 - 3.33 (.745 - A_0)}$$

Time (min.)	A_0	$\log \frac{1}{1 - 3.33 (.745 - A_0)}$	$k_0 t$
3	0.683	0.101	7.4×10^6
4	0.670	0.126	9.2×10^6
5	0.654	0.158	11.5×10^6
6	0.642	0.183	13.3×10^6
7	0.629	0.214	14.8×10^6
8	0.618	0.233	16.9×10^6
9	0.608	0.266	19.3×10^6
10	0.597	0.297	21.6×10^6
11	0.588	0.324	23.6×10^6
12	0.580	0.348	25.3×10^6
13	0.571	0.378	27.3×10^6
14	0.562	0.410	29.8×10^6
15	0.553	0.443	32.3×10^6

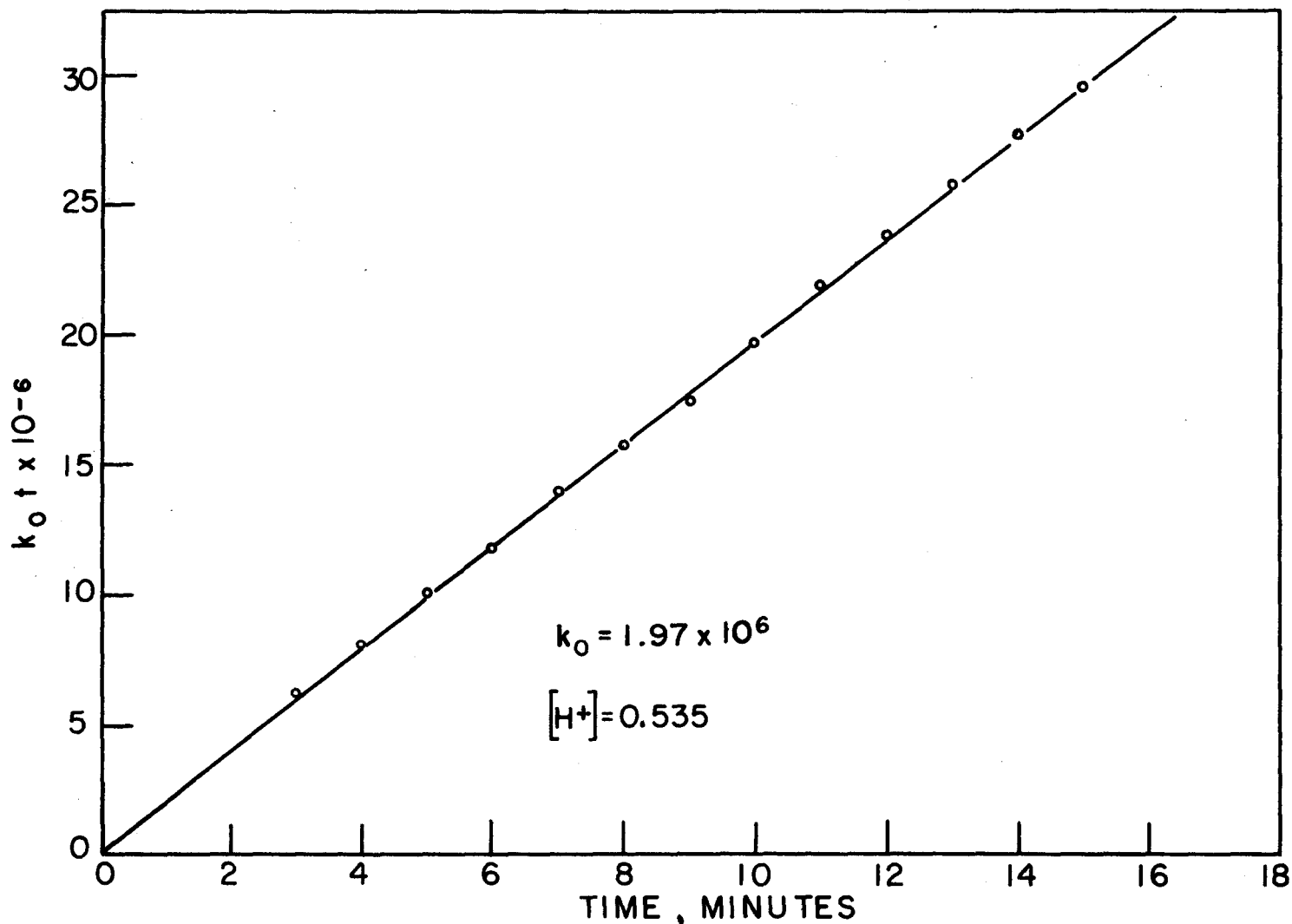


FIGURE 7, REACTION NO. 4

Table 7. Spectrophotometric Data
and Calculation of Reaction 4

$$k_0 t = 3.663 \times 10^7 \log \frac{1}{1 - 2.98 (.751 - A_0)}$$

Time (min.)	A_0	$\log \frac{1}{1 - 2.98 (.751 - A_0)}$	$k_0 t$
3	0.630	0.174	6.4×10^6
4	0.617	0.222	8.1×10^6
5	0.594	0.274	10.1×10^6
6	0.583	0.323	11.8×10^6
7	0.573	0.381	14.0×10^6
8	0.541	0.427	15.7×10^6
9	0.527	0.479	17.5×10^6
10	0.513	0.538	19.7×10^6
11	0.501	0.597	21.9×10^6
12	0.491	0.648	23.8×10^6
13	0.482	0.701	25.7×10^6
14	0.474	0.757	27.8×10^6
15	0.468	0.807	29.6×10^6

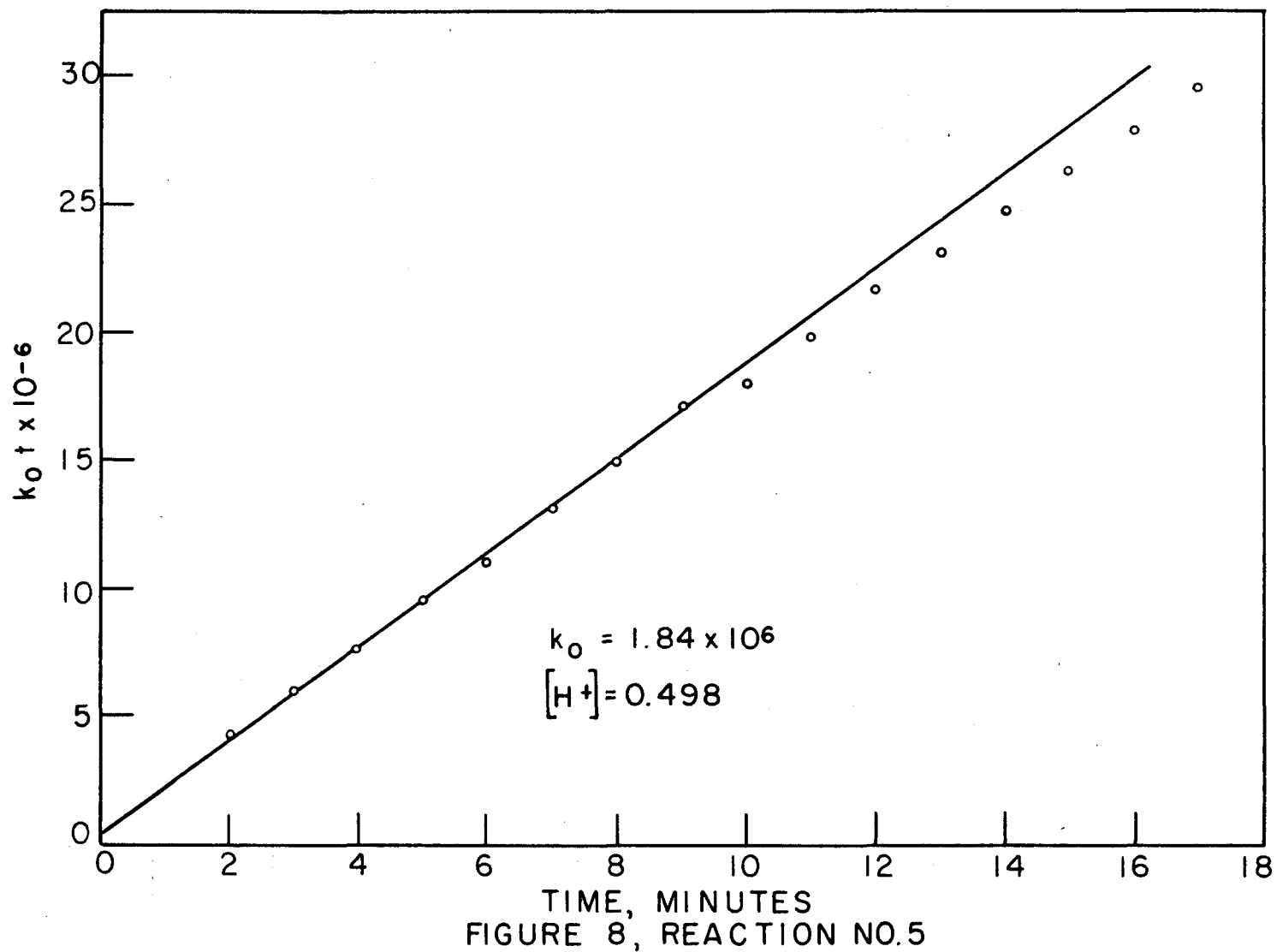


Table 8. Spectrophotometric Data
and Calculation of Reaction 5

$$k_0 t = 2.1 \times 10^8 \log \frac{A_0 + 1.787}{(A_0 - .156) 5330}$$

Time (min.)	A_0	$\log \frac{A_0 + 1.787}{(A_0 - .156) 5330}$	$k_0 t$
2	0.569	0.080	4.2×10^6
3	0.561	0.088	5.9×10^6
4	0.551	0.096	7.6×10^6
5	0.542	0.095	9.5×10^6
6	0.534	0.092	10.9×10^6
7	0.524	0.062	15.0×10^6
8	0.516	0.071	14.9×10^6
9	0.505	0.081	17.0×10^6
10	0.502	0.085	17.9×10^6
11	0.495	0.094	19.7×10^6
12	0.485	0.103	21.6×10^6
13	0.480	0.109	22.9×10^6
14	0.473	0.117	24.6×10^6
15	0.466	0.125	26.2×10^6
16	0.461	0.132	27.7×10^6
17	0.454	0.140	29.4×10^6
18	0.449	0.146	30.6×10^6
19	0.445	0.154	32.4×10^6

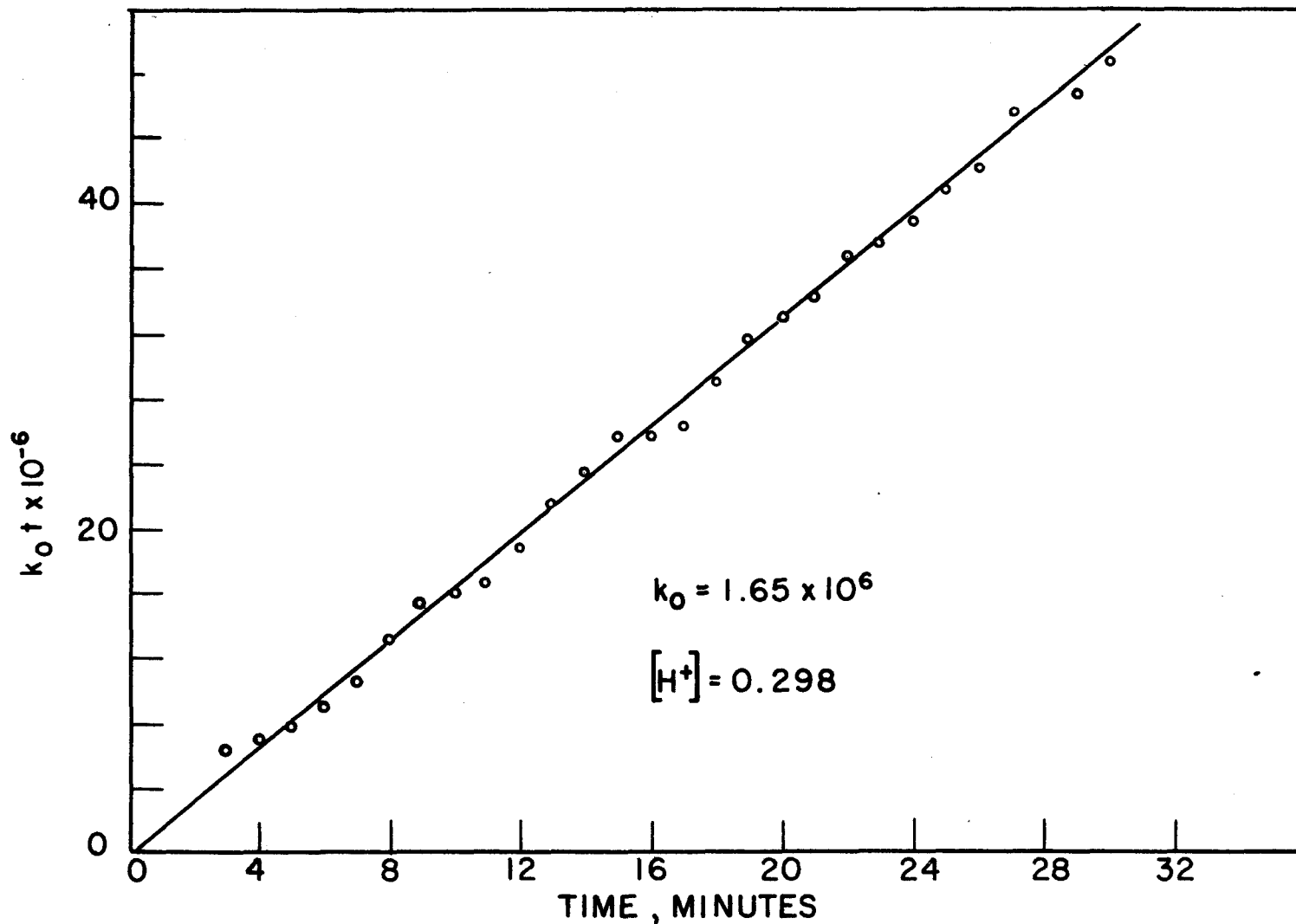


FIGURE 9, REACTION NO.6

Table 9. Spectrophotometric Data
and Calculation of Reaction 6

$$k_0 t = 1.613 \times 10^9 \log \frac{A_0 - .156}{A_0 - .301} \times .663$$

Time (min.)	A_0	$\log \frac{A_0 - .156}{A_0 - .301} \times .663$	$k_0 t$
3	0.579	0.0039	6.3×10^6
4	0.578	0.0043	6.9×10^6
5	0.577	0.0048	7.7×10^6
6	0.576	0.0056	9.0×10^6
7	0.574	0.0063	10.3×10^6
8	0.571	0.0082	13.2×10^6
9	0.569	0.0093	15.3×10^6
10	0.568	0.0099	16.0×10^6
11	0.567	0.0103	16.6×10^6
12	0.565	0.0116	18.7×10^6
13	0.562	0.0133	21.3×10^6
14	0.560	0.0145	23.4×10^6
15	0.558	0.0158	25.5×10^6
16	0.558	0.0158	25.5×10^6
17	0.557	0.0162	26.1×10^6
18	0.554	0.0179	28.9×10^6
19	0.552	0.0193	31.3×10^6
20	0.551	0.0204	32.9×10^6
21	0.549	0.0212	34.2×10^6
22	0.547	0.0223	35.8×10^6
23	0.546	0.0233	37.6×10^6
24	0.545	0.0241	38.9×10^6
25	0.543	0.0253	40.8×10^6
26	0.542	0.0261	42.1×10^6
27	0.539	0.0282	45.5×10^6
28	0.538	0.0286	46.1×10^6
29	0.538	0.0286	46.8×10^6
30	0.536	0.0302	48.7×10^6

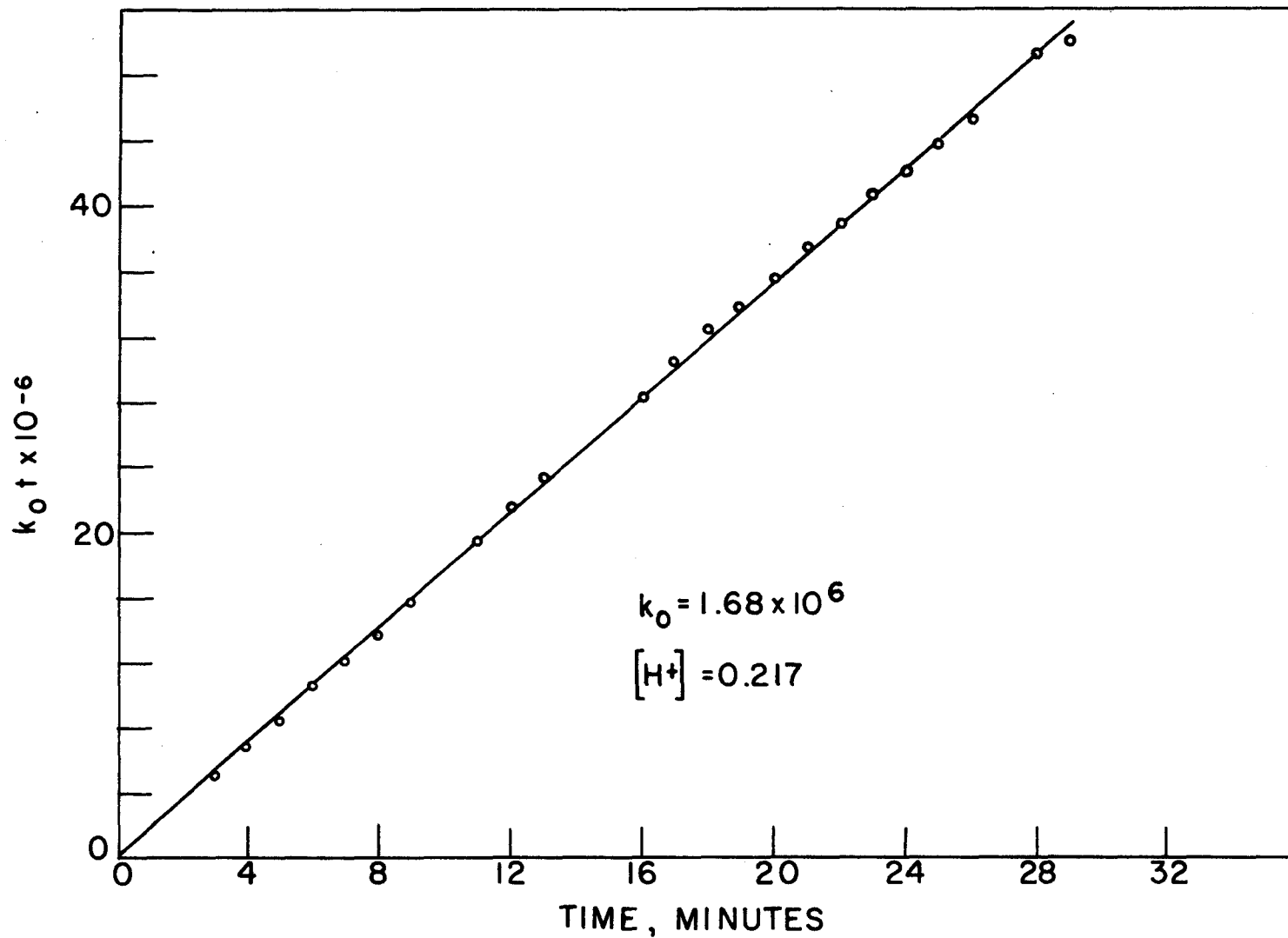


FIGURE 10, REACTION NO.7

Table 10, Spectrophotometric Data
and Calculation of Invariant γ

$$k_0 t = 1.89 \times 10^8 \log \frac{A_0 + 1.47}{(A_0 - .206) .469}$$

Time (min.)	A_0	$\log \frac{A_0 + 1.47}{(A_0 - .206) .469}$	$k_0 t$
3	0.626	0.087	5.1×10^6
4	0.616	0.076	6.8×10^6
5	0.604	0.064	8.3×10^6
6	0.593	0.056	10.6×10^6
7	0.584	0.064	12.1×10^6
8	0.575	0.073	13.8×10^6
9	0.565	0.085	15.7×10^6
10	0.554	0.094	17.8×10^6
11	0.545	0.105	19.5×10^6
12	0.535	0.114	21.5×10^6
13	0.527	0.123	23.8×10^6
14	0.520	0.090	24.8×10^6
15	0.515	0.140	26.5×10^6
16	0.504	0.150	28.4×10^6
17	0.495	0.161	30.4×10^6
18	0.487	0.171	32.3×10^6
19	0.482	0.179	33.8×10^6
20	0.475	0.186	35.5×10^6
21	0.468	0.198	37.8×10^6
22	0.465	0.206	38.9×10^6
23	0.456	0.216	40.8×10^6
24	0.452	0.222	42.0×10^6
25	0.445	0.232	43.8×10^6
26	0.441	0.239	45.2×10^6
27	0.437	0.246	46.4×10^6
28	0.433	0.252	47.6×10^6
29	0.427	0.265	49.7×10^6
30	0.425	0.270	51.0×10^6

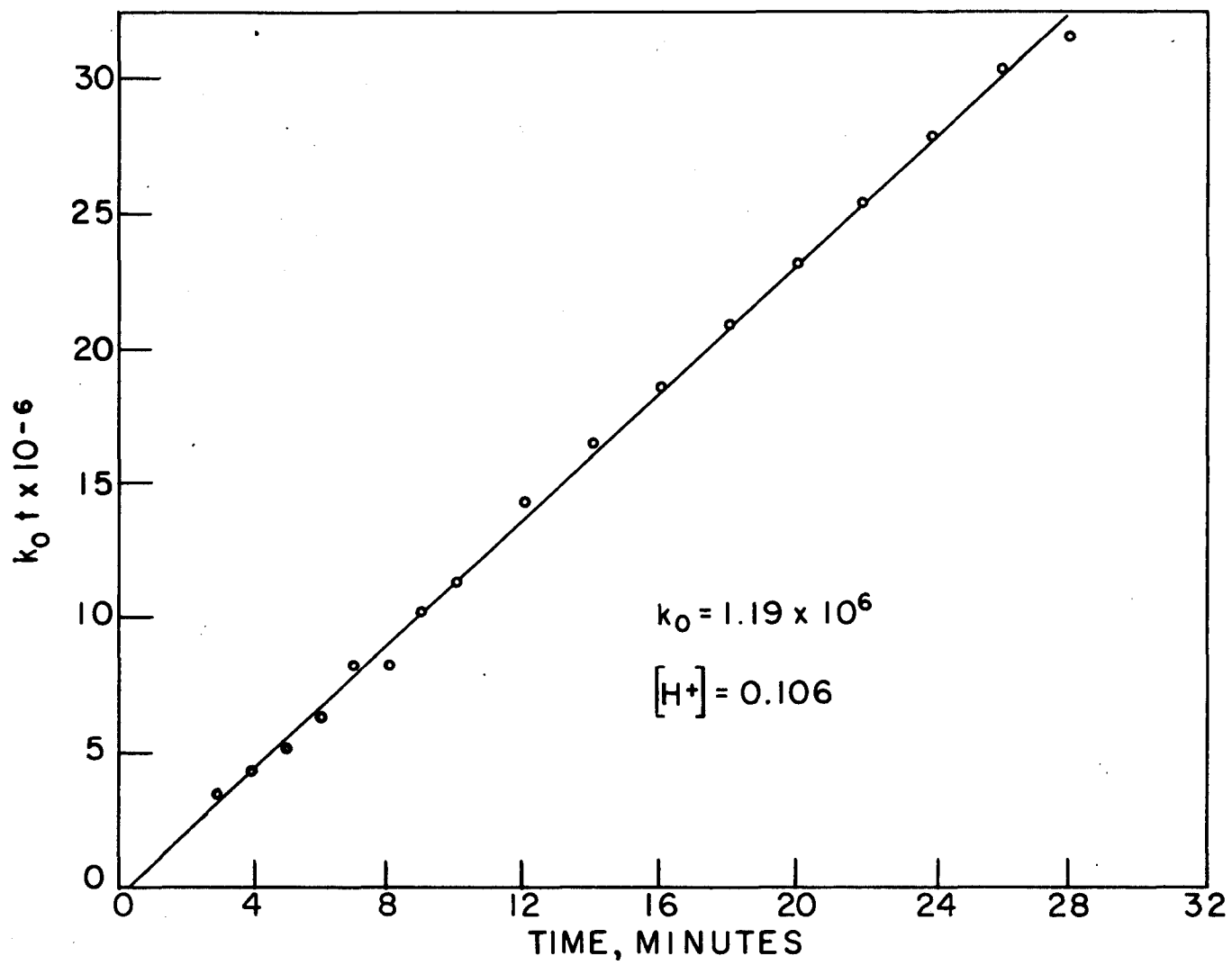


FIGURE II, REACTION NO.8

Table 11. Spectrophotometric Data
and Calculation of Reaction 8

$$k_0 t = 1.156 \times 10^9 \log \frac{A_0 - .103}{A_0 - .173} \times .703$$

Time (Min.)	A_0	$\log \frac{A_0 - .103}{A_0 - .173} \times .703$	$k_0 t$
3	0.535	0.0029	3.5×10^6
4	0.534	0.0036	4.2×10^6
5	0.533	0.0046	5.3×10^6
6	0.532	0.0054	6.2×10^6
7	0.530	0.0071	8.2×10^6
8	0.530	0.0071	8.2×10^6
9	0.528	0.0088	10.2×10^6
10	0.527	0.0097	11.2×10^6
12	0.524	0.0124	14.3×10^6
14	0.522	0.0142	16.4×10^6
16	0.520	0.0161	18.6×10^6
18	0.518	0.180	20.8×10^6
20	0.516	0.0200	23.1×10^6
22	0.514	0.0220	25.4×10^6
24	0.512	0.0241	27.8×10^6
26	0.510	0.0262	30.3×10^6
28	0.508	0.0274	31.6×10^6
30	0.506	0.0306	35.4×10^6

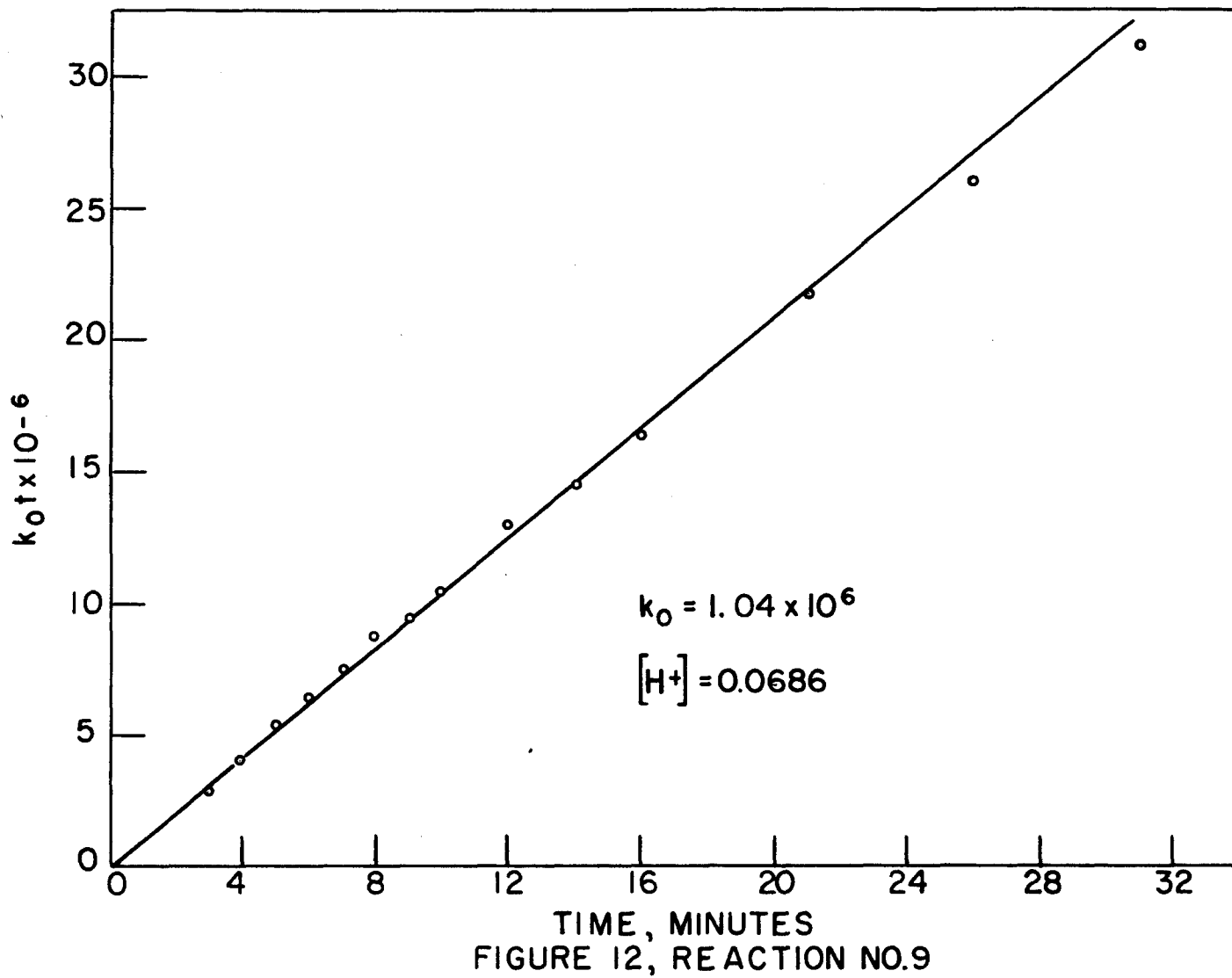


Table 12. Spectrophotometric Data
and Calculation of Reaction 9

$$k_0 t = 7.45 \times 10^8 \log \frac{(A_0 - .205)(.704)}{A_0 - .541}$$

Time (min.)	A_0	$\log \frac{(A_0 - .205)(.704)}{A_0 - .541}$	$k_0 t$
3	0.675	0.004	2.98×10^6
4	0.651	0.006	4.5×10^6
5	0.647	0.007	5.2×10^6
6	0.644	0.008	6.0×10^6
7	0.641	0.010	7.5×10^6
8	0.637	0.012	8.3×10^6
9	0.635	0.013	9.7×10^6
10	0.632	0.014	10.4×10^6
12	0.625	0.018	13.4×10^6
14	0.621	0.020	14.9×10^6
16	0.616	0.022	16.4×10^6
21	0.605	0.030	22.4×10^6
26	0.593	0.035	26.0×10^6
31	0.582	0.042	31.3×10^6
36	0.573	0.049	36.3×10^6
41	0.562	0.057	42.5×10^6
46	0.555	0.064	47.7×10^6

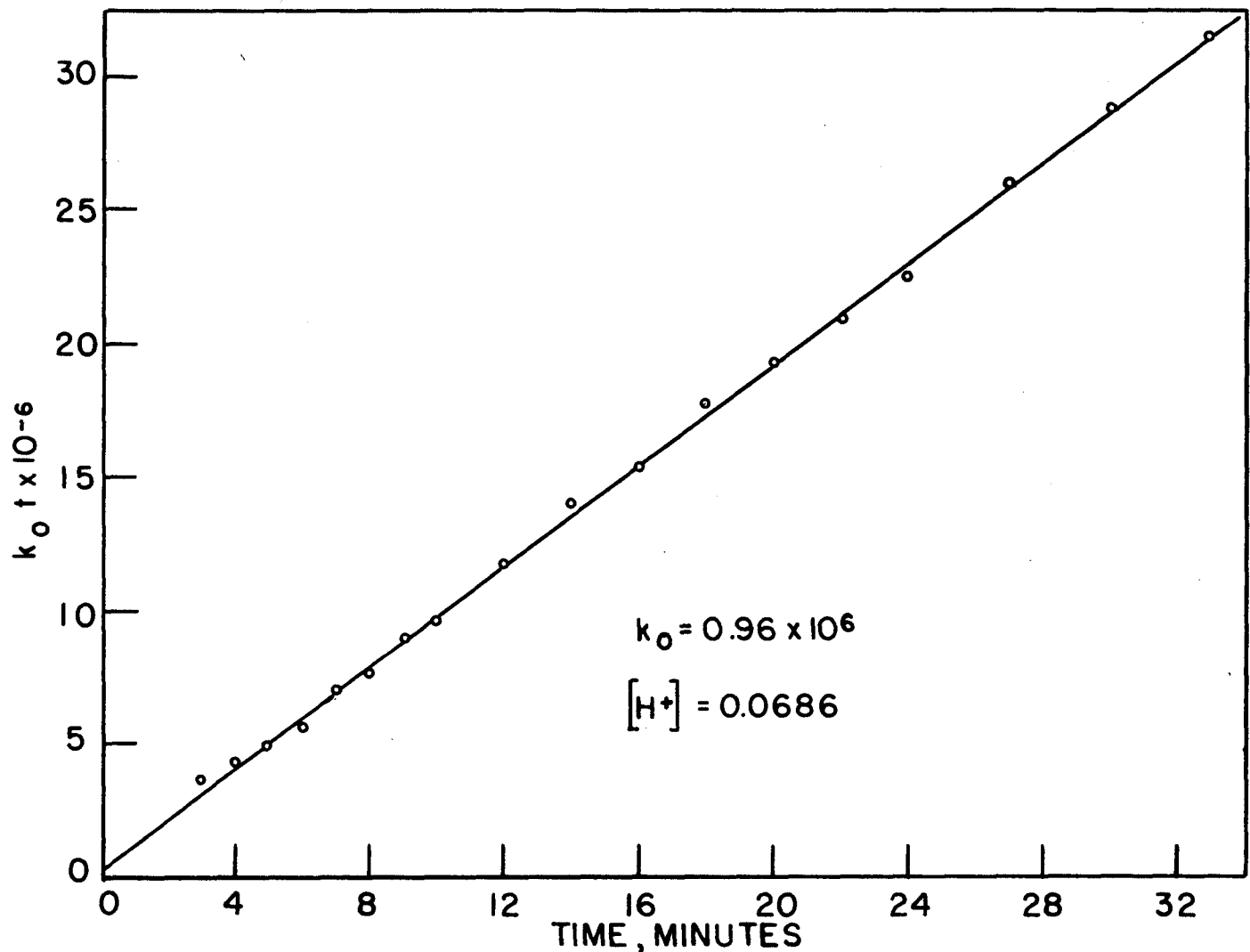


FIGURE 13, REACTION NO.10

Table 13. Spectrophotometric Data
and Calculation of Reaction 10

$$k_0 t = .745 \times 10^9 \log \frac{A_0 - .105}{A_0 - .172} \times .704$$

Time (min.)	A_0	$\log \frac{A_0 - .105}{A_0 - .172} \times .704$	$k_0 t$
3	0.330	0.0049	3.7×10^6
4	0.329	0.0048	4.3×10^6
5	0.328	0.0066	4.9×10^6
6	0.327	0.0075	5.6×10^6
7	0.325	0.0092	6.9×10^6
8	0.324	0.0101	7.6×10^6
9	0.322	0.0119	8.9×10^6
10	0.321	0.0128	9.6×10^6
12	0.318	0.0157	11.7×10^6
14	0.315	0.0186	13.9×10^6
16	0.313	0.0206	15.3×10^6
18	0.310	0.0237	17.7×10^6
20	0.308	0.238	19.2×10^6
22	0.306	0.0289	20.8×10^6
24	0.304	0.0302	22.5×10^6
27	0.300	0.0348	25.9×10^6
30	0.297	0.0385	28.7×10^6
33	0.294	0.0422	31.4×10^6

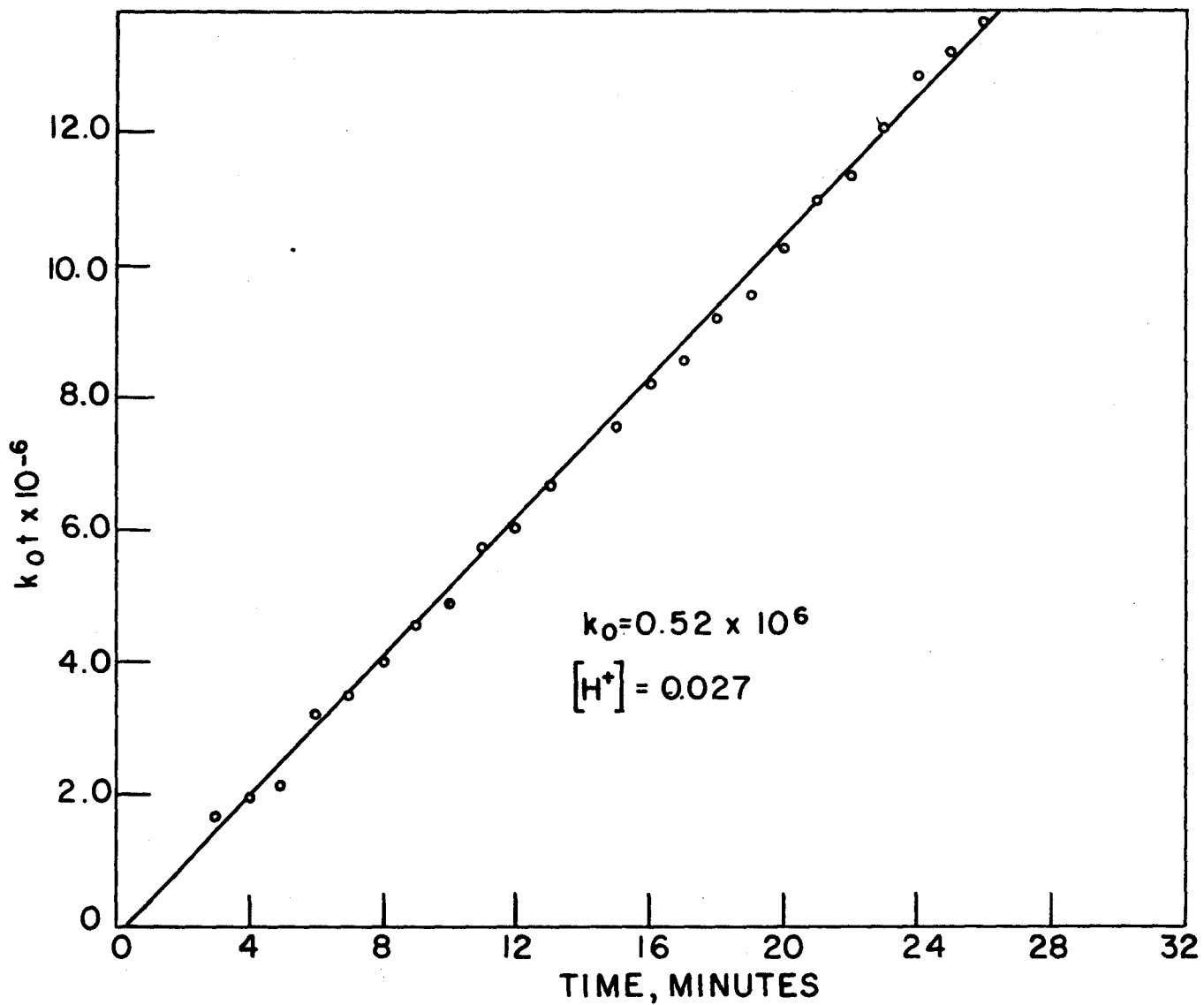


FIGURE 14, REACTION NO. II

Table 14. Spectrophotometric Data and Calculation of Reaction II

$$k^{\circ} t = 2.32 \times 10^8 \log \frac{A^{\circ} - .103}{A^{\circ} - .171} \times .704$$

Time (min.)	A°	$\log \frac{A^{\circ} - .103}{A^{\circ} - .171} \times .704$	$k^{\circ} t$
3	0.286	0.0033	1.6×10^6
4	0.283	0.0064	1.9×10^6
5	0.284	0.0073	2.1×10^6
6	0.280	0.0108	3.25×10^6
7	0.279	0.0118	3.4×10^6
8	0.277	0.0136	4.0×10^6
9	0.275	0.0155	4.5×10^6
10	0.274	0.0165	4.8×10^6
11	0.271	0.0195	5.7×10^6
12	0.270	0.0205	6.0×10^6
13	0.268	0.0226	6.6×10^6
14	0.266	0.0248	7.3×10^6
15	0.265	0.0258	7.5×10^6
16	0.263	0.0280	8.2×10^6
17	0.262	0.0291	8.5×10^6
18	0.260	0.0314	9.5×10^6
19	0.259	0.0325	9.5×10^6
20	0.257	0.0350	10.2×10^6
21	0.255	0.0374	10.9×10^6
22	0.254	0.0387	11.3×10^6
23	0.252	0.0412	12.0×10^6
24	0.250	0.0439	12.8×10^6
25	0.249	0.0452	13.2×10^6

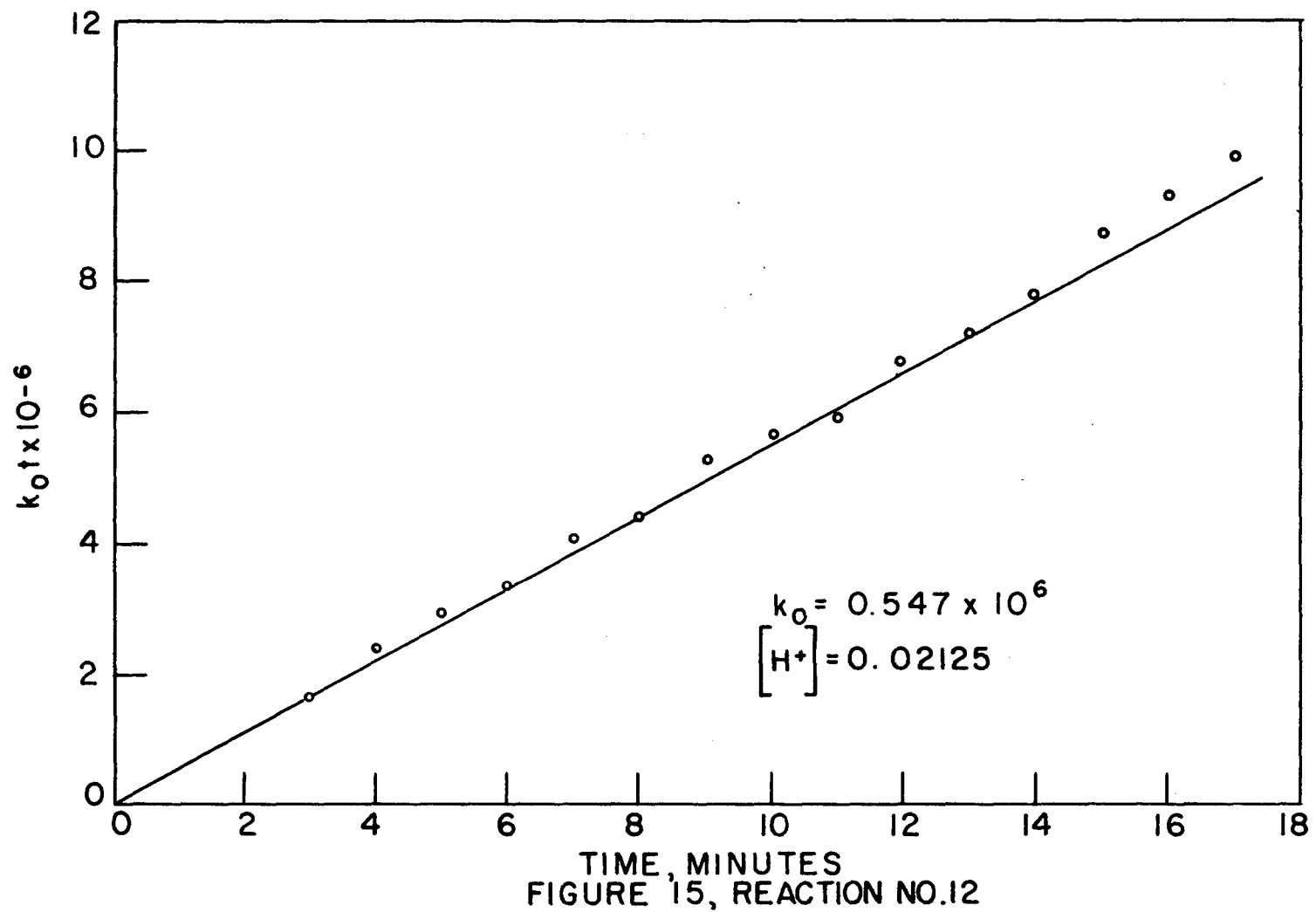


Table 15. Spectrophotometric Data
and Calculation of Reaction 12

$$k_0 t = 5.26 \times 10^7 \log \frac{(A_0 - .205)}{A_0 - .491} \times .532$$

Time (min.)	A_0	$\log \frac{(A_0 - .205)}{A_0 - .491} \times .532$	$k_0 t$
3	0.630	0.031	1.6×10^6
4	0.624	0.044	2.3×10^6
5	0.619	0.055	2.9×10^6
6	0.615	0.064	3.4×10^6
7	0.610	0.077	4.1×10^6
8	0.608	0.083	4.4×10^6
9	0.602	0.099	5.2×10^6
10	0.599	0.107	5.6×10^6
11	0.597	0.106	6.0×10^6
12	0.592	0.129	6.8×10^6
13	0.589	0.138	7.3×10^6
14	0.586	0.148	7.8×10^6
15	0.581	0.166	8.8×10^6
16	0.578	0.177	9.3×10^6
17	0.575	0.189	9.95×10^6
18	0.571	0.206	10.9×10^6
19	0.568	0.218	11.5×10^6
20	0.566	0.228	12.0×10^6

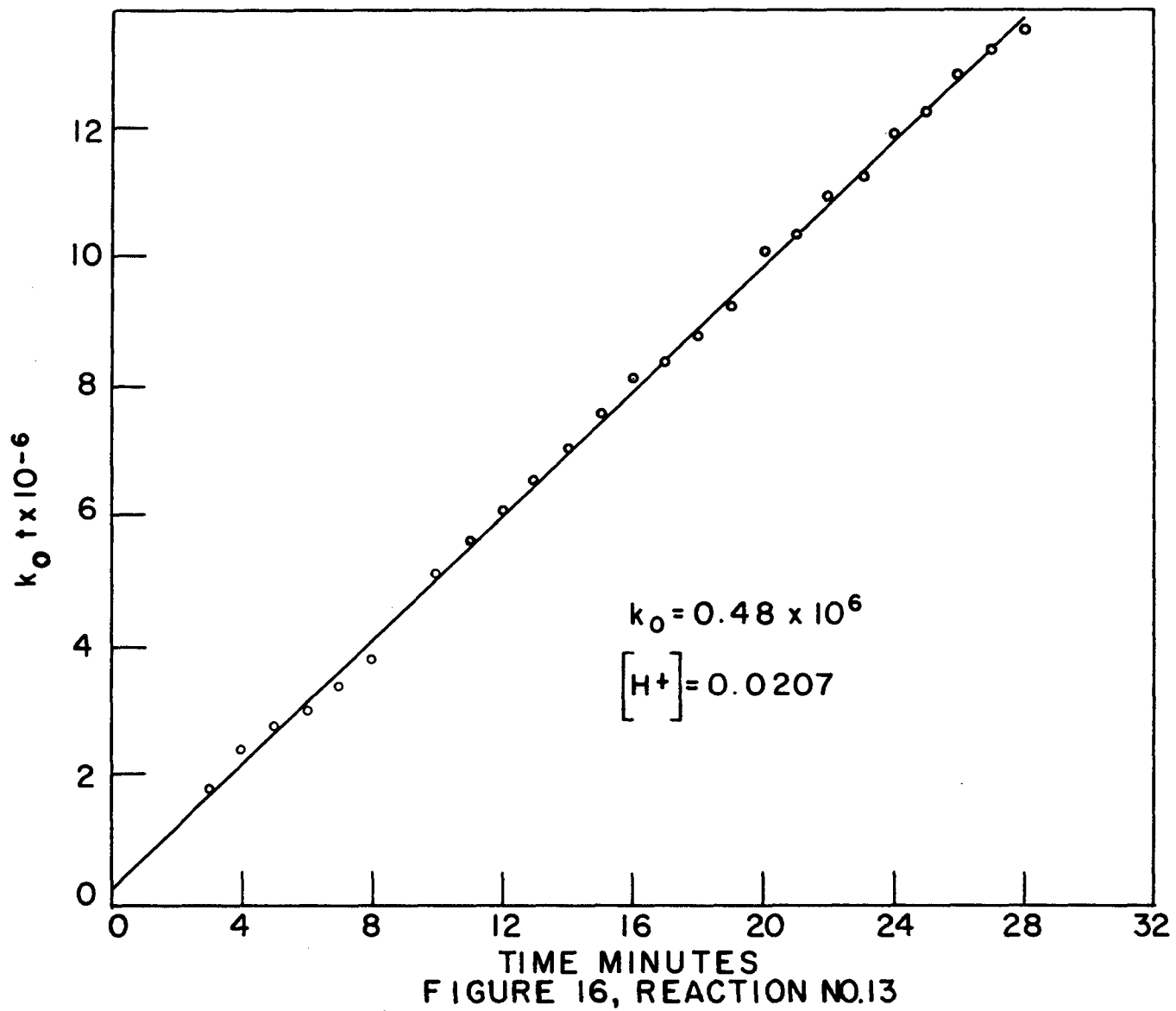


Table 16. Spectrophotometric Data and Calculation of Molarities

$$K_2 = 2.85 \times 10^6 \frac{A_0 - .105}{A_0 - .175} \times .704$$

Time (min.)	A_0	$\log \frac{A_0 - .105}{A_0 - .175} \times .704$	K_2
-------------	-------	--	-------

2	0.250	0.077	1.7 x 10 ⁶
4	0.277	0.095	2.3 x 10 ⁶
6	0.294	0.110	2.9 x 10 ⁶
8	0.300	0.116	3.3 x 10 ⁶
10	0.314	0.125	3.8 x 10 ⁶
12	0.312	0.124	3.8 x 10 ⁶
14	0.306	0.121	3.5 x 10 ⁶
15	0.304	0.120	3.5 x 10 ⁶
16	0.302	0.119	3.4 x 10 ⁶
17	0.301	0.118	3.4 x 10 ⁶
18	0.299	0.117	3.3 x 10 ⁶
19	0.298	0.116	3.2 x 10 ⁶
20	0.295	0.115	3.1 x 10 ⁶
21	0.294	0.114	3.0 x 10 ⁶
22	0.292	0.113	2.9 x 10 ⁶
23	0.290	0.112	2.8 x 10 ⁶
24	0.286	0.110	2.6 x 10 ⁶
25	0.284	0.109	2.5 x 10 ⁶
26	0.282	0.108	2.4 x 10 ⁶
27	0.281	0.107	2.4 x 10 ⁶
28	0.280	0.106	2.3 x 10 ⁶
29	0.278	0.105	2.2 x 10 ⁶
30	0.276	0.104	2.1 x 10 ⁶
31	0.275	0.103	2.1 x 10 ⁶
32	0.274	0.102	2.0 x 10 ⁶
33	0.273	0.101	2.0 x 10 ⁶
34	0.272	0.100	1.9 x 10 ⁶
35	0.271	0.099	1.9 x 10 ⁶
36	0.270	0.098	1.8 x 10 ⁶
37	0.269	0.097	1.8 x 10 ⁶
38	0.268	0.096	1.7 x 10 ⁶
39	0.267	0.095	1.7 x 10 ⁶
40	0.266	0.094	1.6 x 10 ⁶
41	0.265	0.093	1.6 x 10 ⁶
42	0.264	0.092	1.5 x 10 ⁶
43	0.263	0.091	1.5 x 10 ⁶
44	0.262	0.090	1.4 x 10 ⁶
45	0.261	0.089	1.4 x 10 ⁶
46	0.260	0.088	1.3 x 10 ⁶
47	0.259	0.087	1.3 x 10 ⁶
48	0.258	0.086	1.2 x 10 ⁶
49	0.257	0.085	1.2 x 10 ⁶
50	0.256	0.084	1.1 x 10 ⁶
51	0.255	0.083	1.1 x 10 ⁶
52	0.254	0.082	1.0 x 10 ⁶
53	0.253	0.081	1.0 x 10 ⁶
54	0.252	0.080	0.9 x 10 ⁶
55	0.251	0.079	0.9 x 10 ⁶
56	0.250	0.078	0.8 x 10 ⁶
57	0.249	0.077	0.8 x 10 ⁶
58	0.248	0.076	0.7 x 10 ⁶
59	0.247	0.075	0.7 x 10 ⁶
60	0.246	0.074	0.6 x 10 ⁶
61	0.245	0.073	0.6 x 10 ⁶
62	0.244	0.072	0.5 x 10 ⁶
63	0.243	0.071	0.5 x 10 ⁶
64	0.242	0.070	0.4 x 10 ⁶
65	0.241	0.069	0.4 x 10 ⁶
66	0.240	0.068	0.3 x 10 ⁶
67	0.239	0.067	0.3 x 10 ⁶
68	0.238	0.066	0.2 x 10 ⁶
69	0.237	0.065	0.2 x 10 ⁶
70	0.236	0.064	0.1 x 10 ⁶
71	0.235	0.063	0.1 x 10 ⁶
72	0.234	0.062	0.0 x 10 ⁶
73	0.233	0.061	0.0 x 10 ⁶
74	0.232	0.060	0.0 x 10 ⁶
75	0.231	0.059	0.0 x 10 ⁶
76	0.230	0.058	0.0 x 10 ⁶
77	0.229	0.057	0.0 x 10 ⁶
78	0.228	0.056	0.0 x 10 ⁶
79	0.227	0.055	0.0 x 10 ⁶
80	0.226	0.054	0.0 x 10 ⁶
81	0.225	0.053	0.0 x 10 ⁶
82	0.224	0.052	0.0 x 10 ⁶
83	0.223	0.051	0.0 x 10 ⁶
84	0.222	0.050	0.0 x 10 ⁶
85	0.221	0.049	0.0 x 10 ⁶
86	0.220	0.048	0.0 x 10 ⁶
87	0.219	0.047	0.0 x 10 ⁶
88	0.218	0.046	0.0 x 10 ⁶
89	0.217	0.045	0.0 x 10 ⁶
90	0.216	0.044	0.0 x 10 ⁶
91	0.215	0.043	0.0 x 10 ⁶
92	0.214	0.042	0.0 x 10 ⁶
93	0.213	0.041	0.0 x 10 ⁶
94	0.212	0.040	0.0 x 10 ⁶
95	0.211	0.039	0.0 x 10 ⁶
96	0.210	0.038	0.0 x 10 ⁶
97	0.209	0.037	0.0 x 10 ⁶
98	0.208	0.036	0.0 x 10 ⁶
99	0.207	0.035	0.0 x 10 ⁶
100	0.206	0.034	0.0 x 10 ⁶

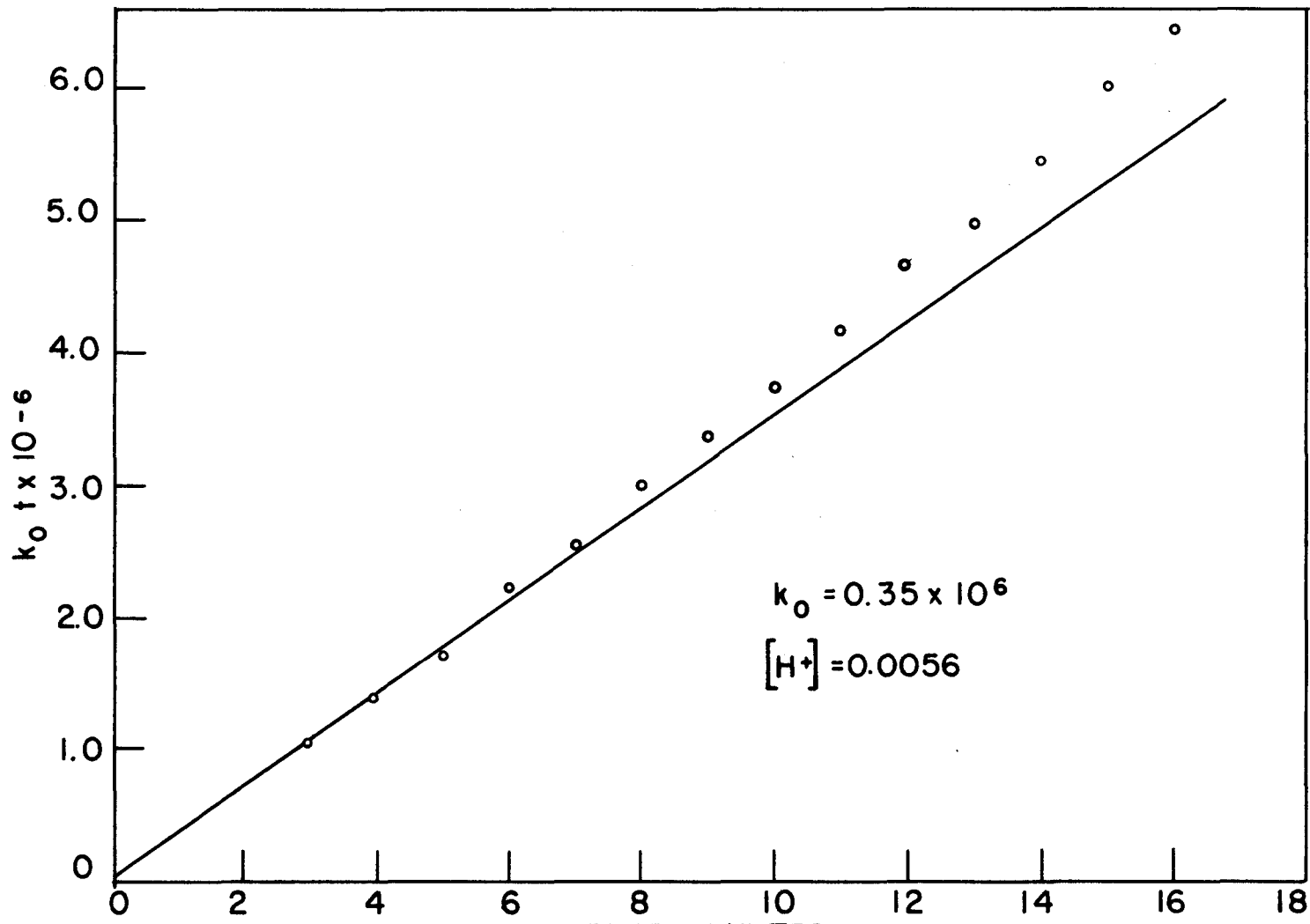


FIGURE 17, REACTION NO. 14

Table 17. Spectrophotometric Data
and Calculation of Reaction 14

$$k_0 t = 6.07 \times 10^7 \log \frac{A_0 - .104}{A_0 - .159} \times .704$$

Time (min.)	A_0	$\log \frac{A_0 - .104}{A_0 - .159} \times .704$	$k_0 t$
3	0.305	0.0172	1.1×10^6
4	0.300	0.0225	1.4×10^6
5	0.295	0.0282	1.7×10^6
6	0.288	0.0368	2.2×10^6
7	0.284	0.0421	2.6×10^6
8	0.279	0.0492	3.0×10^6
9	0.275	0.0553	3.4×10^6
10	0.271	0.0617	3.8×10^6
11	0.267	0.0685	4.2×10^6
12	0.263	0.0768	4.7×10^6
13	0.260	0.0816	5.0×10^6
14	0.256	0.0899	5.5×10^6
15	0.252	0.0987	6.0×10^6
16	0.249	0.1058	6.4×10^6
17	0.245	0.1160	7.0×10^6
18	0.242	0.1241	7.6×10^6
19	0.239	0.1328	8.1×10^6
20	0.236	0.1421	8.6×10^6

nical(II) increases noticeably. Secondly, at λ_{max} two distinct values for the molar absorptivity of mono(1,10-phenanthroline)nickel(II) are recorded, namely, 1.58×10^3 and 1.35×10^3 . This resulted from the use of two different stock solutions of 1,10-phenanthroline, both carefully prepared in the manner described on page 8. The concentration of both of these solutions was known and both gave the same value for the molar absorptivity of the 1,10-phenanthroline ion. However, the 1,10-phenanthroline solutions on standing gained a slightly yellow cast and the molar absorptivity at λ_{max} increased. It should be emphasized that none of the above discrepancies are large enough to have an appreciable effect on the calculated rate constant. The failure of some of the reaction plots to pass through the origin can be accounted for by one or more of these factors, but in all cases the slope is only slightly affected.

All reactions were performed at $25.0 \pm 0.2^\circ\text{C}$., using thermostated cell compartments. Perchlorate was the only anion present in the solutions. The nickel(II) perchlorate solution and the acid were mixed and diluted in a volumetric flask. After reaching temperature equilibrium in a thermostated water bath, the required amount of 1,10-phenanthroline solution was added and the reaction solution was diluted to volume, shaken thoroughly and a portion transferred to an absorbance cell. Unless the time of reaction was quite long, all readings were then taken on this sample. The time required for dilution, mixing and transfer was about two minutes.

An excess of nickel(II) to 1,10-phenanthroline was used in Reaction 6 and in Reactions 8 through 14. In these reactions two effects altered

the calculated rate after a period of time. These were the dissociation of the mono(1,10-phenanthroline)nickel(II) complex and the formation of the bis(1,10-phenanthroline)nickel(II) complex. At low acidities the latter reaction became more predominant and caused the slope to turn upward after a period of time. This was particularly true of Reaction 14 and is believed to have resulted in a k_0 value larger than the true value.

The ionic strength of the solution for Reaction 10 was 0.5 while for Reaction 9, at the same acidity, the ionic strength was only 0.069 molar. Reaction 11 was prepared with carbon dioxide free solutions in order to make sure that a nickel(II) carbonate complex was not affecting the rate.

(2) Rate of dissociation. A solution of 1,10-phenanthroline and excess nickel(II) ion at equilibrium has nearly all the 1,10-phenanthroline present as the mono(1,10-phenanthroline)nickel(II) complex. If this solution is aliquoted into a strong acid environment, some dissociation of this nickel(II)-1,10-phenanthroline complex occurs and some 1,10-phenanthrolium ion forms. If this dissociation reaction is followed over the first small fraction of its progress, the reverse reaction may be neglected. Using the simple reaction mechanism proposed in Equation (1) the following expressions can be used:

$$\frac{d[\text{NiPh}^{++}]}{dt} = -k_{1d}[\text{NiPh}^{++}], \quad [13]$$

$$2.3 \log \frac{[\text{NiPh}^{++}]_T}{[\text{NiPh}^{++}]_0} = -k_{1d}t \quad [14]$$

where T refers to the initial concentration and 0 to the observed concentration.

Using Equation [12], it can be shown that

$$\log \left[\frac{1}{\epsilon_{\text{HPh}} \text{Ph}_2\text{L} - A_0} \right] = \frac{k_{1d} t}{2.3} - \log [1(\epsilon_{\text{HPh}} - \epsilon_{\text{HPh}^+}) (\text{HPh}^+)_0] \quad [15]$$

Therefore, a plot of the left hand expression in Equation [15] against t gives a slope $\frac{k_{1d}}{2.3}$ and an intercept equal to $-\log [1(\epsilon_{\text{HPh}} - \epsilon_{\text{HPh}^+}) (\text{HPh}^+)_0]$.

Table 3 lists the dissociation reactions where k_0^1 is used instead of k_{1d} , since the observed rate constants calculated with Equation [15] varied with acidity. The data for Reactions 15 through 19 are found in Tables 18 through 22 and in Figures 18 through 22.

The dissociation reactions were performed under varying acidic conditions, from 0.02 to 4.5 molar hydrogen ion. These rates were also followed at two wavelengths, 277.5 and 310m μ . A 1,10-phenanthroline blank was again determined for each acidity. The apparent large increase in the molar absorptivity of the 1,10-phenanthroline in 4.5 molar hydrochloric acid is due to the formation of the diprotomated-1,10-phenanthroline ion, H_2Ph^{++} . Fig. 23 is a plot of the molar absorptivity of 1,10-phenanthroline against the acid concentration at a wavelength near the absorption maxima of the diprotomated form(10). The molar absorptivity used for Reaction 15 is actually a composite value of ϵ_{HPh} and $\epsilon_{\text{H}_2\text{Ph}^{++}}$. Since the formation of the diprotomated form is not rate determining, the kinetic calculations are not affected.

The molar absorptivity of mono(1,10-phenanthroline)nickel(II) can be calculated from the intercept of the curves in Figures 18 through 22. These calculated values are given in Table 3, and are used to estimate some of the molar absorptivities used in Table 2. The intercept is

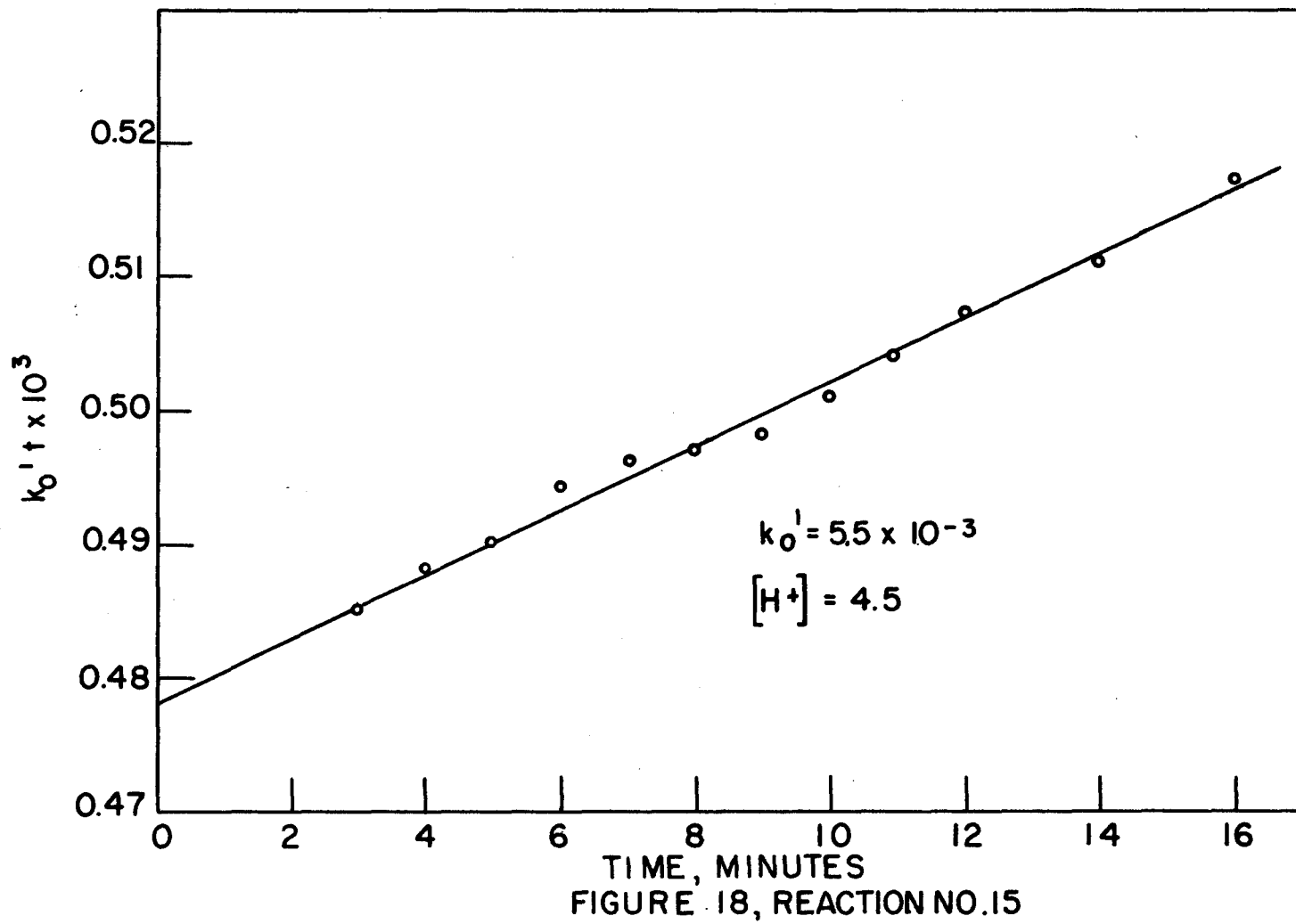


Table 18. Spectrophotometric Data
and Calculation of Reaction 15

$$\log \frac{1}{.754 - A_0} = \frac{k' t}{2.5} - \log [(3.87 \times 10^4 - \epsilon_{2170}) 2.506 \times 10^{-5}]$$

Time (min.)	A_0	$\log \frac{1}{.754 - A_0}$
3	0.427	0.485
4	0.429	0.488
5	0.431	0.490
6	0.434	0.494
7	0.435	0.496
8	0.436	0.497
9	0.437	0.498
10	0.439	0.501
11	0.441	0.504
12	0.443	0.507
14	0.446	0.511
16	0.450	0.517

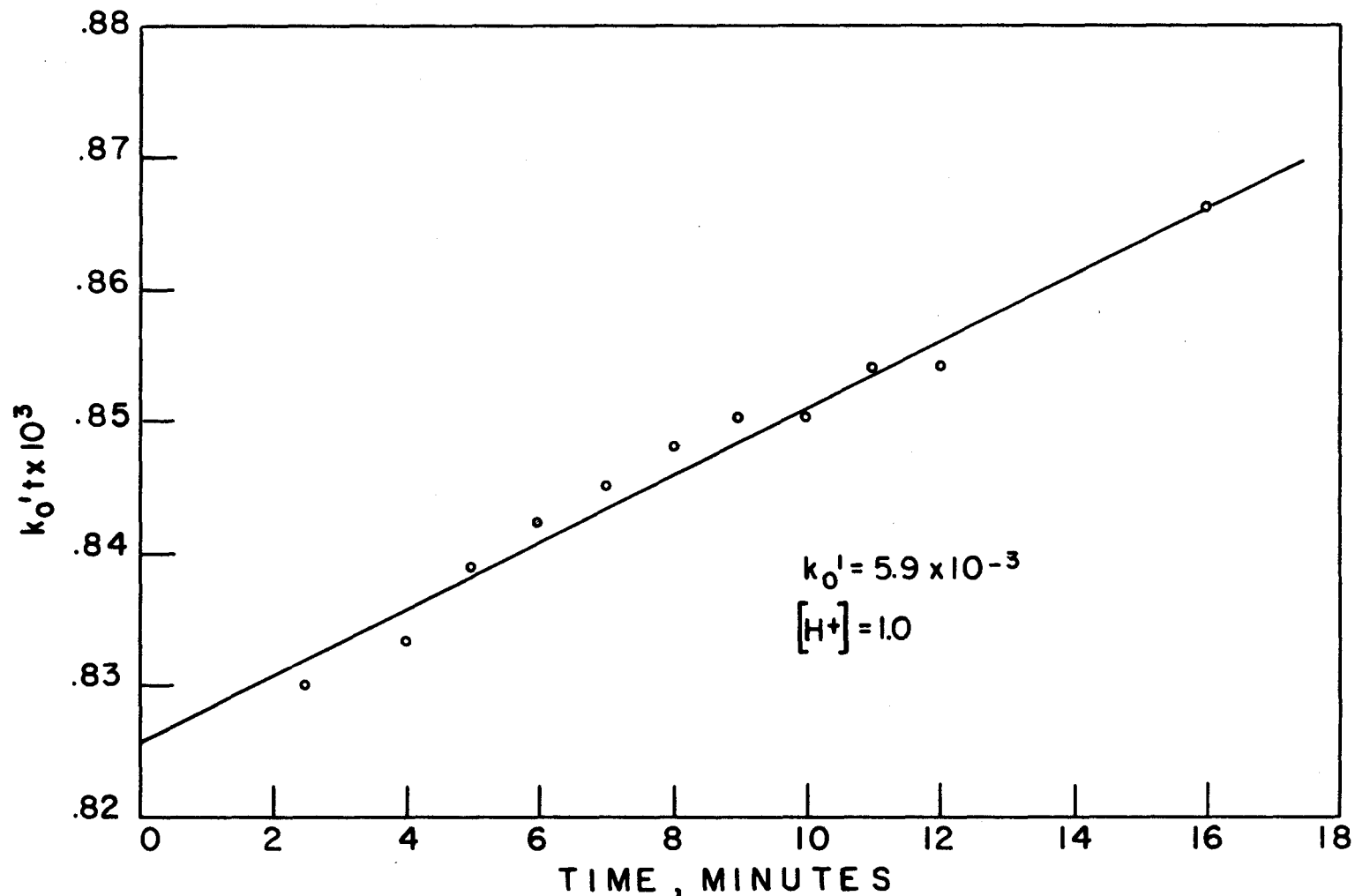


FIGURE 19, REACTION NO.16

Table 19. Spectrophotometric Data
and Calculation of Reaction 16

$$\log \frac{1}{.536 - A_0} = \frac{k'_0 t}{2.5} - \log [2.90 \times 10^4 - \epsilon_{\text{MIPh}}] 1.153 \times 10^{-5}$$

Time (min.)	A_0	$\log \frac{1}{.536 - A_0}$
2.5	0.188	0.830
4	0.189	0.833
5	0.191	0.839
6	0.192	0.842
7	0.193	0.845
8	0.194	0.848
9	0.195	0.851
10	0.195	0.851
11	0.196	0.854
12	0.196	0.854
16	0.200	0.866

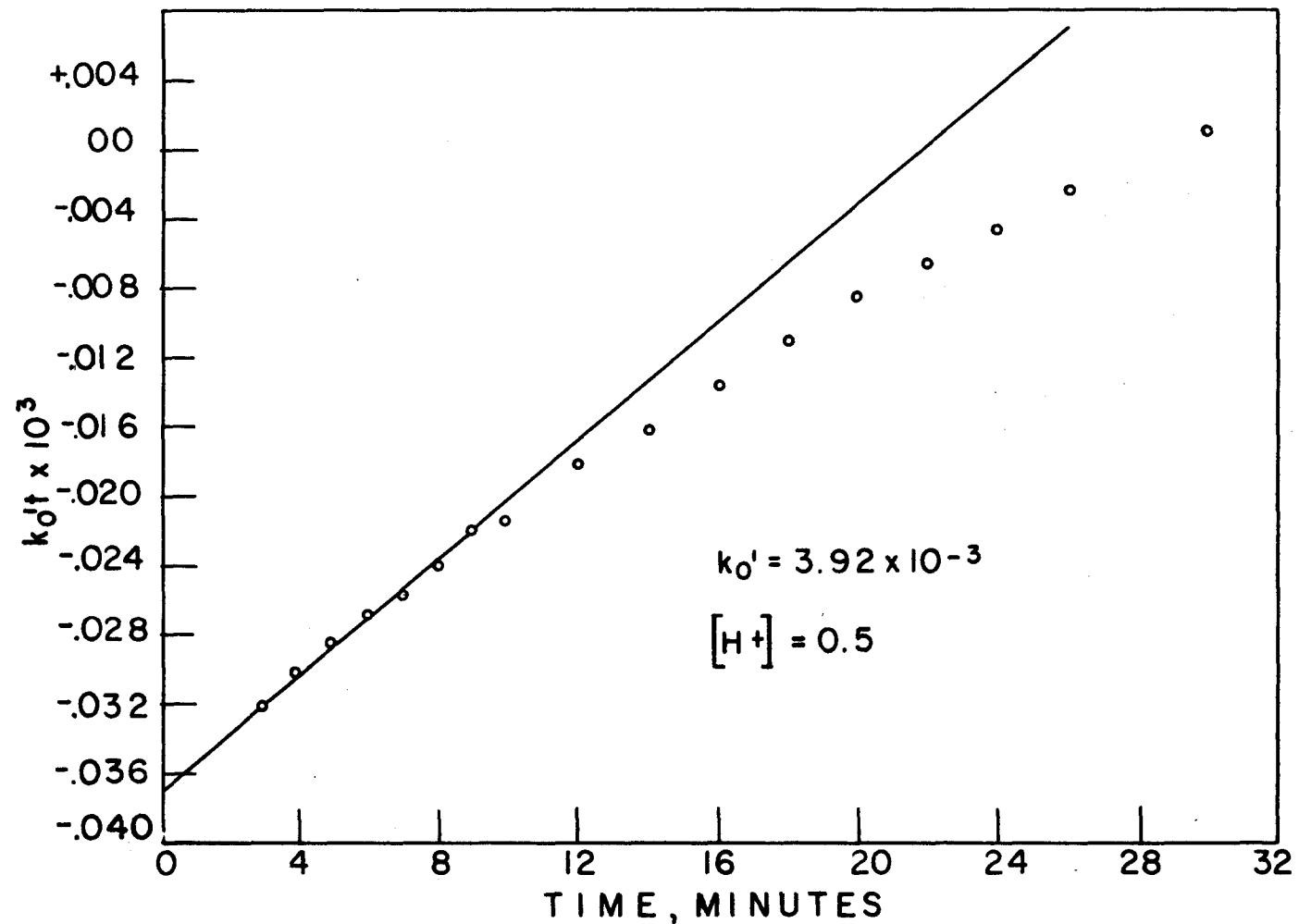


FIGURE 20, REACTION NO.17

Table 20. Spectrophotometric Data
and Calculation of Reaction 17

$$\log \frac{1}{1.482 - A_0} = \frac{k' t}{2.3} \log [5(5.14 \times 10^3 - c_{\text{NIPN}}) 5.76 \times 10^{-5}]$$

Time (min.)	A_0	$\log \frac{1}{1.482 - A_0}$
3	0.405	-0.0322
4	0.410	-0.0302
5	0.414	-0.0286
6	0.418	-0.0269
7	0.421	-0.0257
8	0.425	-0.0241
9	0.429	-0.0224
10	0.432	-0.0212
12	0.439	-0.0183
14	0.444	-0.0162
16	0.450	-0.0137
18	0.456	-0.0112
20	0.462	-0.0086
22	0.466	-0.0069
24	0.471	-0.0048
26	0.476	-0.0026
29	0.481	+0.0009

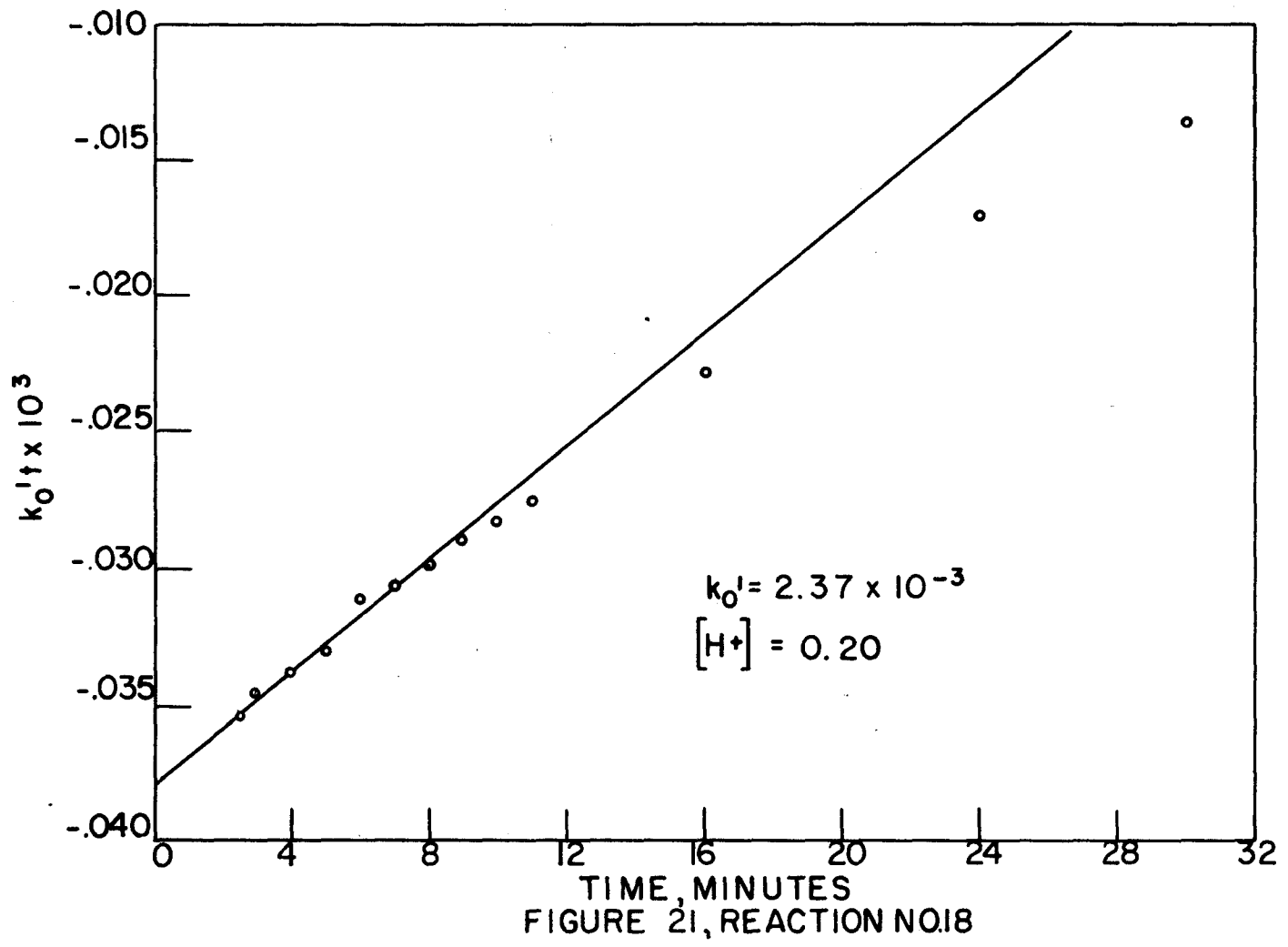


Table 21. Spectrophotometric Data and Calculation of Reaction 18

$$\log \frac{1}{1.482 - A_0} = \frac{K_0'}{2.3} \log [5(5.14 \times 10^5 - \epsilon_{\text{HFM}}) 5.76 \times 10^{-5}]$$

Time (min.)	A_0	$\log \frac{1}{1.482 - A_0}$
2.5	0.297	-0.0324
3	0.399	-0.0346
4	0.401	-0.0358
5	0.405	-0.0350
6	0.405	-0.0362
7	0.409	-0.0306
8	0.411	-0.0298
9	0.415	-0.0290
10	0.415	-0.0282
11	0.417	-0.0274
16	0.428	-0.0228
24	0.441	-0.0170
30	0.459	-0.0157

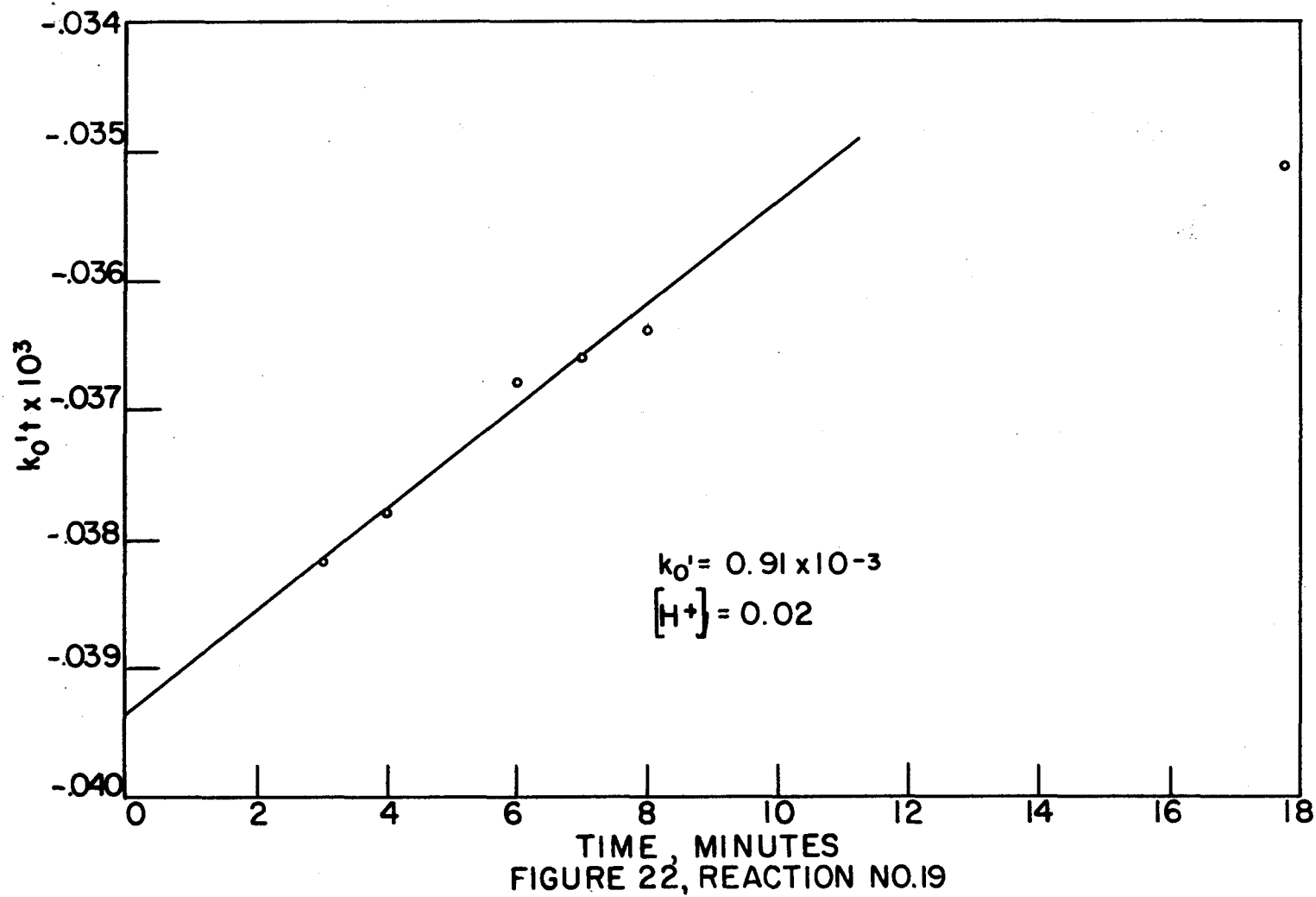


Table 22. Spectrophotometric Data
and Calculation of Reaction 19

$$\log \frac{1}{1.482 - A_0} = \frac{k' t}{2.5} \log [5(5.14 \times 10^3 - \epsilon_{Mn}) 5.76 \times 10^{-5}]$$

Time (min.)	A_0	$\log \frac{1}{1.482 - A_0}$
3	0.390	-0.0382
4	0.391	-0.0378
5	0.393	-0.0370
6	0.3935	-0.0368
7	0.394	-0.0366
8	0.3945	-0.0350
20	0.398	-0.0350

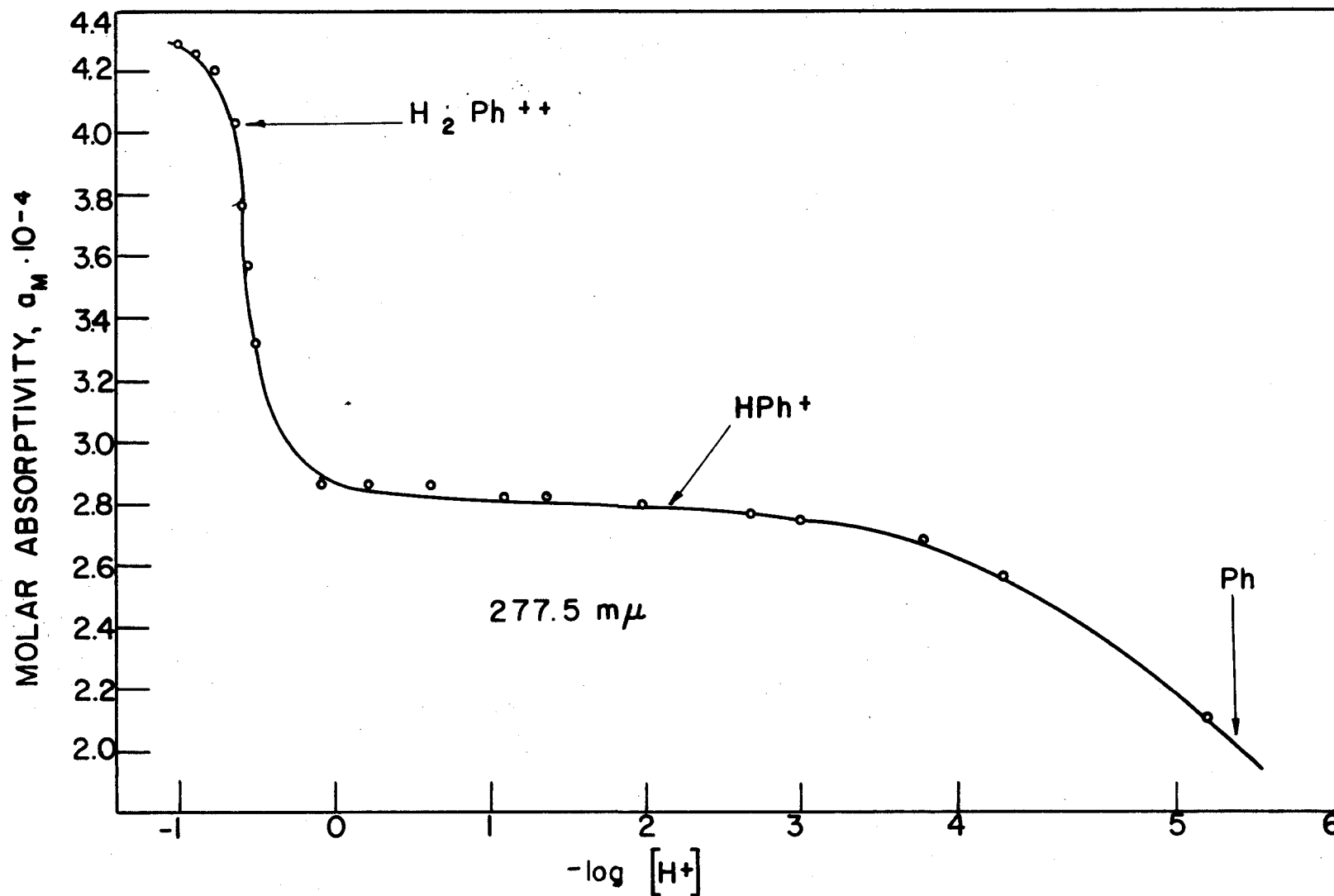


FIGURE 23, SPECTROPHOTOMETRIC EVIDENCE OF MONO- AND DI-PROTONATED PHENANTHROLINE

Table 23. Formation and Dissociation Reactions of the Mono(5-methyl-1,10-phenanthroline)nickel(II) Complex

Formation Reactions

Reaction No.	$[H^+]$	λ (m μ)	ϵ_{MPh}	ϵ_{NiPh}	cell length	Mh_T	Ni_T	k_o
20	0.5295	310	5.43×10^3	2.32×10^3	2 cm.	5.35×10^{-5}	1.526×10^{-3}	1.90×10^6
21	0.4985	310	5.38×10^3	2.32×10^3	1 cm.	5.35×10^{-5}	1.526×10^{-3}	1.91×10^6
22	0.1005	310	5.40×10^3	2.20×10^3	1 cm.	5.35×10^{-5}	1.526×10^{-4}	1.28×10^6
23	0.0415	310	5.38×10^3	2.18×10^3	2 cm.	5.35×10^{-5}	5.375×10^{-5}	7.53×10^5
24	0.02125	310	5.36×10^3	2.18×10^3	2 cm.	5.35×10^{-5}	4.59×10^{-5}	4.90×10^5

Dissociation Reaction

25	0.500	310	5.40×10^3	2.32×10^3	10 cm.	1.07×10^{-5}	3.05×10^{-4}	3.7×10^{-3}
----	-------	-----	--------------------	--------------------	--------	-----------------------	-----------------------	----------------------

obtained by extrapolation to zero time. The apparent molar absorptivity of mono(2,10-phenanthroline)nickel(II) increases with increasing acidity.

b. Mono(5-methyl-1,10-phenanthroline)nickel(II) ion

(1) Rate of formation. Table 1 gives the value of the ionization constant for the 5-methyl-1,10-phenanthroline ion which is used throughout this work. Table 25 lists the various reactions that were studied. The rate data for the formation of the mono(5-methyl-1,10-phenanthroline)nickel(II) complex are treated in the same manner as 1,10-phenanthroline in Equations [11] and [12]. The data for reactions 20 through 24 are presented in Tables 24 through 26 and in the accompanying graphs in Figures 24 through 26.

The experimental techniques were the same as those used with 1,10-phenanthroline. A wavelength of 310m μ was found suitable for following the absorbance changes. The rate of formation was studied over a wide range of acid strength, from 0.55 to 0.001 molar perchloric acid. The reactions were performed at $25.0 \pm 0.2^\circ\text{C}$.

(2) Rate of dissociation. Only one dissociation reaction rate, Reaction 25, was measured. The data are treated in the manner of Equation [15] and are presented in Table 29 and Figure 29.

c. Mono(5-nitro-1,10-phenanthroline)nickel(II) ion

(1) Rate of formation. Table 1 gives the value of the ionization constant for the 5-nitro-1,10-phenanthroline ion, which is used throughout this work. Table 30 lists the various reactions that were studied. The rate data for the formation of the mono(5-nitro-1,10-phenanthroline)nickel(II) are treated in the same manner as 1,10-phenanthroline was in

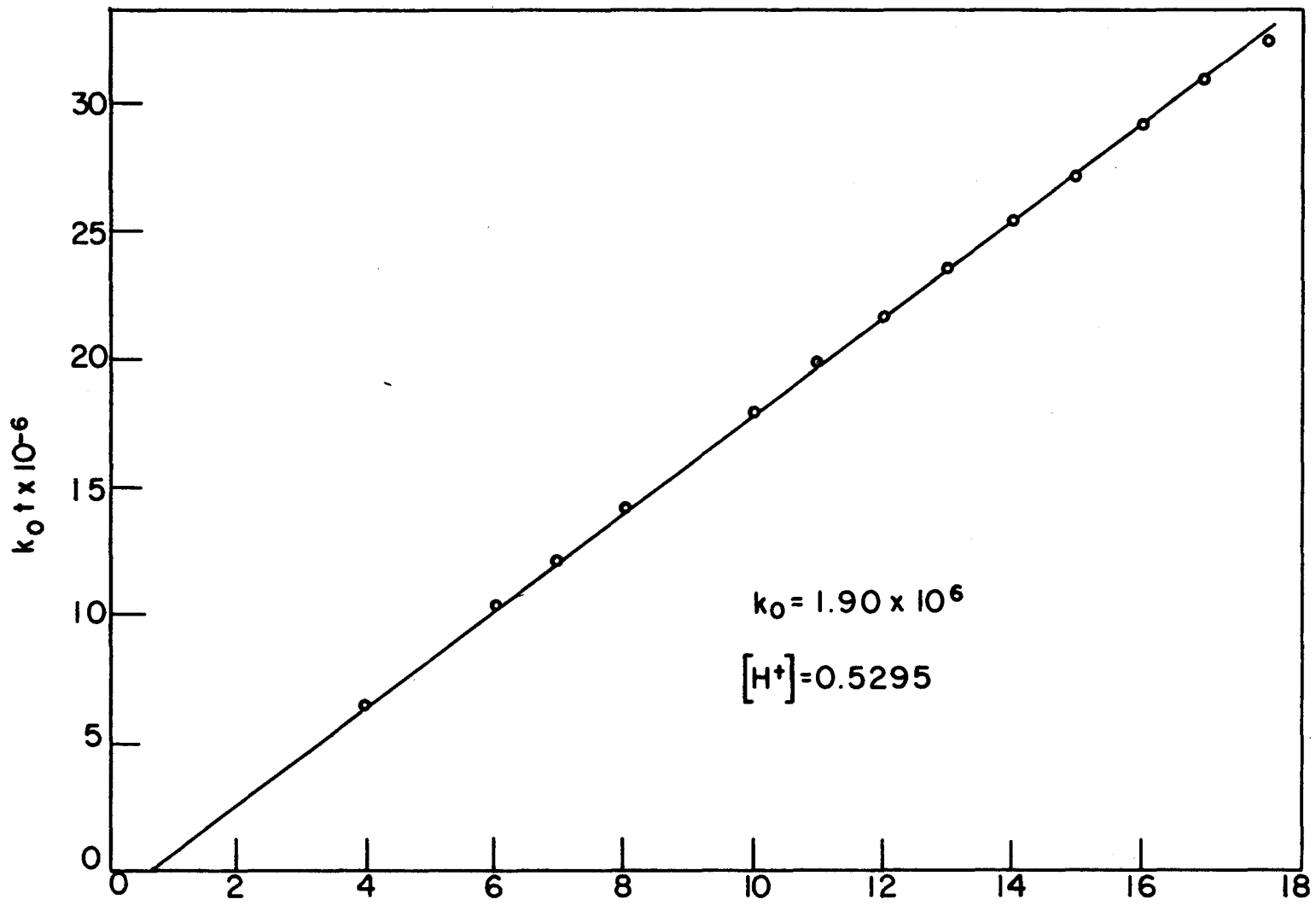


FIGURE 24, REACTION NO. 20

Table 24. Spectrophotometric Data
and Calculation of Reaction 20

$$k_0 t = 1.405 \times 10^8 \log \frac{8.911 + A_0}{(A_0 - .248) 28.5}$$

Time (min.)	A_0	$\log \frac{8.911 + A_0}{(A_0 - .248) 28.5}$	$k_0 t$
3	0.556	0.035	4.6×10^6
4	0.547	0.046	6.5×10^6
5	0.538	0.058	8.2×10^6
6	0.528	0.073	10.3×10^6
7	0.519	0.086	12.1×10^6
8	0.510	0.101	14.2×10^6
9	0.503	0.112	15.7×10^6
10	0.494	0.123	18.0×10^6
11	0.486	0.142	19.9×10^6
12	0.479	0.154	21.6×10^6
13	0.472	0.167	23.5×10^6
14	0.465	0.180	25.3×10^6
15	0.459	0.193	27.1×10^6
16	0.452	0.207	29.1×10^6
17	0.446	0.220	30.9×10^6
18	0.441	0.231	32.4×10^6

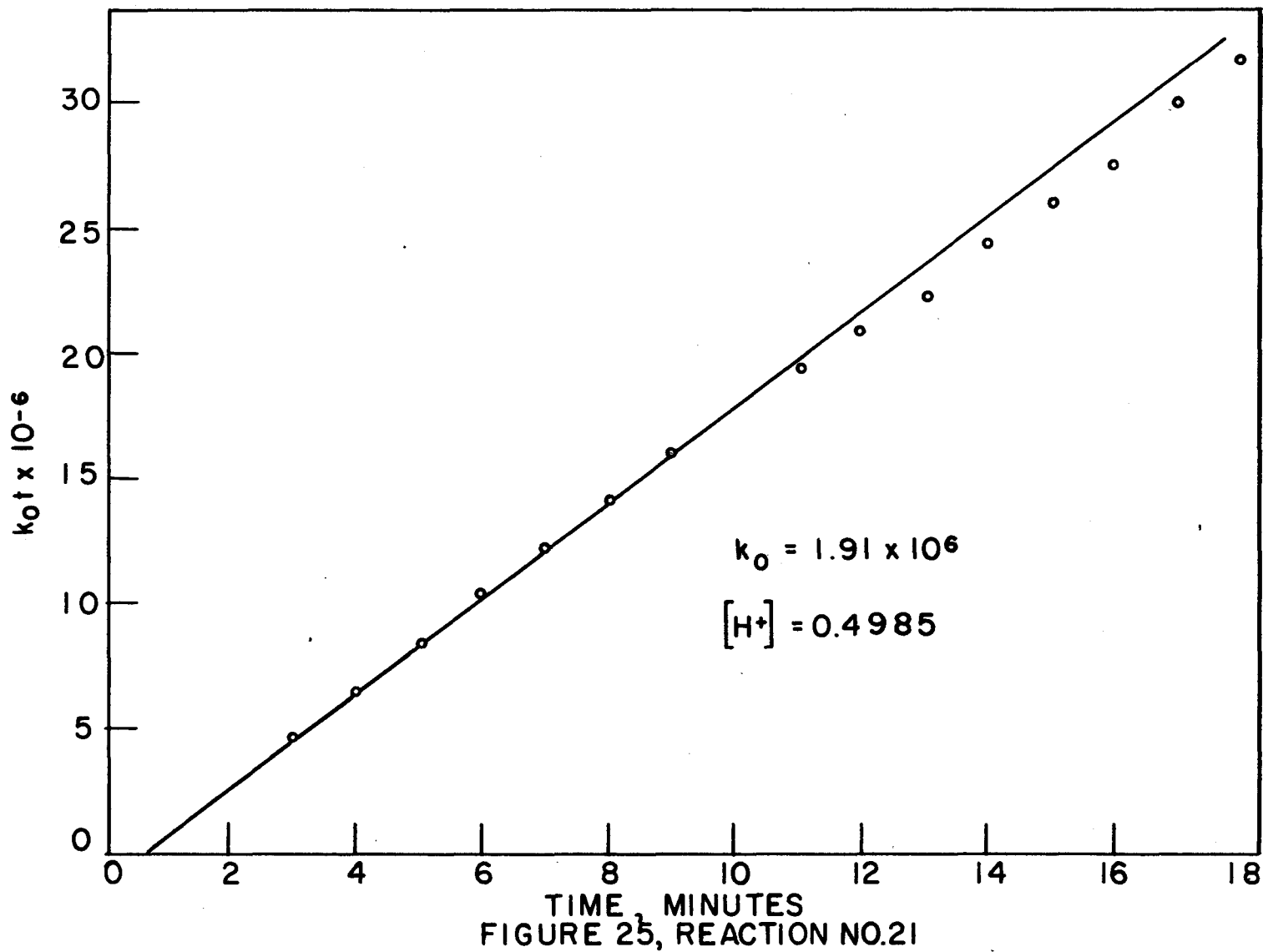


Table 25. Spectrophotometric Data
and Calculation of Reaction k_0

$$k_0^{\circ} = 1.38 \times 10^8 \log \frac{A_0 + k_0 t}{(A_0 - .12k) 28.5}$$

Time (min.)	A_0	$\log \frac{A_0 + k_0 t}{A_0 - .12k} 28.5$	k_0°
3	0.275	0.0350	4.6×10^6
4	0.270	0.0488	6.4×10^6
5	0.265	0.0637	8.4×10^6
6	0.260	0.0788	10.4×10^6
7	0.256	0.0917	12.1×10^6
8	0.251	0.1079	14.2×10^6
9	0.247	0.1202	16.0×10^6
10	0.243	0.1375	17.9×10^6
11	0.240	0.1461	19.3×10^6
12	0.237	0.1572	20.8×10^6
13	0.234	0.1698	22.3×10^6
14	0.230	0.1844	24.3×10^6
15	0.227	0.1965	25.9×10^6
16	0.224	0.2093	27.6×10^6
17	0.220	0.2266	29.9×10^6
18	0.217	0.2398	31.7×10^6
19	0.214	0.2541	33.7×10^6
20	0.211	0.2683	35.4×10^6
21	0.209	0.2783	36.7×10^6
22	0.206	0.2936	38.8×10^6
23	0.204	0.3041	40.1×10^6

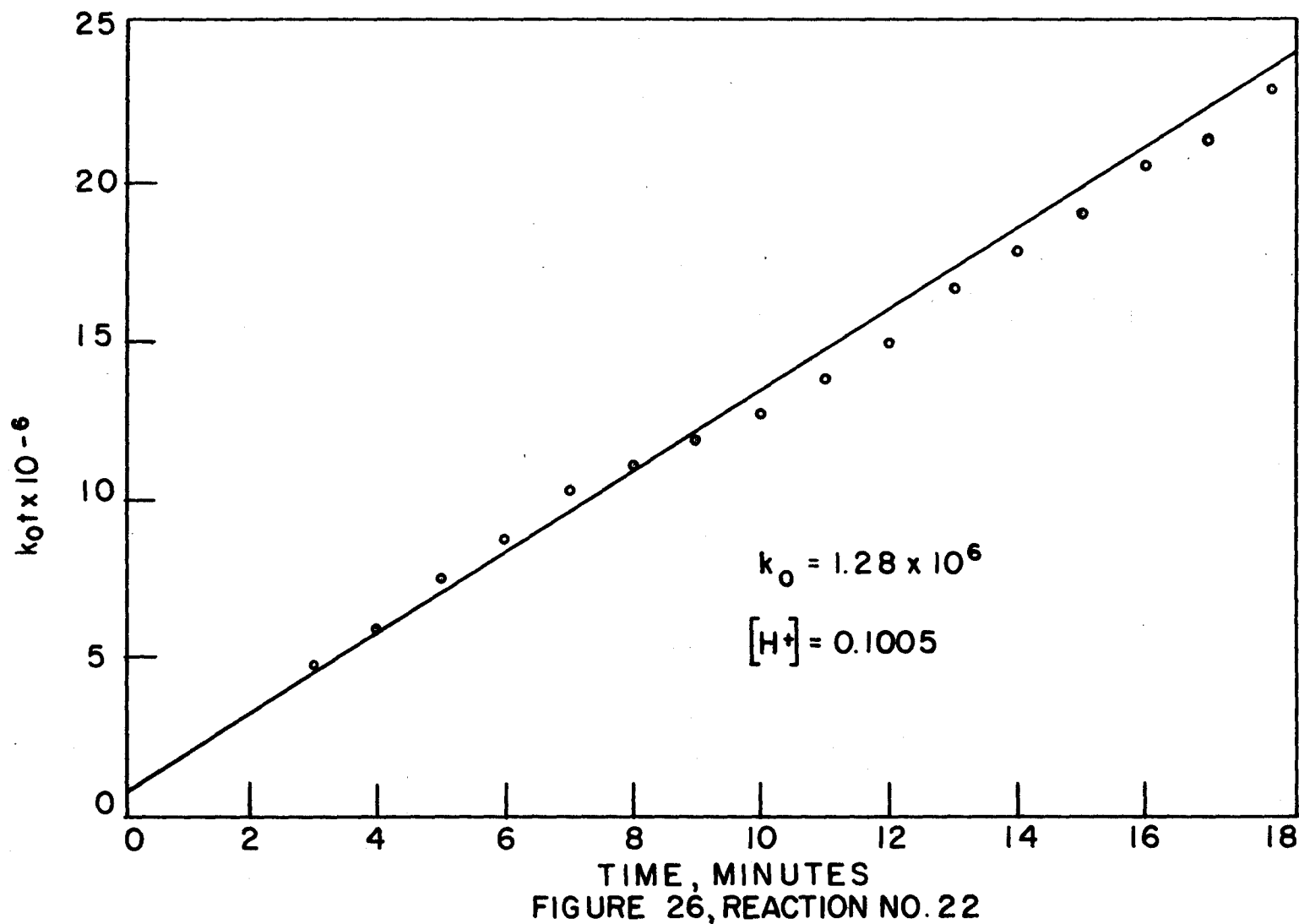


Table 26. Spectrophotometric Data
and Calculation of Reaction 22

$$k_0 t = 3.93 \times 10^8 \log \frac{A_0 + .199}{(A_0 - .118) 2.85}$$

Time (min.)	A_0	$\log \frac{A_0 + .199}{(A_0 - .118) 2.85}$	$k_0 t$
3	0.282	0.012	4.7×10^6
4	0.280	0.015	5.9×10^6
5	0.278	0.019	7.5×10^6
6	0.276	0.022	8.6×10^6
7	0.274	0.026	10.2×10^6
8	0.273	0.028	11.0×10^6
9	0.272	0.030	11.8×10^6
10	0.271	0.032	12.6×10^6
11	0.269	0.035	13.8×10^6
12	0.268	0.038	14.9×10^6
13	0.266	0.042	16.5×10^6
14	0.264	0.045	17.7×10^6
15	0.263	0.048	18.9×10^6
16	0.261	0.052	20.4×10^6
17	0.260	0.054	21.2×10^6
18	0.258	0.058	22.8×10^6
19	0.257	0.061	24.0×10^6
20	0.255	0.064	25.2×10^6

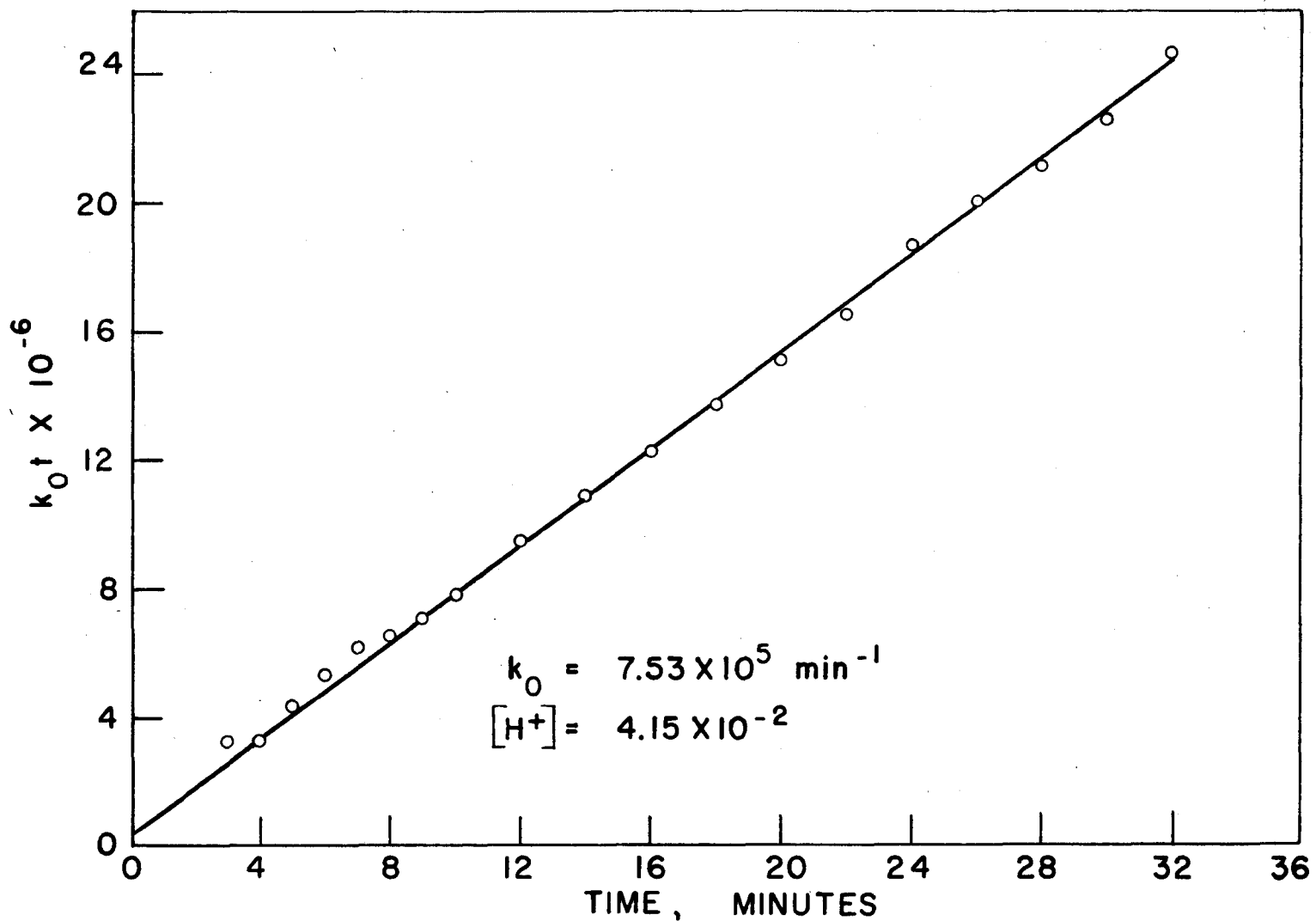


FIGURE 27, REACTION NO. 23

Table 27. Spectrophotometric Data
and Calculation of Reaction 25

$$k_0 t = 7.04 \times 10^3 \left[\frac{.640 \times 10^4}{A_0 - .255} - 1.87 \times 10^4 \right]$$

Time (min.)	A_0	$\frac{.640}{A_0 - .255}$	$k_0 t$
3	0.567	1.927	3.30×10^6
4	0.567	1.927	3.30×10^6
5	0.564	1.932	4.36×10^6
6	0.562	1.946	5.35×10^6
7	0.560	1.958	6.19×10^6
8	0.559	1.962	6.47×10^6
9	0.558	1.970	7.04×10^6
10	0.556	1.981	7.81×10^6
12	0.552	2.005	9.50×10^6
14	0.549	2.025	10.90×10^6
16	0.546	2.045	12.30×10^6
18	0.543	2.065	13.71×10^6
20	0.540	2.085	15.12×10^6
22	0.537	2.105	16.52×10^6
24	0.533	2.135	18.65×10^6
26	0.530	2.155	20.05×10^6
28	0.528	2.179	21.10×10^6
30	0.525	2.199	22.50×10^6
32	0.521	2.229	24.60×10^6

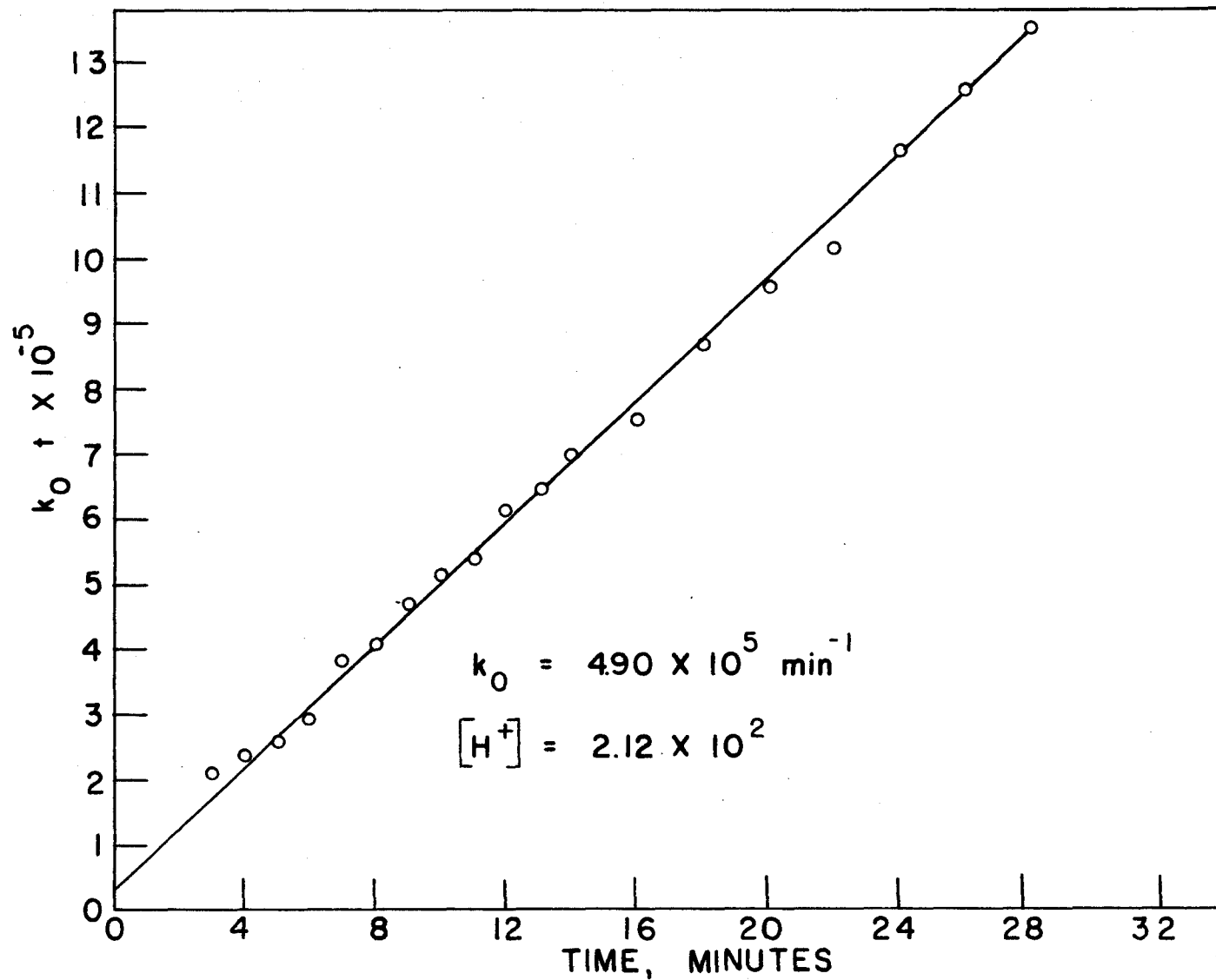


FIGURE 28, REACTION NO. 24

Table 28. Spectrophotometric Measurements
and Calculations of Reaction 24

$$k_0 t = 1.092 \times 10^8 \log \frac{A_0 - .233}{A_0 - .282} \times .878$$

Time (min.)	A_0	$\log \frac{A_0 - .233}{A_0 - .282} \times .878$	$k_0 t$
3	0.569	0.00392	2.10×10^5
4	0.568	0.00216	2.36×10^5
5	0.567	0.00039	2.59×10^5
6	0.565	0.00072	2.96×10^5
7	0.562	0.00350	3.82×10^5
8	0.561	0.00373	4.07×10^5
9	0.559	0.00450	4.70×10^5
10	0.557	0.00463	5.11×10^5
11	0.556	0.00481	5.36×10^5
12	0.555	0.00564	6.15×10^5
13	0.552	0.00589	6.45×10^5
14	0.550	0.00659	6.97×10^5
16	0.548	0.00689	7.52×10^5
18	0.544	0.00732	8.65×10^5
20	0.541	0.00872	9.51×10^5
22	0.539	0.00905	10.11×10^5
24	0.534	0.01063	11.68×10^5
26	0.531	0.01148	12.55×10^5
28	0.528	0.01224	13.50×10^5
30	0.526	0.01294	14.15×10^5
32	0.525	0.01374	15.01×10^5
34	0.519	0.01508	16.48×10^5
36	0.516	0.01605	17.52×10^5
38	0.514	0.01668	18.20×10^5
40	0.511	0.01766	19.50×10^5

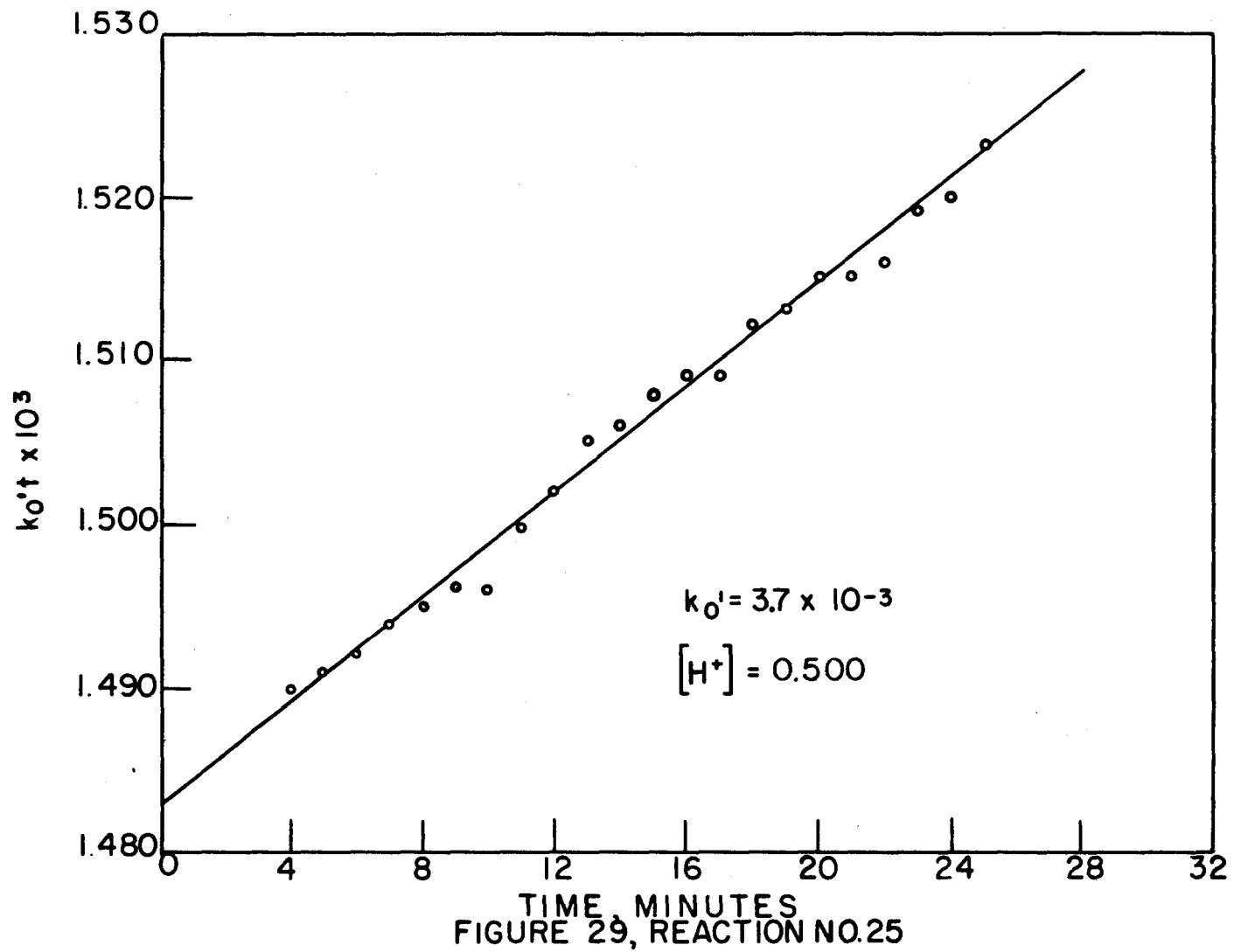


Table 29. Spectrophotometric Data
and Calculation of Reaction 25

$$\log \frac{I_0}{.587 - A_0} = \frac{k'_0 t}{2.3} - \log [(5.40 \times 10^{-3} - c_{\text{MFA}}) 1.07 \times 10^{-5}]$$

Time (min.)	A_0	$\log \frac{I_0}{.587 - A_0}$
4	0.263	1.490
5	0.264	1.491
6	0.265	1.492
7	0.266	1.494
8	0.267	1.495
9	0.268	1.496
10	0.268	1.496
11	0.271	1.500
12	0.272	1.502
13	0.274	1.505
14	0.275	1.506
15	0.276	1.508
16	0.277	1.509
17	0.277	1.509
18	0.279	1.512
19	0.280	1.513
20	0.281	1.515
21	0.281	1.515
22	0.282	1.516
23	0.284	1.519
24	0.285	1.520
25	0.287	1.523

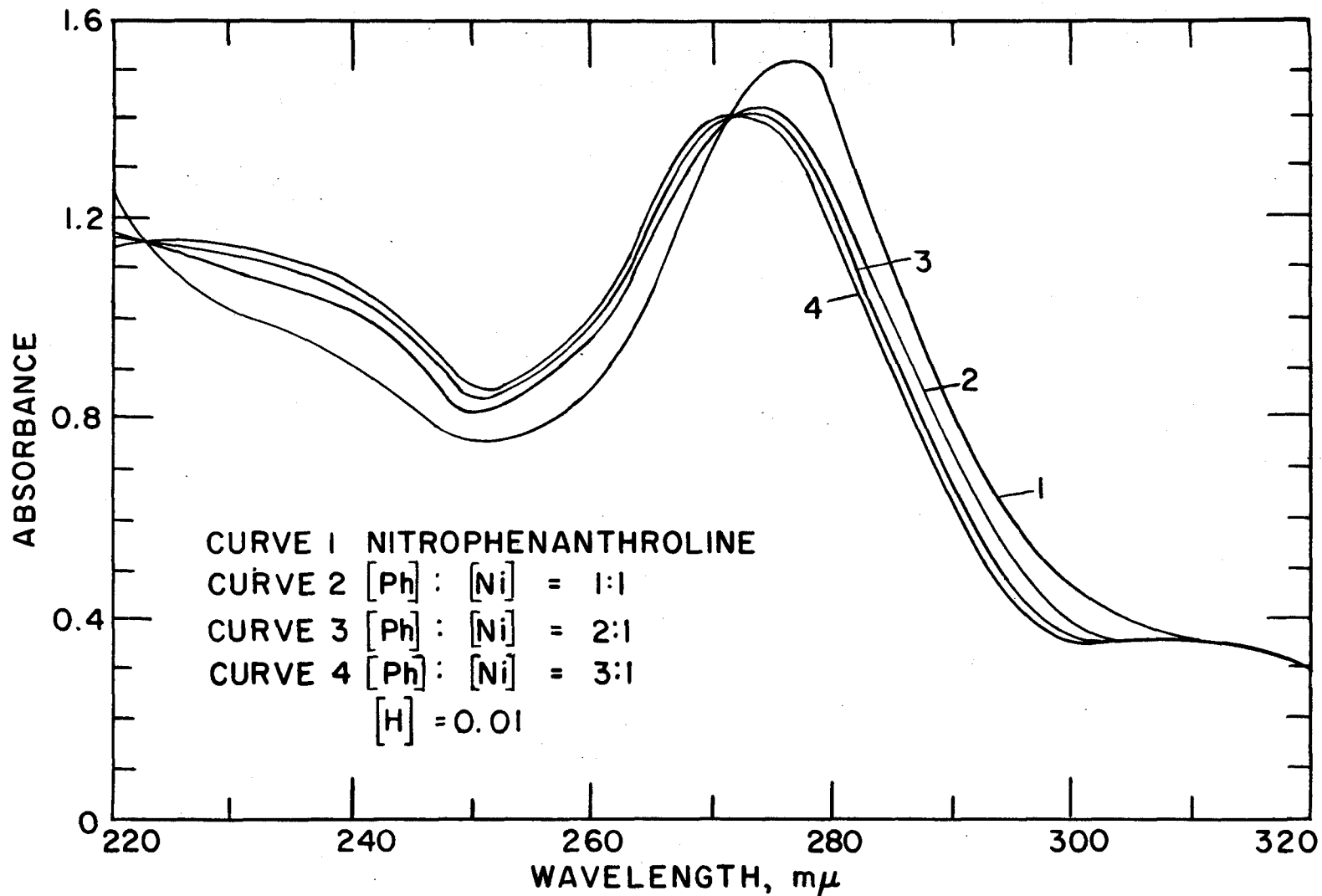


FIGURE 30, ABSORPTION SPECTRA OF NITROPHENANTHROLINE WITH VARYING NICKEL IN ACID SOLUTIONS

Table 30. Formation and Dissociation Reactions
of the Mono(3-nitro-1,10-phenanthroline)nickel(II) Complex

Assoc- tion No.	λ (μ)	Formation Reactions				k_0	
		ϵ_{Mn}	ϵ_{Mn}	cell length	k_1		
26	0.498	1.47×10^4	1.11×10^4	1 cm.	2.794×10^{-5}	1.53×10^{-4}	3.78×10^5
27	0.199	1.45×10^4	1.09×10^4	1 cm.	2.794×10^{-5}	4.59×10^{-5}	2.68×10^5
28	0.100	1.45×10^4	1.08×10^4	1 cm.	2.794×10^{-5}	4.59×10^{-5}	2.51×10^5
29	0.02023	1.52×10^4	1.08×10^4	5 cm.	5.59×10^{-6}	9.18×10^{-6}	1.19×10^5
Dissociation Reactions							
30	1.25	1.47×10^4	1.16×10^4	5 cm.	2.095×10^{-5}	1.145×10^{-4}	1.07×10^{-2}
31	0.50	1.47×10^4	1.11×10^4	5 cm.	2.095×10^{-5}	1.145×10^{-4}	7.75×10^{-3}

Equations [11] and [12]. A wavelength of 290m μ was used to follow the progress of the reaction. Figure 30 shows the spectra of 5-nitro-1,10-phenanthroline in acid solution with varying amounts of nickel(II). The data for Reactions 26 through 29 are presented in Tables 31 through 34 and in the accompanying graphs in Figures 31 through 34. The rate of formation was studied over a wide range of acid strength, from 0.50 to 0.02 molar perchloric acid. The reactions were performed at $25.0 \pm 0.2^\circ\text{C}$., using the same experimental techniques that were used with 1,10-phenanthroline.

(2) Rate of dissociation. The dissociation reactions of mono-(5-nitro-1,10-phenanthroline)nichel(II) were treated in the same manner as was mono(1,10-phenanthroline)nichel(II), using Equation [15]. Table 30 lists the reactions studied at two different acidities. These data are presented in Tables 35 and 36 and the corresponding graphs in Figures 35 and 36.

2. Discussion

Inspection of Tables 2 and 3 clearly indicates that the simple reaction kinetics proposed in Equations [1] and [4] do not completely satisfy the experimental facts. The observed rate constants, k_0 and k'_0 , vary significantly with the acidity of the solution, both increasing with increasing acid concentration. From the excellent fit of data for each individual reaction using Equation [11], it seems apparent that a second order rate reaction is actually occurring which is first order with respect to both nichel(II) and 1,10-phenanthroline. However, it is obvious that the kinetics must be more complicated and must involve

Table 31. Spectrophotometric Data
and Calculation of Reaction 26

$$k_0 t = 5.4 \times 10^7 \log \frac{A_0 + .140}{(A_0 - .310) 5.48}$$

Time (min.)	A_0	$\log \frac{A_0 + .140}{(A_0 - .310) 5.48}$	$k_0 t$
3	0.401	0.035	1.19×10^6
4	0.398	0.047	1.60×10^6
5	0.396	0.055	1.88×10^6
6	0.393	0.068	2.32×10^6
7	0.390	0.082	2.80×10^6
8	0.388	0.091	3.10×10^6
9	0.387	0.096	3.27×10^6
10	0.384	0.110	3.75×10^6
11	0.382	0.121	4.12×10^6
12	0.380	0.132	4.50×10^6
13	0.379	0.136	4.63×10^6
14	0.377	0.148	5.05×10^6
15	0.375	0.159	5.42×10^6
16	0.374	0.166	5.66×10^6
17	0.373	0.171	5.85×10^6
18	0.371	0.184	6.27×10^6
19	0.369	0.196	6.59×10^6
20	0.368	0.203	6.92×10^6

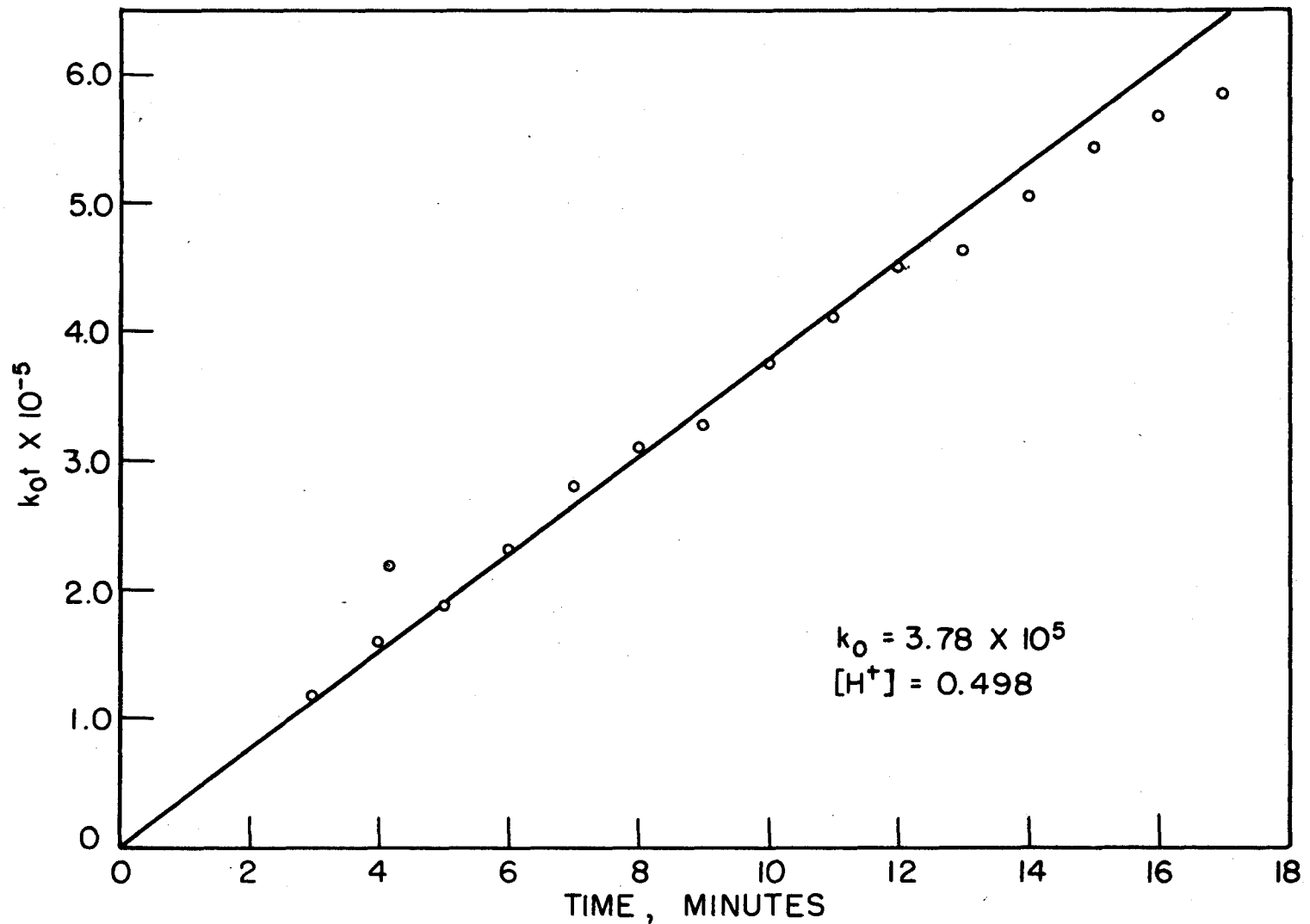


FIGURE 31, REACTION NO. 26

Table 32. Spectrophotometric Data
and Calculation of Reaction 27

$$k_0 t = 9.53 \times 10^7 \log \frac{A_0 - .240}{1.642 (A_0 - .304)}$$

Time (min.)	A_0	$\log \frac{A_0 - .240}{1.642 (A_0 - .304)}$	$k_0 t$
3	0.400	0.007	6.7×10^5
4	0.398	0.011	10.5×10^5
5	0.397	0.013	12.4×10^5
6	0.395	0.017	16.2×10^5
7	0.393	0.021	20.0×10^5
8	0.392	0.023	21.9×10^5
9	0.391	0.025	24.8×10^5
10	0.389	0.030	28.6×10^5
11	0.388	0.032	30.5×10^5
12	0.388	0.032	30.5×10^5
13	0.387	0.034	32.4×10^5
14	0.386	0.036	34.3×10^5
16	0.384	0.041	39.0×10^5
18	0.382	0.046	44.8×10^5
20	0.379	0.054	51.5×10^5
22	0.377	0.060	57.1×10^5
24	0.376	0.062	59.0×10^5
26	0.373	0.071	67.6×10^5
28	0.372	0.074	70.5×10^5
30	0.370	0.081	77.1×10^5

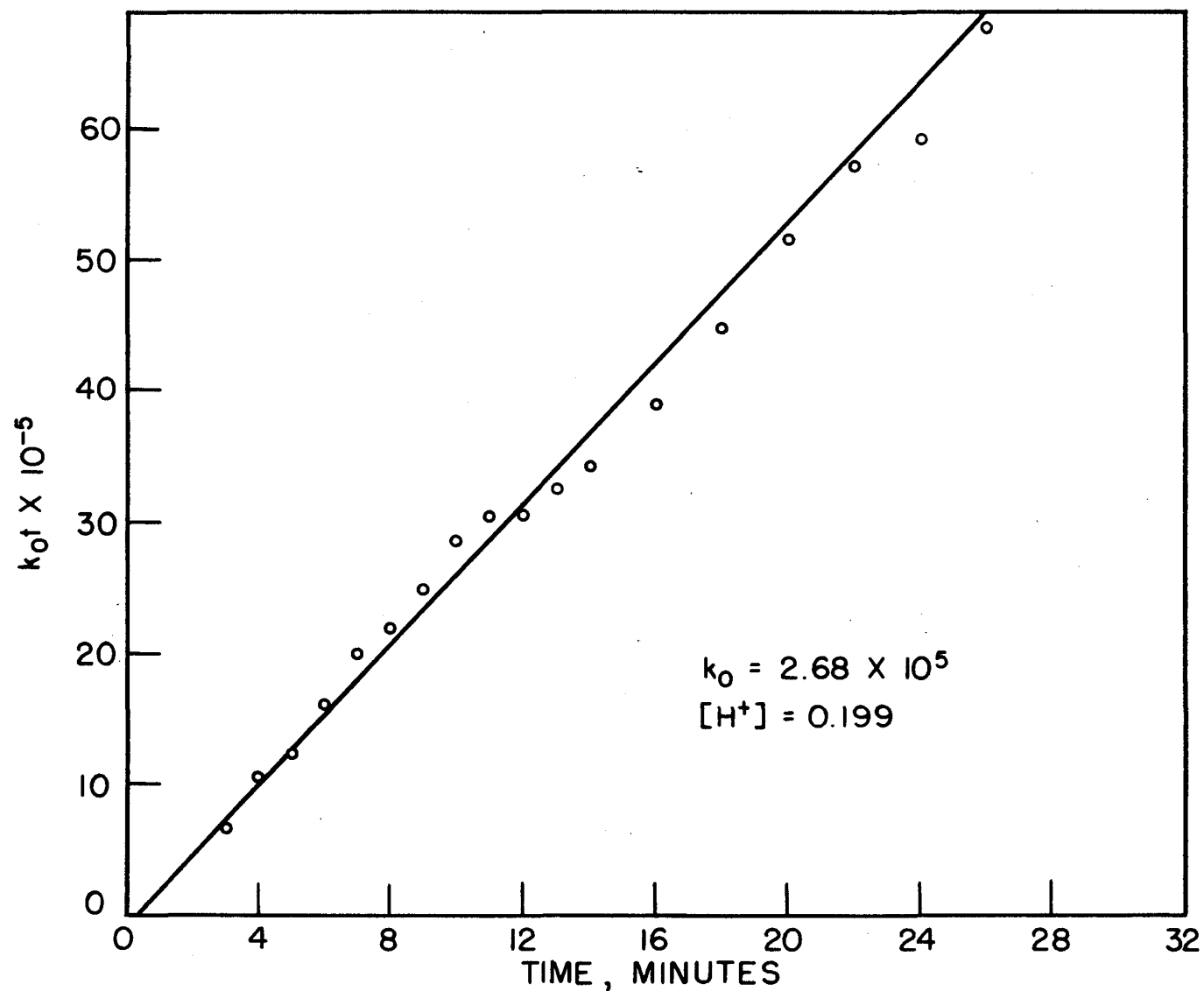


FIGURE 32, REACTION NO. 27

Table 33. Spectrophotometric Data
and Calculation of Reaction 28

$$k_0 t = 4.74 \times 10^7 \log \frac{A_0 - .235}{1.642 (A_0 - .302)}$$

Time (min.)	A_0	$\log \frac{A_0 - .235}{1.642 (A_0 - .302)}$	$k_0 t$
3	0.394	0.082	1.04×10^6
4	0.392	0.086	1.23×10^6
5	0.390	0.090	1.42×10^6
6	0.387	0.097	1.75×10^6
7	0.386	0.099	1.85×10^6
8	0.384	0.093	2.04×10^6
9	0.382	0.098	2.27×10^6
10	0.380	0.093	2.51×10^6
11	0.377	0.062	2.94×10^6
12	0.376	0.064	3.04×10^6
13	0.374	0.070	3.32×10^6
14	0.372	0.076	3.60×10^6
15	0.371	0.079	3.74×10^6
16	0.370	0.082	3.88×10^6
17	0.369	0.085	4.03×10^6
18	0.367	0.092	4.36×10^6
19	0.366	0.095	4.50×10^6
20	0.364	0.102	4.84×10^6
21	0.363	0.106	5.03×10^6
22	0.362	0.110	5.21×10^6
23	0.361	0.114	5.40×10^6
24	0.360	0.118	5.60×10^6
25	0.358	0.126	5.97×10^6
26	0.357	0.150	6.16×10^6
27	0.357	0.150	6.16×10^6
28	0.356	0.154	6.35×10^6
29	0.356	0.154	6.35×10^6
30	0.354	0.144	6.85×10^6
32	0.352	0.153	7.25×10^6
34	0.351	0.159	7.54×10^6

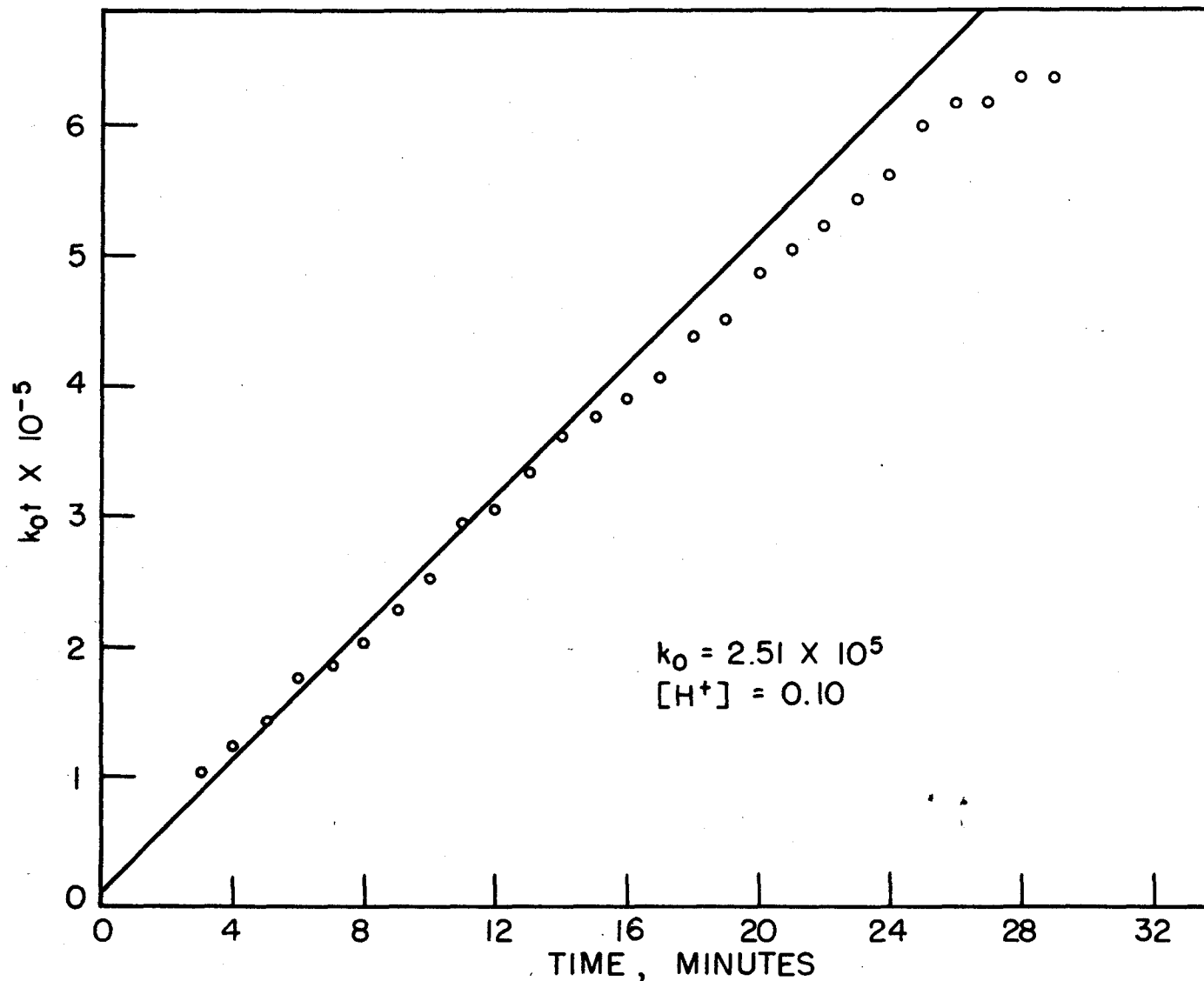


FIGURE 33, REACTION NO. 28

Table 54. Spectrophotometric Data
and Calculation of Reaction 29

$$k_0 t = 4.81 \times 10^7 \log \frac{A_0 - .222}{(A_0 - .301) 1.642}$$

Time (min.)	A_0	$\log \frac{A_0 - .222}{(A_0 - .301) 1.642}$	$k_0 t$
3	0.419	0.0072	3.5×10^3
4	0.417	0.0102	4.9×10^3
5	0.415	0.0133	6.4×10^3
6	0.413	0.0164	7.9×10^3
7	0.412	0.0181	8.7×10^3
8	0.411	0.0197	9.5×10^3
9	0.410	0.0214	10.3×10^3
10	0.408	0.0248	12.0×10^3
11	0.406	0.0283	13.1×10^3
12	0.405	0.0301	14.3×10^3
13	0.404	0.0319	15.4×10^3
14	0.403	0.0337	16.2×10^3
15	0.402	0.0356	17.1×10^3
16	0.401	0.0375	18.0×10^3
17	0.400	0.0394	19.0×10^3
18	0.399	0.0414	19.4×10^3
19	0.398	0.0434	20.9×10^3
20	0.397	0.0454	21.9×10^3
21	0.396	0.0470	22.6×10^3
22	0.395	0.0496	23.9×10^3
23	0.395	0.0496	23.9×10^3
24	0.394	0.0517	24.9×10^3
25	0.393	0.0548	26.4×10^3
26	0.393	0.0548	26.4×10^3
27	0.392	0.0560	27.0×10^3
28	0.391	0.0583	28.1×10^3
29	0.390	0.0606	29.2×10^3
30	0.390	0.0606	29.2×10^3

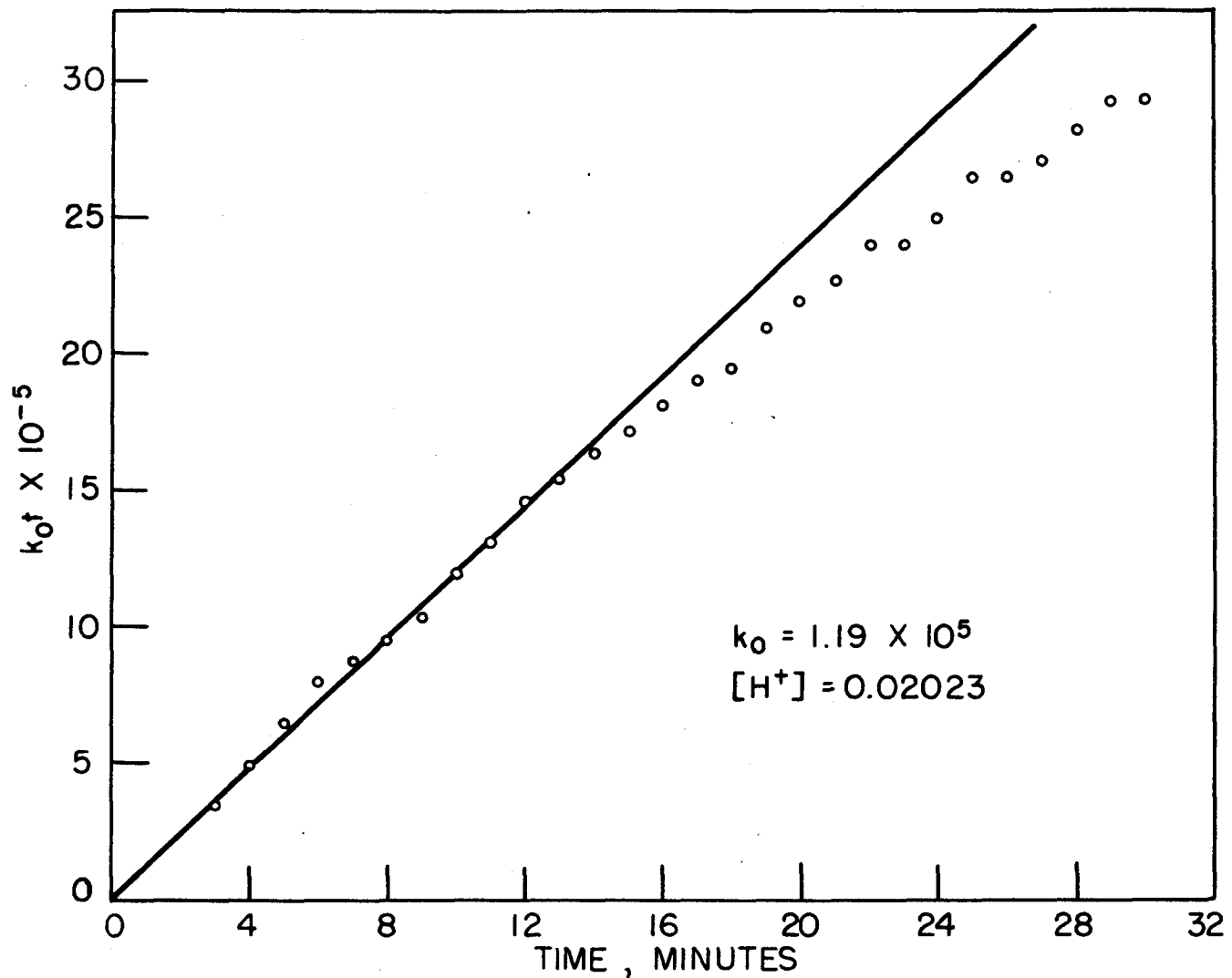


FIGURE 34, REACTION NO.29

Table 25. Spectrophotometric Data and Calculation of Reaction 30

$$\log \frac{1}{1.940 - A_0} = \frac{K_0 t}{2.3} - \log [5 (1.47 \times 10^4 - \epsilon_{\text{HMP}}) 2.075 \times 10^{-5}]$$

Time (min.)	A_0	$\log \frac{1}{1.940 - A_0}$
3	1.880	0.495
4	1.834	0.514
5	1.836	0.517
6	1.836	0.517
7	1.845	0.520
8	1.847	0.523
9	1.850	0.526
10	1.853	0.528
11	1.856	0.527
13	1.861	0.526
15	1.866	0.528
17	1.873	0.526
19	1.878	0.528
21	1.880	0.527
23	1.885	0.526
25	1.893	0.607
30	1.307	0.633
36	1.313	0.644
40	1.318	0.652

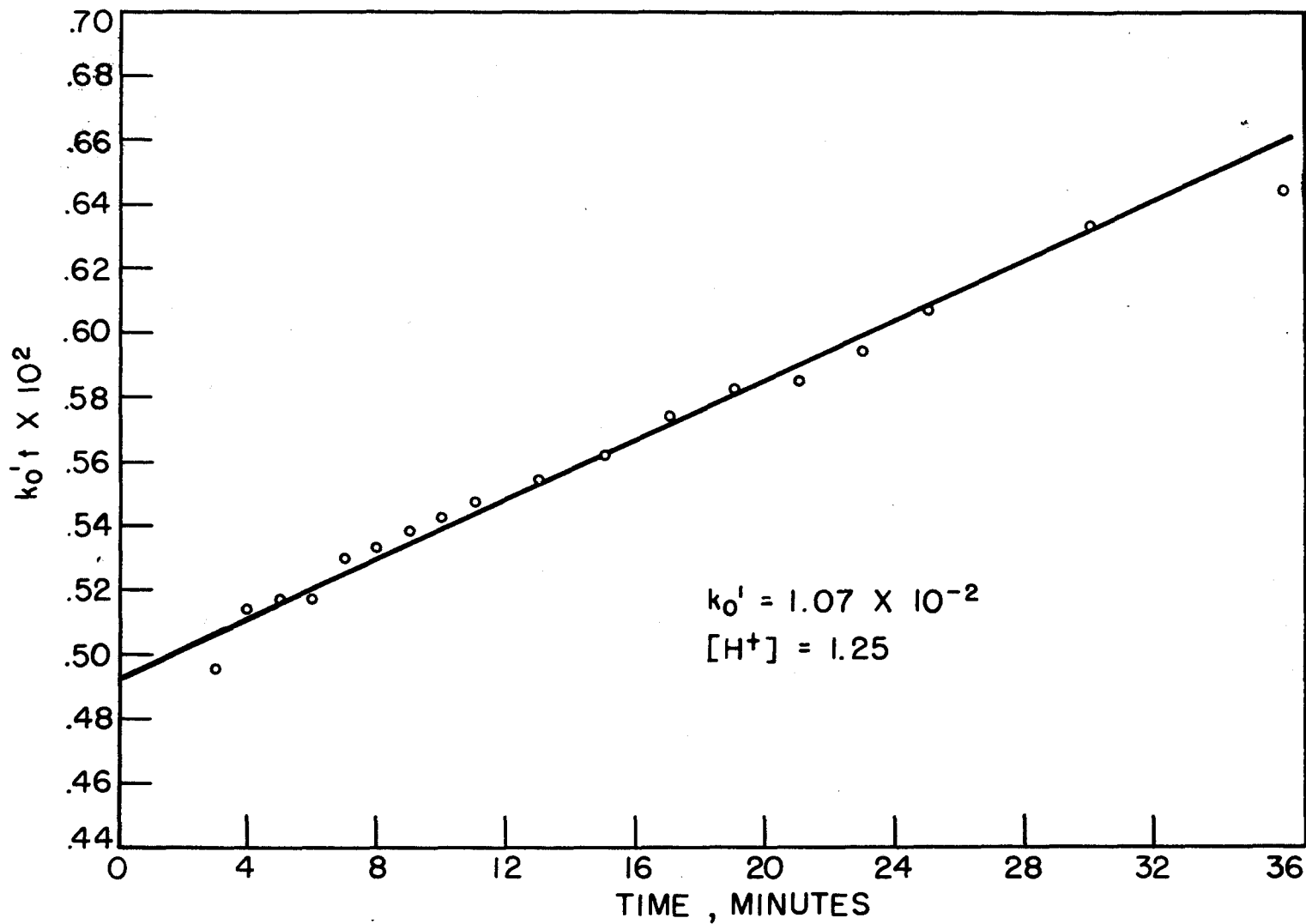


FIGURE 35, REACTION NO. 30

Table 36. Spectrophotometric Data
and Calculation of Reaction 31

$$\log \frac{1}{1.54 - A_0} = \frac{k_0 t}{2.3} - \log [5(1.47 \times 10^4 - c_{\text{MFA}}) 2.095 \times 10^{-5}]$$

Time (min.)	A_0	$\log \frac{1}{1.54 - A_0}$
3	1.170	0.432
4	1.172	0.434
5	1.180	0.444
6	1.181	0.445
7	1.187	0.452
8	1.189	0.454
9	1.190	0.456
10	1.195	0.460
11	1.195	0.460
12	1.195	0.460
13	1.200	0.468
14	1.205	0.472
16	1.201	0.470
18	1.212	0.484
20	1.219	0.494
22	1.216	0.490
24	1.222	0.496
26	1.229	0.507
28	1.225	0.502
30	1.235	0.512
32	1.250	0.509
34	1.241	0.504
36	1.255	0.512

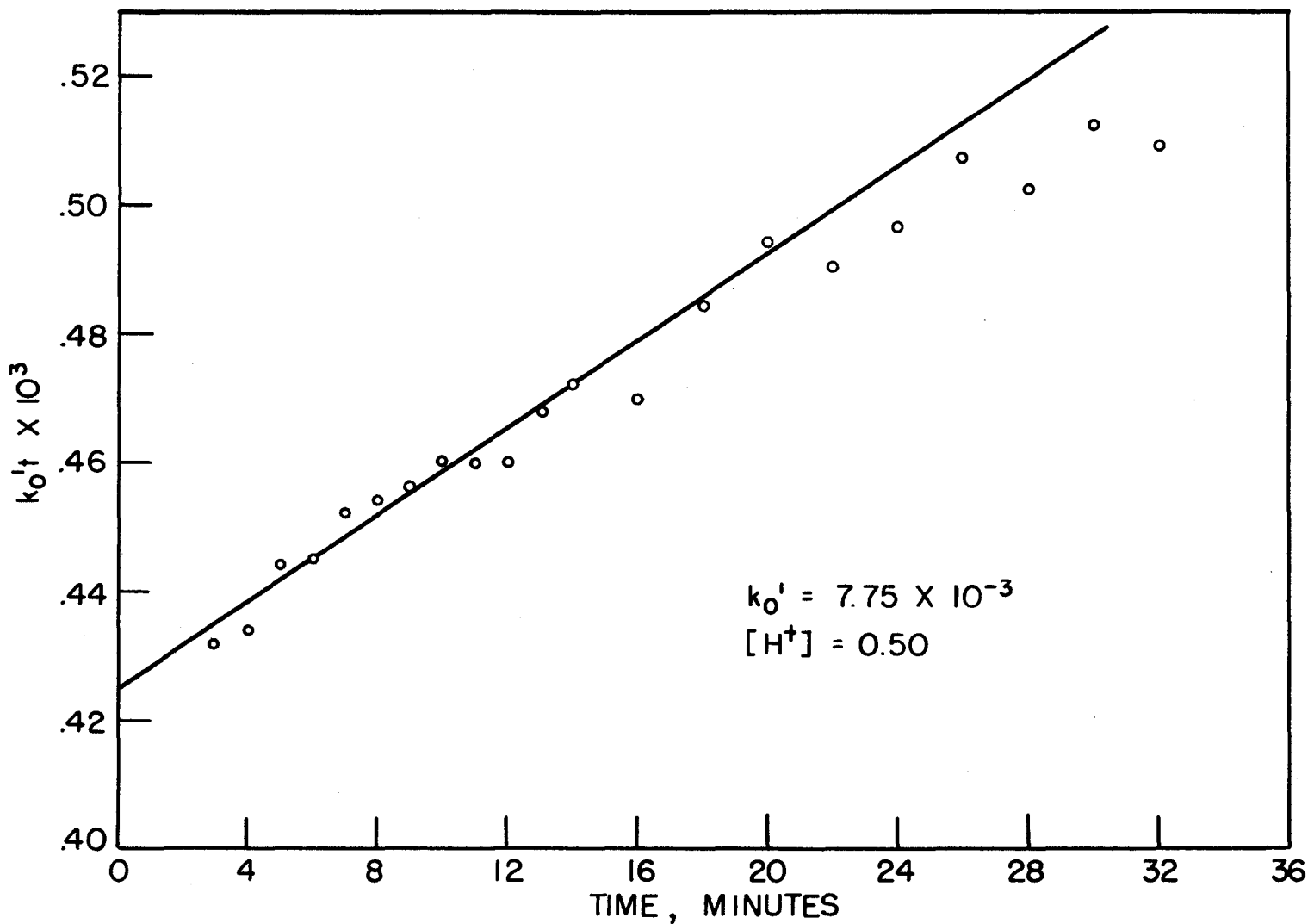


FIGURE 36, REACTION NO. 31

hydrogen ion concentration. It is convenient to examine these data in terms of k_0 and k'_0 , the observed second order rate constants, which actually are variable with acidity. The following discussion refers to the rate constants for the *trans*(1,10-phenanthroline)nickel(II) reaction; the 2-methyl-1,10-phenanthroline and 5-nitro-1,10-phenanthroline systems are considered later.

In Figure 37, where the $\log k_0$ is plotted against pH, it can be seen from the s-shaped curve that the hydrogen ion concentration cannot enter into the kinetic expression as a given constant power. In fact, at either extreme of high and low acid concentration, the observed rate constant is not greatly affected.

The change of k_0 with acidity cannot be due to hydrolysis of nickel(II) at these acidities. The hydrolysis of nickel(II) ion has been studied by Gayer and Warkner (16) and is not appreciable in solutions below pH 8.

In Figure 38, k_0 is plotted against the hydrogen ion concentration. If a reaction were occurring directly between the less active 1,10-phenanthroline ion and nickel(II), in addition to the reaction between free 1,10-phenanthroline and nickel(II), then the points in Figure 38 would fall on a straight line. Such a mechanism has been suggested by Evans (17) with the iron(II) and 2,8'-biimidazole reaction but only holds over a limited range of acid strength. For the nickel(II)-1,10-phenanthroline system the reactions would be those of Equations (1), and (4) and the following:



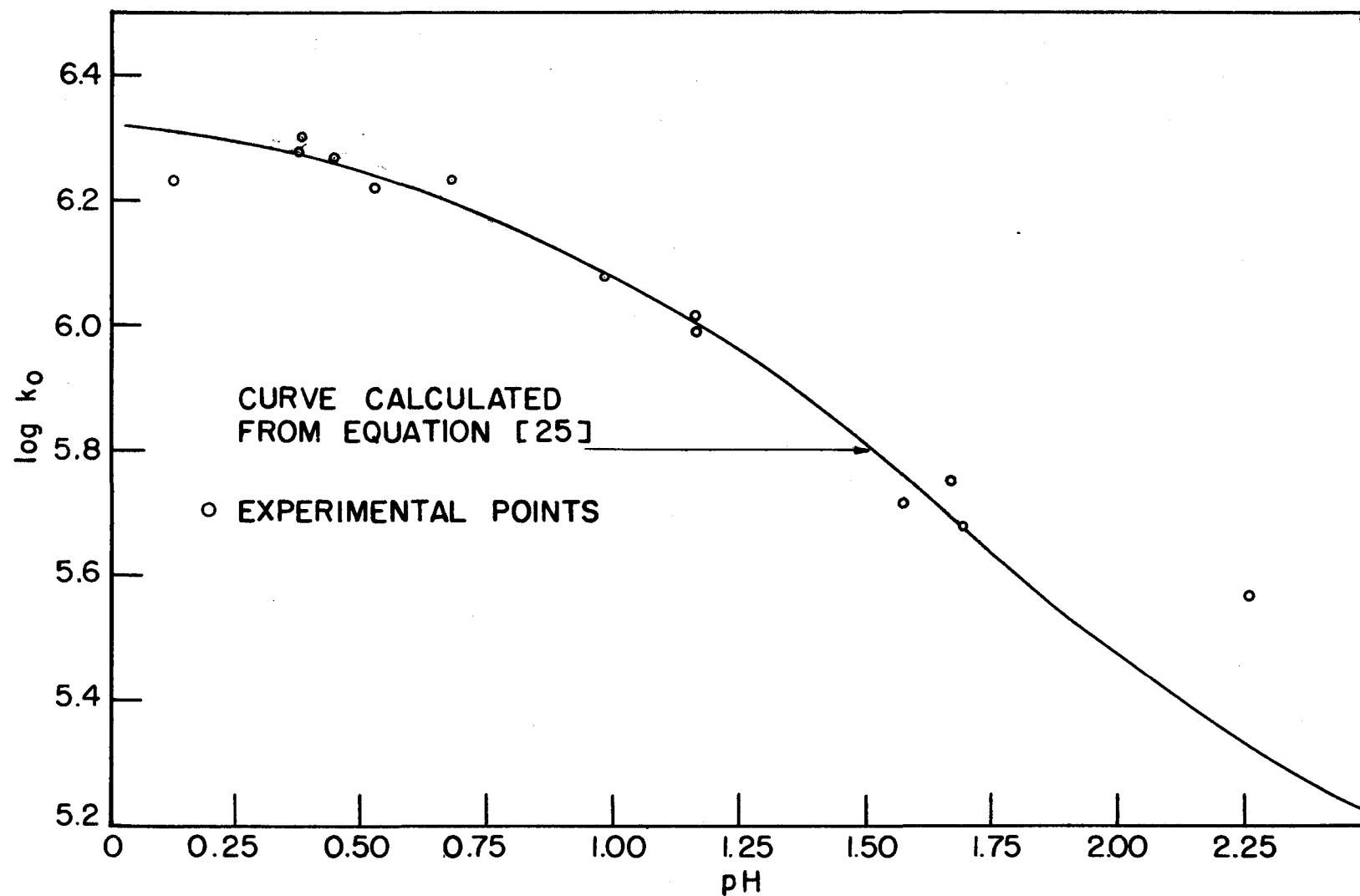


FIGURE 37, EFFECT OF pH ON MONO(PHENANTHROLINE) NICKEL RATE CONSTANT

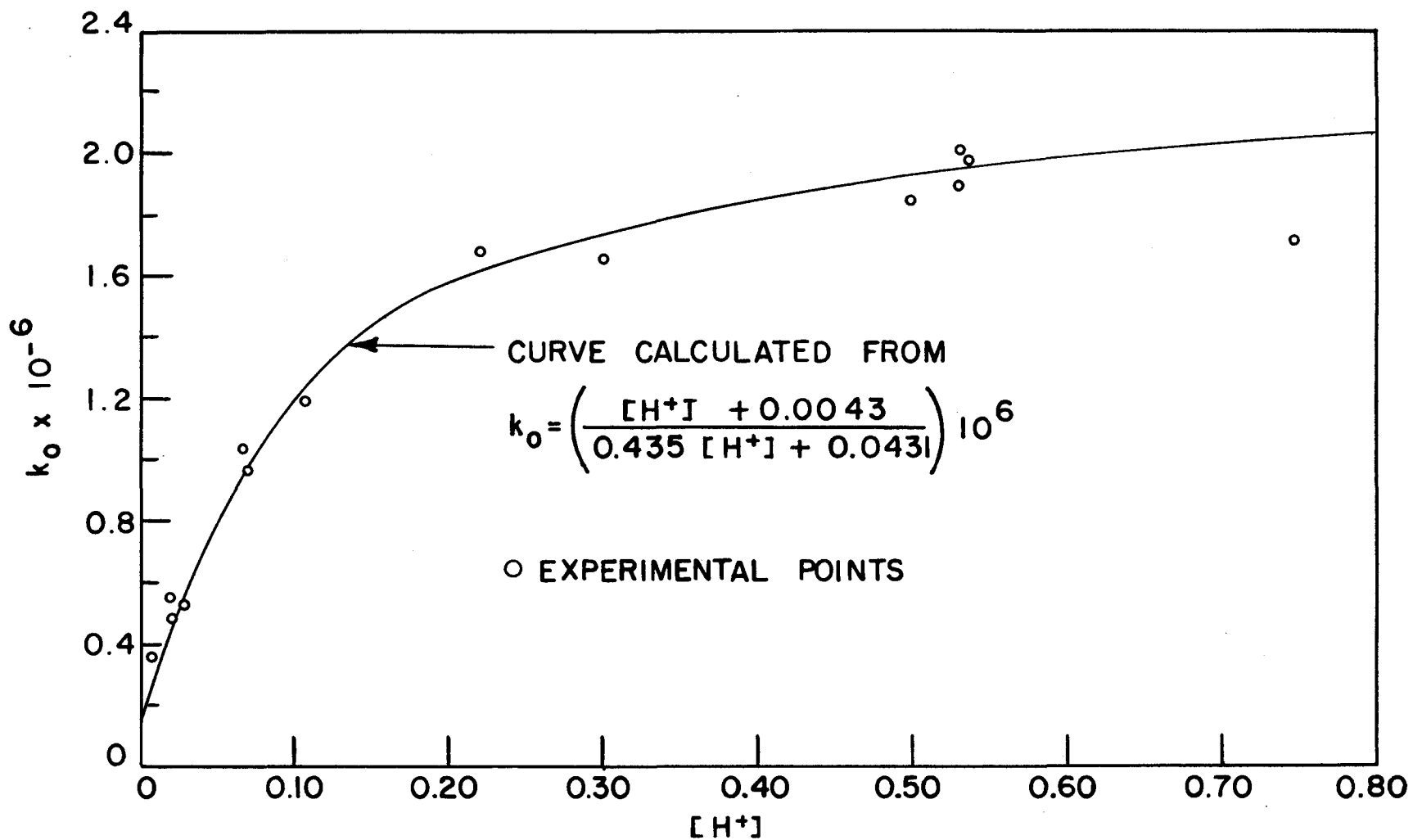


FIGURE 38, EFFECT OF ACIDITY ON FORMATION RATE CONSTANT OF NICKEL PHENANTHROLINE

If the reverse reaction is neglected,

$$\frac{d[\text{H}_2\text{Pn}^{++}]}{dt} = k_{15}[\text{H}^{++}][\text{Pn}] + k_6[\text{H}^{++}][\text{Pn}^+], \quad [17]$$

and therefore,

$$k_6 = k_{15} + \frac{(\text{H}^+)_0 k_6}{k_8} \quad [18]$$

If only the mechanism of Equations [1], and [4] were correct, then the points in Figure 3B would fall on a straight horizontal line. While if the above simple combination of reactions in Equation [17] were correct, the points in Figure 3B would fall on a straight line of the slope $\frac{k_6}{k_8}$. The points do not fall on a straight line, but even deviate in 0.1 molar perchloric acid. Reaction 10 shows that bond strength does not greatly alter the rate up to 0.5 molar sodium perchlorate. However, it seems significant that the alcohol(IX)-1,10-phenanthroline system also fits an expression such as Equation [18] over a very limited range of acidity. It would be reasonable to assume that the reaction between the alcohol(IX) ion and the 1,10-phenanthroline molecule proceeds in a stepwise fashion, one nitrogen-atom bond forming in each step. With 1,10-phenanthroline itself, this replacement of water molecules from alcohol(IX) by the double nitrogen would be expected to follow in rapid sequence with no way of distinguishing the steps. If, however, the 1,10-phenanthroline ion combines directly with alcohol(IX), the molecule must lose the proton before completing the doublet. This reaction sequence may be pictured as seen in Figure 3D, where the left hand side begins with the species formed by the displacement of one water molecule from the aquated alcohol(IX) ion by the 1,10-phenanthroline ion. The entire sequence can be written:

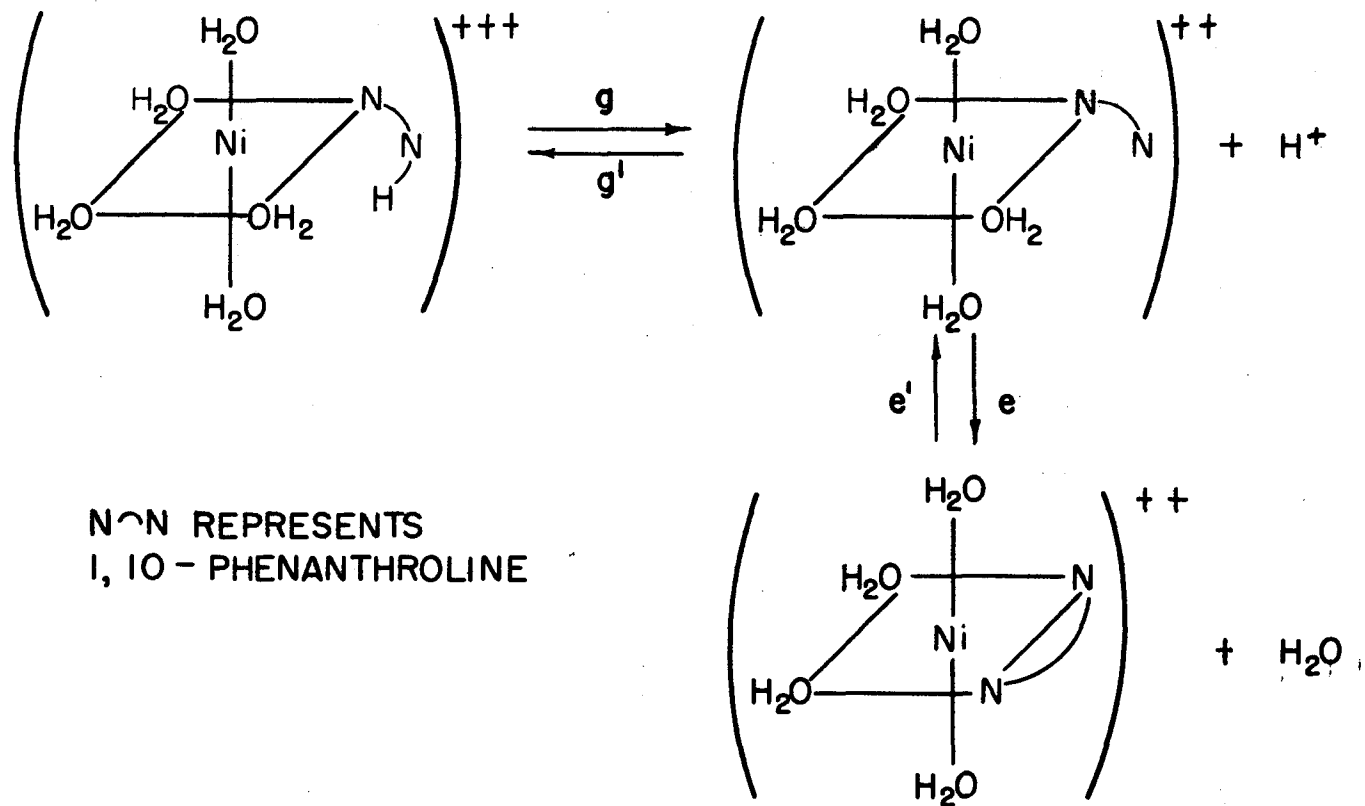


FIGURE 39, PROPOSED MECHANISM FOR REACTION BETWEEN THE PHENANTHROLIUM ION AND NICKEL ION



where, Ni^{++} is $\text{Ni}(\text{H}_2\text{O})_6^{++}$, B^{+++} is $\text{Ni}(\text{H}_2\text{O})_5\text{HPh}^{+++}$, A^{++} is $\text{Ni}(\text{H}_2\text{O})_5\text{Ph}^{++}$, and NiPh^{++} is $\text{Ni}(\text{H}_2\text{O})_4\text{Ph}^{++}$. Since B^{+++} and A^{++} are presumed to be unstable intermediates of negligible concentration, it is possible to make the steady state approximation, setting both of their rates of formation equal to zero. In this way it can be shown by neglecting a' that:

$$\frac{d[\text{NiPh}^{++}]}{dt} = \frac{\text{a}fg[\text{H}^+] + \text{a}a'K_2(\text{f}' + \text{g})}{K_2\text{f}'\text{g}'[\text{H}^+] + K_2(\text{a} + \text{a}')(\text{f}' + \text{g})} [\text{Ni}^{++}][\text{Ph}]. \quad (20)$$

The observed rate constant, k_o , is now dependent on the hydrogen ion concentration and can be written:

$$k_o = \frac{[\text{H}^+] + \text{m}}{n[\text{H}^+] + \text{p}}, \quad (21)$$

where

$$\text{m} = \frac{\text{a}K_2(\text{f}' + \text{g})}{\text{f}'\text{g}}, \quad \text{n} = \frac{K_2\text{f}'\text{g}'}{\text{a}fg} \quad \text{and} \quad \text{p} = \frac{(\text{a} + \text{a}')(\text{f}' + \text{g})K_2}{\text{a}fg}.$$

Another possible mechanism for the formation of mono(1,10-phenanthroline)nickel(II) may be postulated as an acid catalyzed reaction, where the intermediate formed by the replacement of one water molecule from the aquated nickel ion by 1,10-phenanthroline goes to the product faster by the elimination of a hydronium ion. This mechanism is pictured in Figure 40. The reaction sequence may be written:

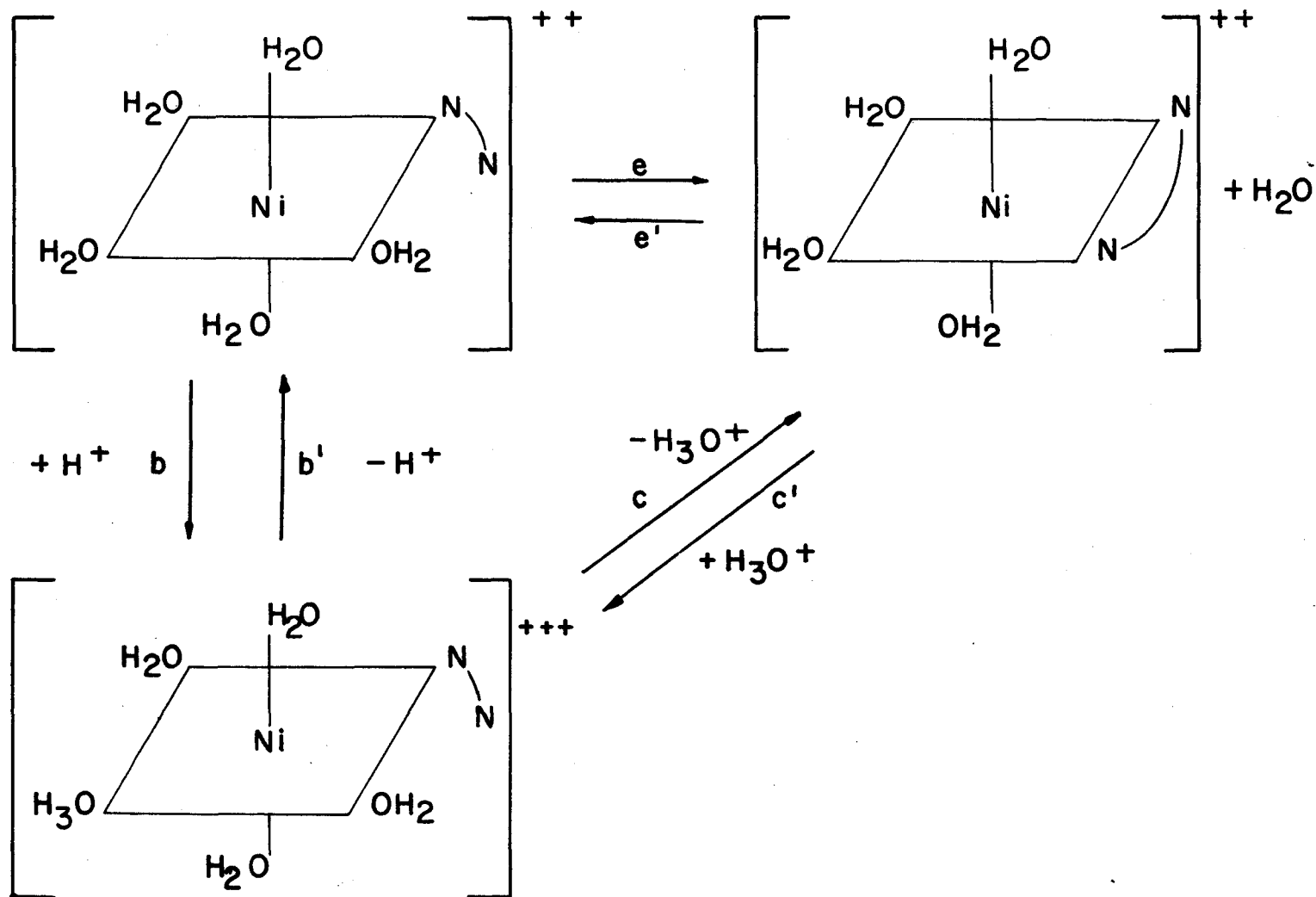
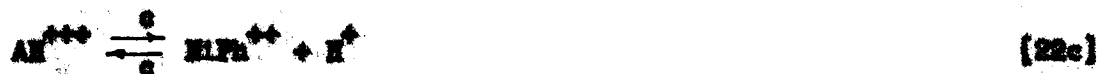


FIGURE 40, PROPOSED MECHANISM FOR ACID CATALYSIS OF REACTION BETWEEN PHENANTHROLINE AND NICKEL ION



where A^{++} is $\text{Ni}(\text{H}_2\text{O})_5\text{Ph}^{++}$ and AH^{+++} is $\text{Ni}(\text{H}_2\text{O})_4(\text{H}_3\text{O})\text{Ph}^{+++}$. Since A^{++} and AH^{+++} are unstable intermediates, the steady state approximations can again be made. Neglecting c' and e' , it can be shown that:

$$\frac{d[\text{HPh}^{++}]}{dt} = \frac{abc[\text{H}^+] + ce(b' + c)}{bc[\text{H}^+] + (a' + e)(b' + c)} [\text{Ni}^{++}][\text{Ph}] \quad [23]$$

The observed rate constant, k_o , can again be expressed as in Equation [21], where the coefficients are now, $m = \frac{c(b' + c)}{bc}$, $n = 1/a$, and $p = \frac{(a' + e)(b' + c)}{abc}$.

It can be seen that Equation [21] corresponds qualitatively to the effect of acid strength on the rate constant. At very low acidity k_o is equal to n/p , which by either mechanism is $\frac{ac}{a' + e}$, and is hydrogen ion independent or equal to k_{12} . At intermediate acidity k_o changes with acidity, while at very high acidity k_o again becomes constant, this time equal to $1/n$. The values of the coefficients, m , n , and p , can be evaluated by solving simultaneous equations for a series of three values of k_o at various hydrogen ion concentrations. However, their values are more easily determined if either extreme value of k_o is known. If at high acidity the major fraction of the reaction proceeds through the hydrogen ion dependent path, then $f[\text{HPh}^{++}][\text{Ni}^{++}] \gg a[\text{Ph}][\text{Ni}^{++}]$ or $c[\text{AH}^{+++}] \gg e[\text{A}^{++}]$. It can then be shown that $f[\text{H}^+] \gg \frac{aK_a(a' + e)}{e}$ or that $c[\text{H}^+] \gg \frac{c(b' + c)}{e}$, and hence

at high hydrogen ion concentration:

$$k_o = \frac{[H^+]}{n[H^+] + p} \quad [24]$$

Therefore, if the assumption that the hydrogen ion dependent path is pre-dominant at high acidities is correct, a plot of $1/k_o$ against $1/[H^+]$ should give a straight line of intercept n and slope p . This plot is shown in Figure 41 and the data are presented in Table 37. The values of n and p from this plot can be used to determine m from data at lower acidities, which in turn gives a corrected graph. By successive approximation, numerical values for these constants may be determined:

$$k_o = \frac{[H^+] + .0043}{.435[H^+] + .0431} 10^6 \quad [25]$$

The same procedure was applied to 5-methyl-1,10-phenanthroline as shown in Table 37 and Figure 42 and to 5-nitro-1,10-phenanthroline as in Table 37. The following expressions can be written for k_o :

$$\text{MePh} \quad k_o = \frac{([H^+] + .0056)}{(.45[H^+] + .045)} 10^6, \quad [26]$$

$$\text{NO}_2\text{Ph} \quad k_o = \frac{([H^+] + .0068)}{(.23[H^+] + .0181)} 10^5 \quad [27]$$

The proposed mechanisms of the nickel(II)-1,10-phenanthroline reactions can also be applied to the rate of dissociation of the complexes. With either mechanism it can be seen that the observed rate constant, k_o , should increase as the hydrogen ion concentration increases. Using the steady state approximation and neglecting a and f in the mechanism in Equations [19a-d] it can be shown that:

$$\frac{d[\text{NiPh}^{++}]}{dt} = \frac{e'f'g'[H^+] + a'e'(f'+g)}{f'g'[H^+] + (a'+e)(f'+g)} [\text{NiPh}^{++}]. \quad [28]$$

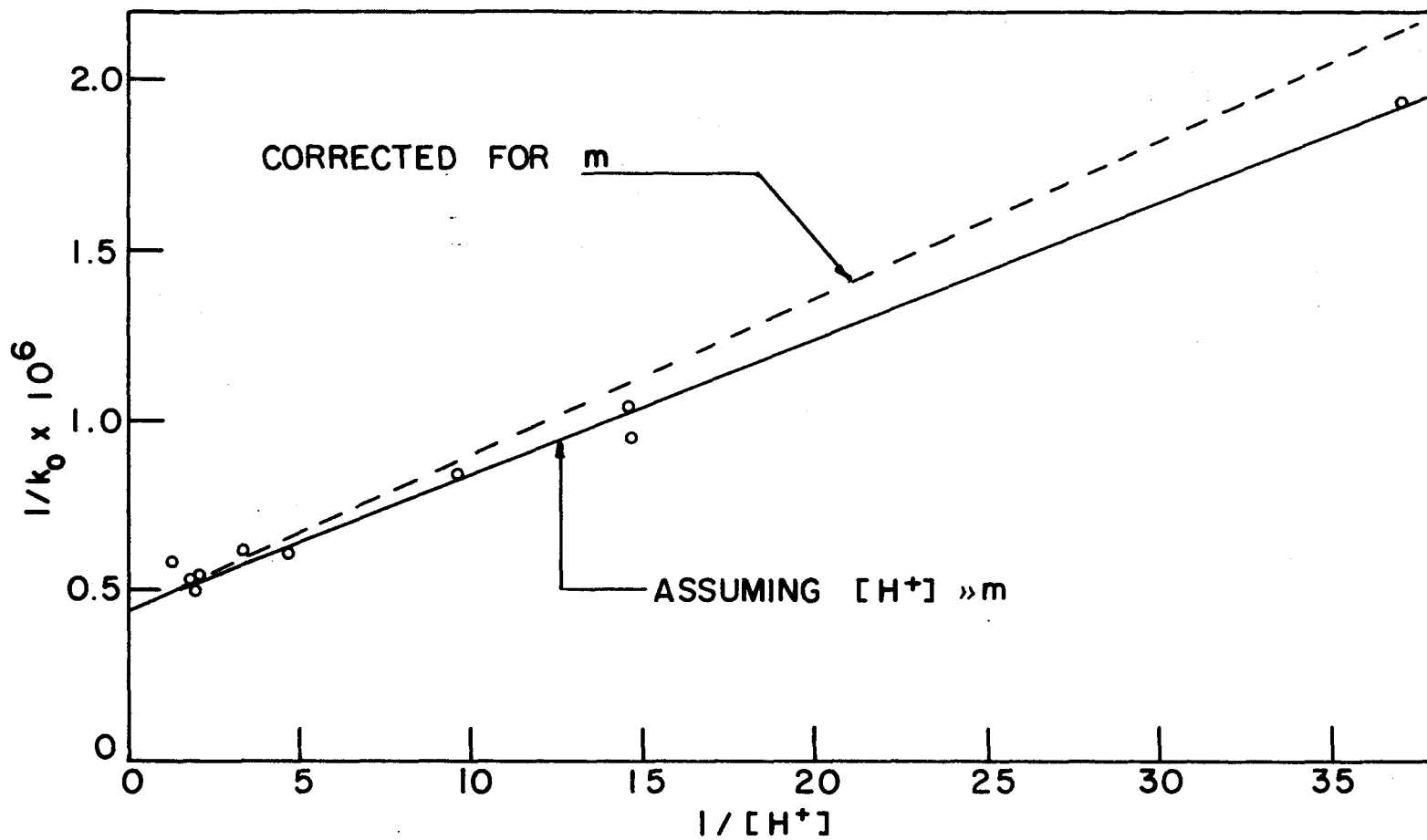


FIGURE 41, ACID DEPENDENCE OF MONO(PHENANTHROLINE)NICKEL FORMATION RATE

Table 37. Acid Dependence of Rate
of Formation of Nickel(II)-1,10-Phenanthrolines

Reaction No.	$\frac{1}{k_0}$	$\frac{1}{[H^+]}$
<u>1,10-phenanthroline</u>		
1	0.59	1.3
2	0.53	1.9
3	0.50	1.9
4	0.51	1.9
5	0.54	2.0
6	0.61	3.4
7	0.60	4.6
8	0.84	9.5
9	0.96	14.6
10	1.04	14.6
11	1.93	37.0
<u>5-methyl-1,10-phenanthroline</u>		
20	0.53	1.9
21	0.52	2.0
22	0.78	10.0
23	1.33	24.1
24	2.04	47.1
<u>5-nitro-1,10-phenanthroline</u>		
26	0.27	2.0
27	0.38	5.0
28	0.40	10.0
29	0.84	49.5

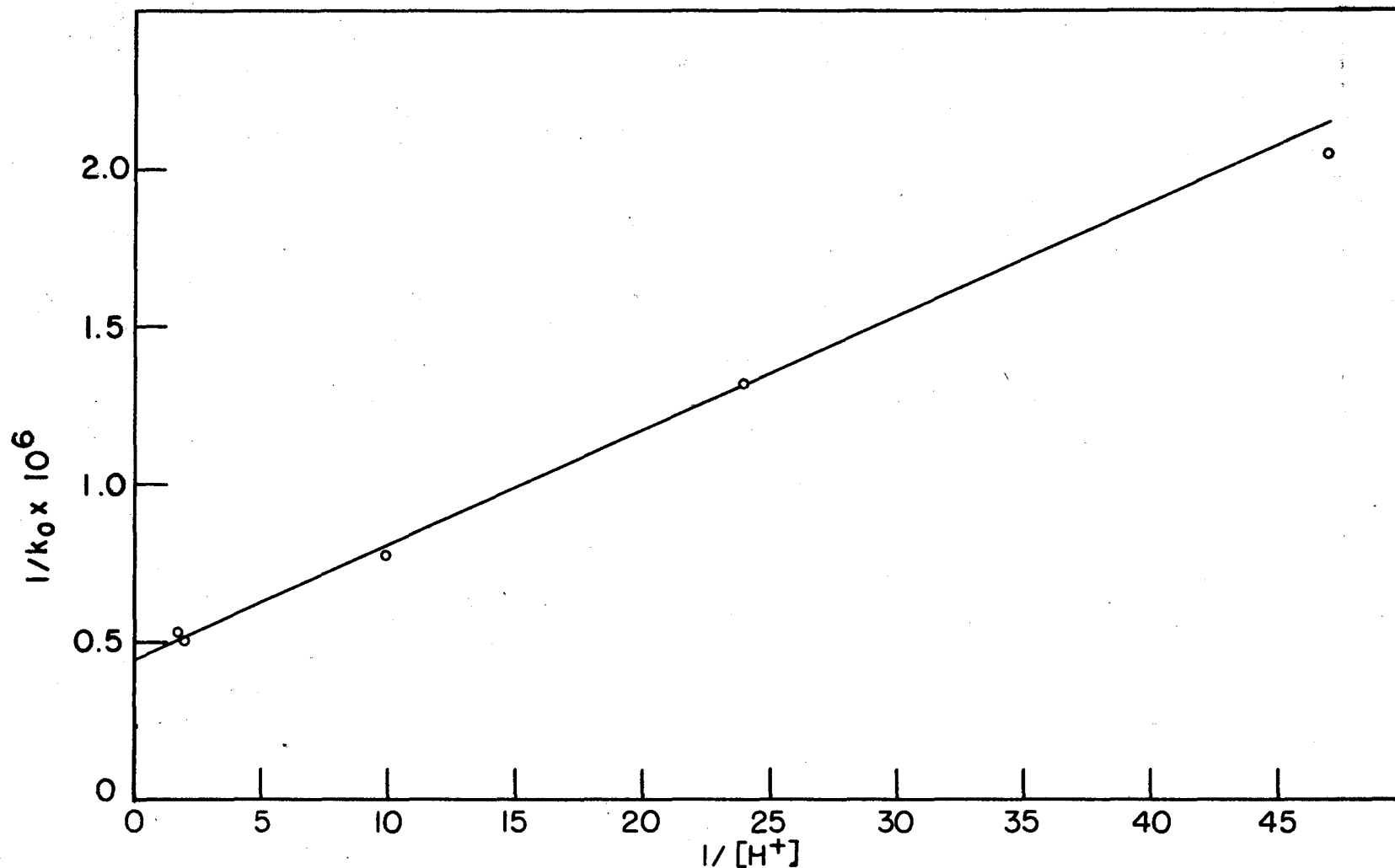


FIGURE 42, ACID DEPENDENCE OF MONO(METHYLPHENANTHROLINE) NICKEL FORMATION RATE

The observed rate of dissociation constant, k'_0 , is therefore dependent on the hydrogen ion concentration:

$$k'_0 = \frac{[H^+] + q}{r[H^+] + s} \quad [29]$$

where $q = \frac{a'(f' + g)}{f'g'}$, $r = 1/e'$, and $s = \frac{(a' + e')(f' + g)}{e'f'g'}$.

Similarly using the mechanism in Equations [22a-d] and neglecting a it can be shown that:

$$-\frac{d[NiPh^{++}]}{dt} = \frac{a'b'c'[H^+] + a'e'(b' + c)[NiPh^{++}]}{bc[H^+] + (a' + e)(b' + c)} \quad [30]$$

The observed rate constant, k'_0 , can again be expressed as in Equation [29] where

$$q = \frac{e'(b' + c)}{b'c'}, \quad r = \frac{bc}{a'b'c'} \quad \text{and} \quad s = \frac{(a' + e)(b' + c)}{a'b'c'}$$

At high hydrogen ion concentration a plot of $1/k'_0$ against $1/[H^+]$ gives a straight line as in Figure 43, indicating that q is small. The coefficients in Equation [29] can then be evaluated giving:

$$k'_0 = \frac{[H^+] + .015}{.14[H^+] + .060} \cdot 10^{-3} \quad [31]$$

From the theoretical values of the coefficients in Equations [21] and [29] it can be shown that the following relation should hold:

$$\frac{p}{n} \times \frac{r}{s} = 1 \quad [32]$$

However, the numerical values obtained for these coefficients give a product approximately equal to .23. The order of magnitude is correct and

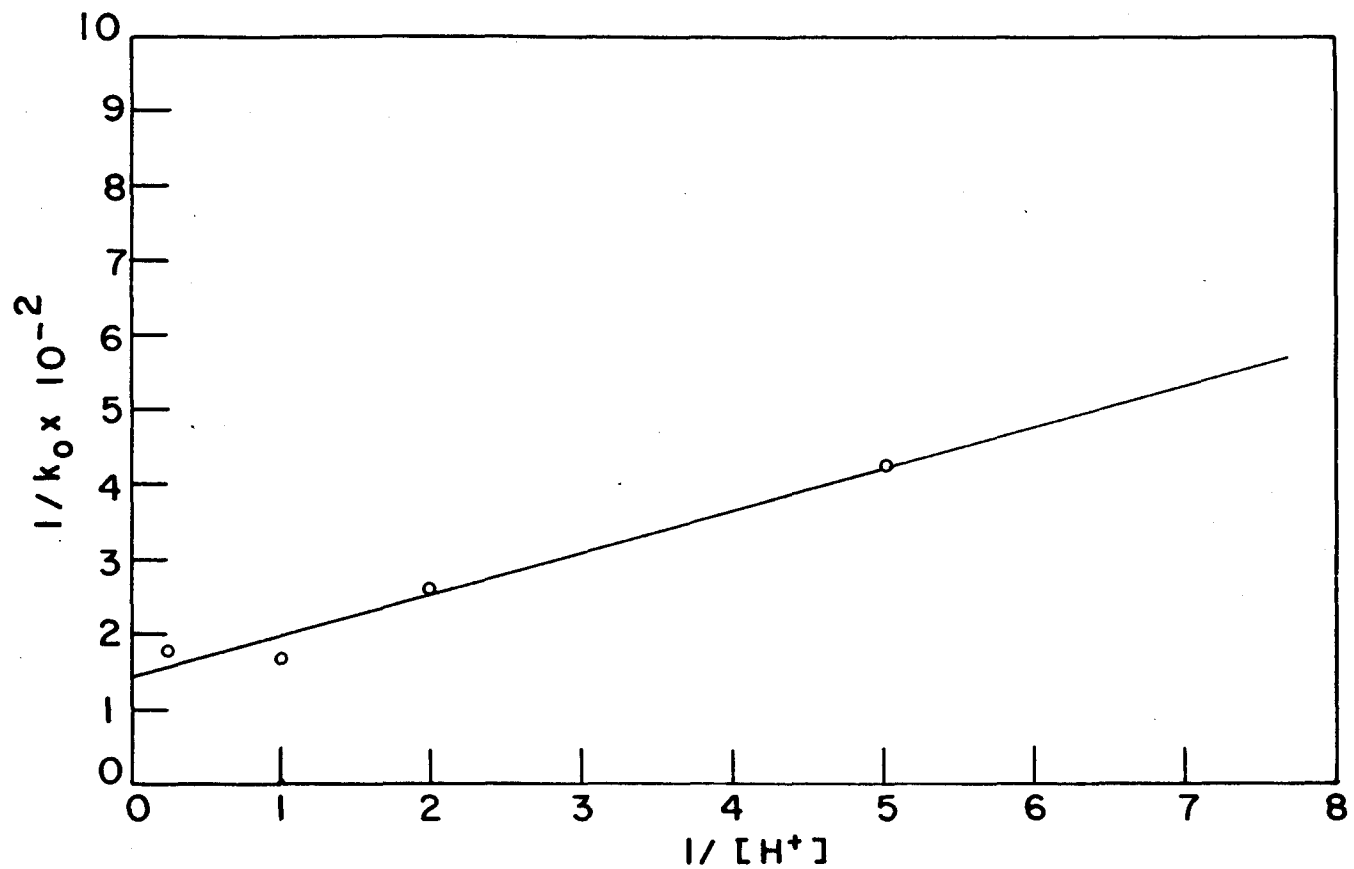


FIGURE 43, ACID DEPENDENCE OF MONO(PHENANTHROLINE)NICKEL DISSOCIATION RATE

the lack of precise agreement may be due to an insufficient number of reaction studies for accurate evaluation of r and s . However, it may also be due to the formation above 0.5 molar acid of a stable complex between mono(1,10-phenanthroline)nickel(II) and hydrogen ion. It was observed in the dissociation reactions that an immediate increase in absorbance occurred when mono(1,10-phenanthroline)nickel(II) was placed in solutions of high acidity. This could not be due to the formation of the 1,10-phenanthrolium ion because the dissociation does not proceed that rapidly. Neither could it be due to the formation of an unstable species such as B^{+++} or AH^{+++} since estimated values of e' and c' are too large to allow their rapid formation. It has been suggested (6, 29) that one of the reasons for the unusual stability of the 1,10-phenanthroline complexes is the formation of a double bond between the metal ion and 1,10-phenanthroline. This would result in the distribution of a negative charge on the 1,10-phenanthroline molecule. It would then be conceivable that in highly acid solutions a proton is associated with the 1,10-phenanthroline portion of the complex but not with the nitrogens. In other words, a complex, $Ni(H_2O)_4PhH^{+++}$, has formed. If such a complex existed, its presence would be expected to affect the rate of dissociation of mono(1,10-phenanthroline)nickel(II) and therefore cause p/n to be different than r/s . Whatever the nature of the complex between nickel(II), 1,10-phenanthroline and hydrogen ion, such a complex does seem to exist to a measurable extent in solutions above 0.5 molar perchloric acid.

Several people (22, 24), have suggested a stable protonated 1,10-phenanthroline-metal ion complex. For instance, the species $FeHPh_3^{+4}$

has been suggested to account for the acid dependence of ferriin dissociation. It is readily apparent that the effect of hydrogen ion concentration on the kinetics and equilibria of the nickel(II)-1,10-phenanthroline complexes is much more complicated than previously supposed. Considerably more work needs to be done to test the reaction mechanism proposed here.

As was pointed out for Reaction 14, whose k_0 value falls off the calculated curve, it is difficult to study the rates in less acid solution due to the interference of the bis(1,10-phenanthroline)nickel(II) formation. At low acidities the 1,10-phenanthroline also begins to coat the glass surface of its container.

Reactions 9 and 10 illustrated that the formation reaction was not greatly affected by ionic strength up to 0.5 molar sodium perchlorate. However, Reaction 1 at 0.75 molar perchloric acid may be slower due to the ionic strength effects.

The expressions for the coefficients in Equations [21] and [29] can be simplified somewhat by assuming the proton transfer reactions such as [19c] and [22b] to be very rapid reactions so that:

$$(f' + g) = e, \quad (b' + c) = c \quad [35]$$

From Equations [28] and [31] it can be seen that for the mechanism given in Equations [19a-d], e is greater than a' and therefore the following values of the rate constants can be estimated:

$$e = 6.6 \times 10^6$$

$$e' = 7.2 \times 10^{-3}$$

$$a = 1.0 \times 10^5$$

$$f = 2.6 \times 10^2$$

On the other hand from Equations [25] and [25] it can be seen that for the mechanism given in Equations [22a-d], a' is greater than e and therefore the following values of the rate constants can be estimated:

$$a = 2.3 \times 10^6$$

$$c' = 1.7 \times 10^{-2}$$

$$e' = 2.5 \times 10^{-4}$$

There appears to be no simple way of distinguishing these two mechanisms. Both mechanisms involve the combination of two positively charged ions and both require a proton transfer between unstable intermediates. If the acid catalysed reaction were to require the displacement of a trans hydronium ion then the effect of acidity would be different for the bis and tris complexes. On the other hand if the mechanism were an acid catalysed displacement of an adjacent hydronium ion or a phenanthrolium ion mechanism, the acidity effect should be much the same for the bis and tris complexes as for the mono complex.

The observed rate constant, k_o , changes approximately fivefold when comparing the reaction rate of 1,10-phenanthroline and 5-nitro-1,10-phenanthroline. However, k_o is the sum of two expressions, one of which is dependent on the acidity. The effect of the nucleophilic character of the ring nitrogens on the rate of reaction is best seen in Figure 44 where $\log k_{1f}$ is plotted against pK_a . There is approximately a threefold

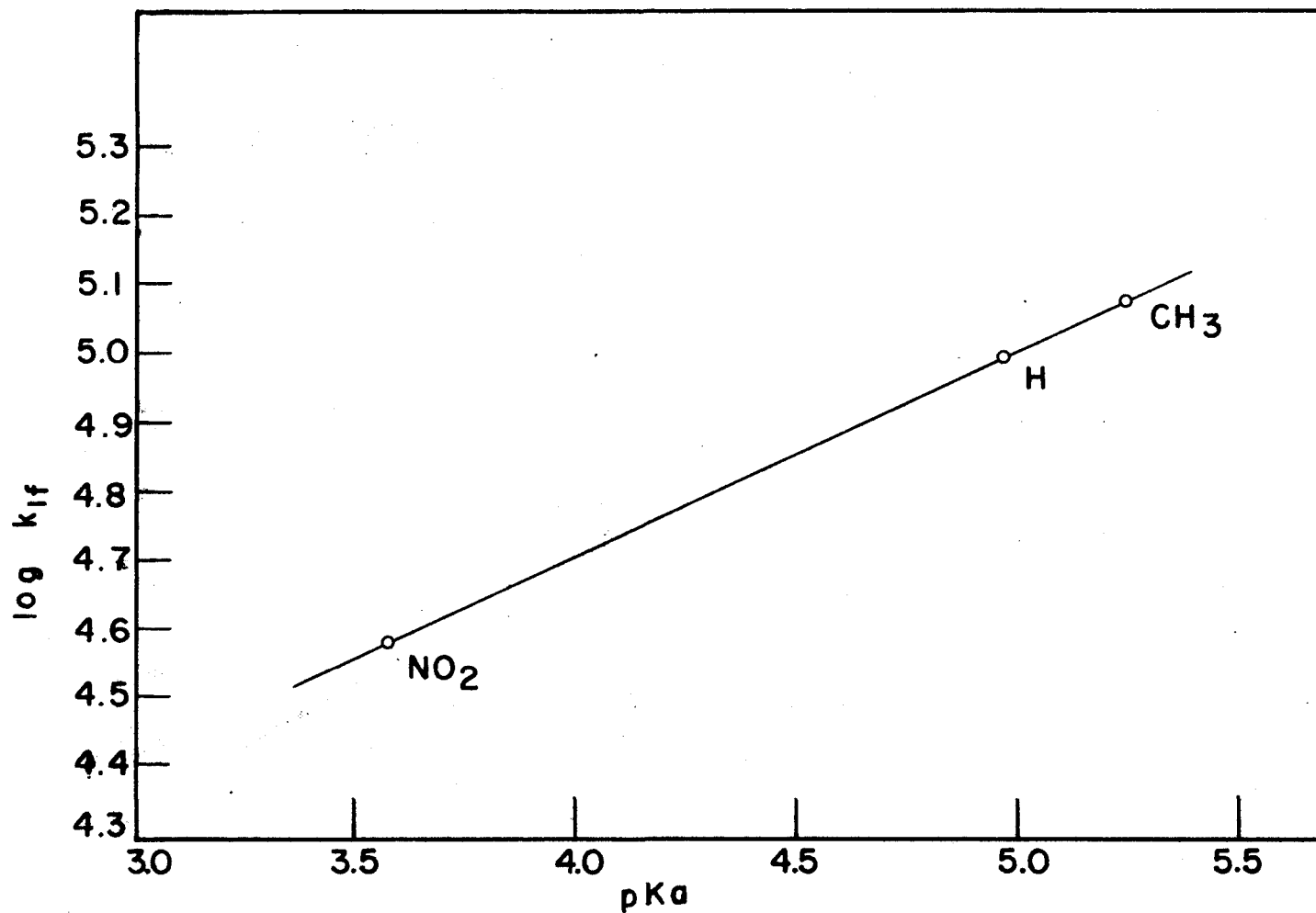


FIGURE 44, SUBSTITUENT EFFECT ON MONO (PHENANTHROLINE) NICKEL RATE CONSTANT

change in rate for a fortyfold change in K_2 . In short, the rate of reaction of nichal(II) ion with 1,10-phenanthroline is not very sensitive to changes in the nucleophilic character of the ring nitrogen.

6. The Bis(1,10-phenanthroline)nichel(II) Complexes

1. Experimental

If the rate of formation of the bis(1,10-phenanthroline)nichel(II) complex is very slow compared to the rate of formation of the mono(1,10-phenanthroline)nichel(II) complex, it is possible to assume that all the nichal(II) has reacted to form the mono-complex before the bis-complex begins to form. Thus, by neglecting the reverse reaction and assuming negligible nichal(II) concentration, the following equations can be written:

$$\frac{d([\text{MLPh}_2^{++}])}{dt} = k_{22}([\text{MLPh}^{++}][\text{Ph}] - \frac{k_2 K_2}{[I^+]} [\text{MLPh}^{++}][\text{MLPh}^+]) \quad [34]$$

$$k_{22}^0 = \frac{2.303}{K_2(\text{Ph}_Y - 2\text{ML}_Y)} \log \left[\frac{\text{Ph}_Y - \text{ML}_Y - [\text{MLPh}_2^{++}]}{\text{ML}_Y - [\text{MLPh}_2^{++}]} \cdot \frac{\text{ML}_Y}{\text{Ph}_Y - \text{ML}_Y} \right] \quad [35]$$

The bis(1,10-phenanthroline)nichel(II) concentration can be measured from the absorbance of the solution:

$$[\text{MLPh}_2^{++}] = \frac{\epsilon_{\text{MLPh}_2^{++}} \text{Ph}_Y - (\epsilon_{\text{MLPh}^{++}} - \epsilon_{\text{MLPh}}) \text{ML}_Y - \lambda/\delta}{\epsilon_{\text{MLPh}^{++}} + \epsilon_{\text{MLPh}} - \epsilon_{\text{MLPh}_2^{++}}} \quad [36]$$

The molar absorptivities of the bis- and tris(1,10-phenanthroline)nichel(II) complexes were measured by mixing a series of solutions containing the same amount of nichal(II) and varying amounts of 1,10-phenanthroline. These solutions were prepared at pH 7 in order to eliminate any 1,10-

phenanthroline absorbance and were measured shortly after mixing to prevent any decrease in absorbance due to loss of 1,10-phenanthroline on the glass surfaces. At 310m μ a nearly linear plot of absorbance against 1,10-phenanthroline concentration was obtained until the phenanthroline concentration exceeded three times the nickel(II) concentration. The following relationship was approximately true:

$$\epsilon_{NiPh} = \frac{1}{2} \epsilon_{NiPh_2} = \frac{1}{3} \epsilon_{NiPh_3}$$

The actual values of the molar absorptivities are presented in the section on equilibrium constants. Table 38 and Figure 45 present a typical rate study (Reaction 32) using Equations [35] and [36].

2. Discussion.

The points in Figure 45 fall on a continuous upward curve rather than on a straight line. This might be attributed to the formation of tris(1,10-phenanthroline)nickel(II). However, the slope of the best straight line from the point when $k_{2f}t$ is zero gives k_{2f} a value of $1.7 \times 10^5 \text{ min.}^{-1}$. Since at this acidity k_0 is $2.2 \times 10^5 \text{ min.}^{-1}$, the original assumption that the second reaction is much slower than the first is not correct. The kinetic system, therefore, is one of competitive consecutive, reversible reactions with prior equilibria. This system cannot be treated with mathematical simplicity unless the 1,10-phenanthroline is present in large excess and even then may not be resolvable if k_{2f} is large. Furthermore, as mentioned earlier, the limitations of the 1,10-phenanthroline absorbance in the ultraviolet and the solubility of the 1,10-phenanthroline perchlorate when using the visible region, prevent the convenient use of

Table 38. Spectrophotometric Data and Calculation of Reaction 32

$$[H^+] = 2.45 \times 10^{-3}$$

$$F_{H_2} = 1.64 \times 10^{-4}$$

$$H_{H_2} = 7.65 \times 10^{-5}$$

1-cm. cell 510m μ

$$k_{2r} = 4.66 \times 10^7 \log \left(\frac{A_0 - .226}{A_0 - .266} \times .874 \right)$$

Time (min.)	A_0	$\log \frac{A_0 - .226}{A_0 - .266} \times .874$	$k_{2r} \times 10^{-5}$
3	0.687	-0.019	-8.9
4	0.679	-0.016	-7.5
5	0.628	-0.014	-6.5
6	0.605	-0.010	-4.7
7	0.587	-0.008	-3.7
8	0.563	-0.004	-1.9
9	0.549	+0.001	-0.5
10	0.531	0.005	1.4
11	0.516	0.006	2.8
12	0.502	0.010	4.6
13	0.489	0.012	5.5
14	0.478	0.016	7.4
15	0.467	0.020	9.3
16	0.457	0.024	11.2
17	0.448	0.028	13.0
18	0.440	0.031	14.4
19	0.432	0.035	16.3
20	0.425	0.039	18.2
21	0.418	0.043	20.0
22	0.411	0.047	21.9
23	0.405	0.053	24.7
24	0.399	0.056	26.1
25	0.394	0.059	27.5
26	0.388	0.065	30.3
27	0.383	0.069	32.2
28	0.378	0.074	34.5
29	0.373	0.079	36.8
30	0.368	0.085	39.6

Table 3B (continued)

Time (min.)	λ	$\frac{\lambda - .286}{\lambda - .286} \times .874$	$k_{22} \times 10^{-3}$
31	0.364	0.090	41.9
32	0.360	0.097	44.3
33	0.357	0.100	46.6
34	0.354	0.104	48.5
35	0.351	0.109	50.8
37	0.344	0.121	56.4
39	0.337	0.136	63.4
41	0.327	0.147	68.9
43	0.317	0.161	75.1
45	0.305	0.173	80.6
47	0.319	0.192	89.5
50	0.314	0.203	95.5

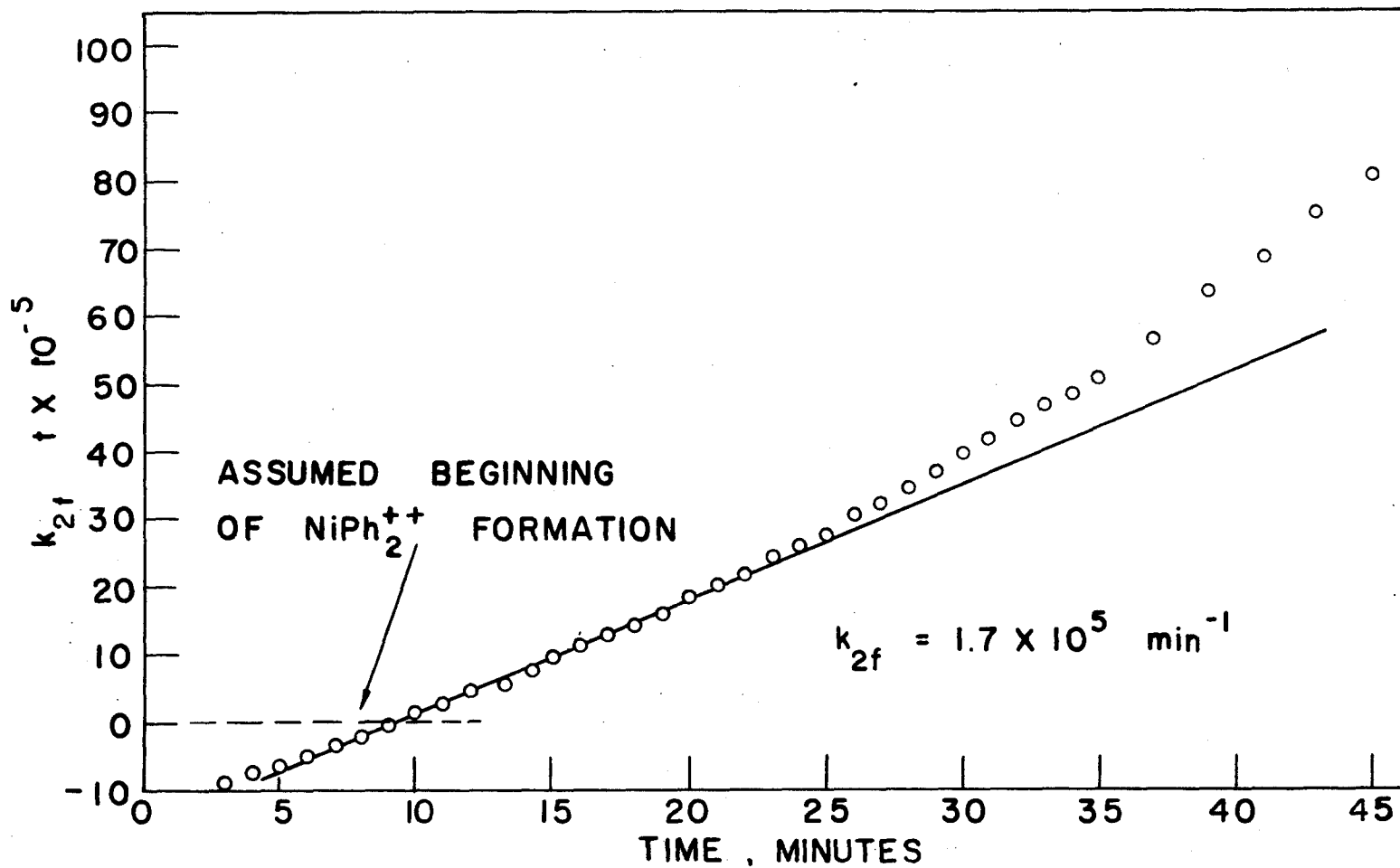


FIGURE 45, REACTION NO. 32

a large excess of 1,10-phenanthroline in these rate studies.

The data obtained using Equation [35] can be used as an approximation for k_2f . The true value should be between 2×10^4 and $2 \times 10^5 \text{ min}^{-1}$. Similar data for 5-methyl-1,10-phenanthroline and 5-nitro-1,10-phenanthroline indicate their k_{2f} and k_{1f} values are in approximately the same relationship. Hence the change of the nucleophilic character of the 1,10-phenanthroline nitrogens does not appear to affect the rate of formation of the bis-complex any more than with the mono-complex.

B. The Tris(1,10-phenanthroline)nickel(II) Complexes

1. Experimental

The rate of formation study of the tris(1,10-phenanthroline)nickel(II) complex can be treated in the same manner as the bis(1,10-phenanthroline)-nickel(II) complex. Using the approximations:

$$\text{Ph}_T = [\text{NPh}^+] + 2[\text{NiPh}_2^{++}] + 3[\text{NiPh}_3^{+++}] \quad [37]$$

$$\text{Ni}_T = [\text{NiPh}_2^{++}] + [\text{NiPh}_3^{+++}] , \quad [38]$$

and neglecting the reverse reaction it can be shown that:

$$k_2f = \frac{2.5[\text{H}^+]}{K_2(\text{Ph}_T - 3\text{Ni}_T)} \log \frac{\text{Ph}_T - 2\text{Ni}_T - [\text{NiPh}_3^{+++}]}{\text{Ni}_T - [\text{NiPh}_3^{+++}]} \times \frac{\text{Ni}_T}{\text{Ph}_T - 2\text{Ni}_T} . \quad [39]$$

The rate study for Reaction 35, which is presented in Table 39 and Figure 46, was calculated using Equation [39] and the following expression for the concentration of the tris(1,10-phenanthroline)nickel(II):

Table 39. Spectrophotometric data and calculation of Reaction 33

$$[M^+] = 2.02 \times 10^{-3}$$

$$M_T = 1.153 \times 10^{-4}$$

$$M_T = 3.06 \times 10^{-5}$$

1-cm. cell 310m μ

$$k_{33} = 1.62 \times 10^7 \log \left(\frac{A_0 - .152}{A_0 - .240} \times .565 \right)$$

Time (min.)	A_0	$\log \left(\frac{A_0 - .152}{A_0 - .240} \times .565 \right)$	k_{33}^t
3	0.308	-0.132	-24.0
4	0.313	-0.127	-23.1
5	0.300	-0.122	-22.2
7	0.480	-0.112	-20.4
9	0.463	-0.104	-18.92
12	0.441	-0.090	-16.40
17	0.412	-0.068	-12.40
22	0.390	-0.048	- 8.74
27	0.372	-0.026	- 4.73
32	0.359	-0.008	- 1.43
33	0.356	-0.005	- 0.55
34	0.353	0.002	0.36
35	0.351	0.006	1.09
36	0.350	0.007	1.27
37	0.347	0.013	2.37
38	0.345	0.016	2.91
39	0.342	0.022	4.00
40	0.341	0.024	4.37
41	0.340	0.026	4.73
42	0.338	0.030	5.46
43	0.336	0.034	6.39
44	0.334	0.039	7.10
45	0.332	0.044	8.01
46	0.331	0.046	8.37
47	0.330	0.048	8.74
48	0.329	0.050	9.10
49	0.327	0.056	11.2
50	0.326	0.058	10.6

Table 39 (continued)

Time (min.)	A_0	$\log \left(\frac{A_0 - .152}{A_0 - .240} \times .365 \right)$	$k_{1/2}^{\text{app}}$
52	0.323	0.066	12.0
54	0.321	0.071	12.9
56	0.319	0.077	14.0
58	0.317	0.083	15.1
60	0.315	0.089	16.2
62	0.312	0.098	17.8
64	0.311	0.102	18.6
66	0.309	0.109	19.8
68	0.307	0.116	21.1

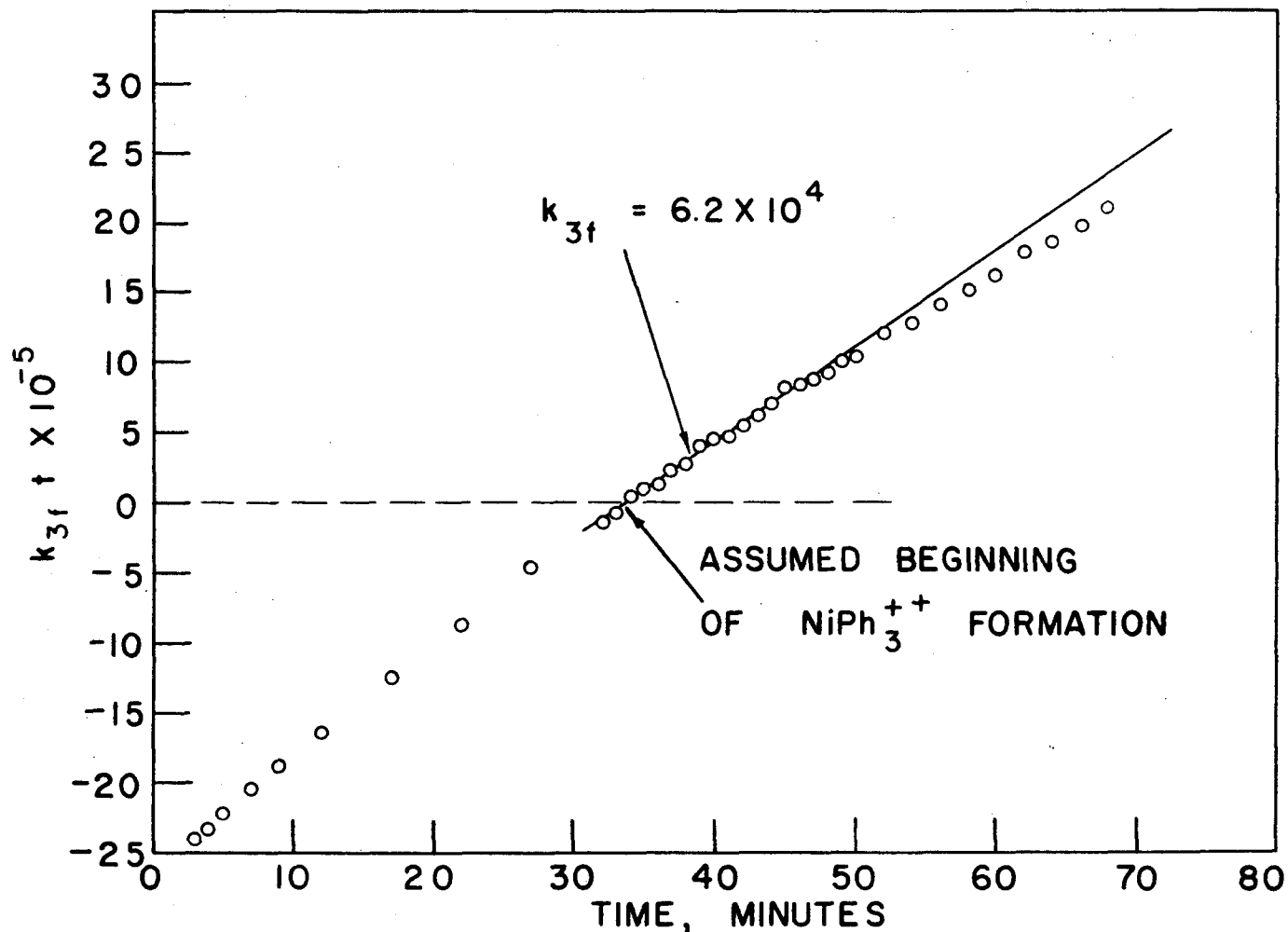


FIGURE 46, REACTION NO. 33

$$[\text{NiPh}_3] = \frac{c_{\text{NiPh}}^0 V_{\text{H}_2} - (2c_{\text{NiPh}}^0 - c_{\text{NiPh}_2}^0) K_3 - A_d/A}{c_{\text{NiPh}}^0 + c_{\text{NiPh}_2}^0 - c_{\text{NiPh}_3}^0} \quad [40]$$

2. Discussion

The values obtained for k_{XF} by these approximations is $6.2 \times 10^4 \text{ min}^{-1}$, which indicates that the approximations are poor and that the concentration of the mono(1,10-phenanthroline)nickel(II) complex is not negligible before the tris(1,10-phenanthroline)nickel(II) starts to form. It is possible to estimate the k_{XF} value from the equilibrium constant, K_3 and the dissociation rate constant, k_{M} . The latter value has been reported (2) to be $5.4 \times 10^{-4} \text{ min}^{-1}$ in 510 molar hydrochloric acid. Using this value and the K_3 value obtained in the next section, the value for k_{XF} is $2 \times 10^4 \text{ min}^{-1}$. Since the reported value of k_{M} may be acid dependent this would represent the maximum value expected for k_{XF} .

5-methyl-1,10-phenanthroline and 5-nitro-1,10-phenanthroline gave reaction rates of a similar nature to those observed for 1,10-phenanthroline. There is no pronounced change in the relative rates of formation of the tris-complexes compared to the mono-complexes.

Additional study to determine the actual rates of formation of the bis- and tris-complexes needs to be done. This might be accomplished in the visible region with an absorbance cell of longer path length than 10 centimeters. It might also be accomplished by preparation of the pure solid mono- and bis-complexes, provided their rates of solution were fairly rapid.

H. Equilibrium Constants

The equilibrium dissociation constants were calculated for the mono-(1,10-phenanthroline)nichel(II) complexes and for the tris(1,10-phenanthroline)nichel(II) complex from absorbance data on solutions that were at equilibrium conditions at 25°C.

For K_1 , the absorbance measurements were made with excess nichel(II) to assure the absence of bis(1,10-phenanthroline)nichel(II), so that:

$$K_1 = \frac{K_a}{[H^+]} \frac{([Ni_T] - [NiPh^{++}])([Ph_T] - [NiPh^{++}])}{[NiPh^{++}]} \quad [41]$$

and

$$[NiPh^{++}] = \frac{c_{NiPh} Ph_T - A/\epsilon}{c_{NiPh} - c_{NiPh}} \quad [42]$$

Table 40 presents the values of K_1 obtained and the data used for the calculation of K_1 with 1,10-phenanthroline, 5-methyl-1,10-phenanthroline and 5-nitro-1,10-phenanthroline.

The equilibrium constant K_2 was calculated only for the unsubstituted tris(1,10-phenanthroline)nichel(II) complex. Absorbance measurements were made at equilibrium with solutions containing an excess of 1,10-phenanthroline to nichel(II) so that the assumptions in Equations [43] and [44] were valid and the calculations of K_2 possible.

$$Ni_T = [NiPh_2^{++}] + [NiPh_3^{++}] \quad [43]$$

$$Ph_T = 2[NiPh_2^{++}] + 3[NiPh_3^{++}] + [NiPh^+] \quad [44]$$

where it is assumed that $[Ni^{++}]$ and $[NiPh^{++}]$ are negligible.

Table 40. Equilibrium Constants for the
 Mono(1,10-phenanthroline)nickel(II) Complexes

$[H^+]$	M_{Ni}	M_{L}	A_{λ}/l	λ (m μ)	K_1
<u>Mono(1,10-phenanthroline)nickel(II) Complexes</u>					
0.0202	5.76×10^{-5}	1.91×10^{-4}	0.082	310	1.48×10^{-9}
0.199	5.76×10^{-5}	1.91×10^{-4}	0.124	310	2.22×10^{-9}
0.498	5.76×10^{-5}	1.91×10^{-4}	0.175	310	2.95×10^{-9}
0.217	6.52×10^{-5}	3.06×10^{-4}	0.137	310	2.24×10^{-9}
0.510	1.16×10^{-3}	1.55×10^{-3}	0.190	277.5	2.44×10^{-9}
0.531	1.30×10^{-3}	1.55×10^{-3}	0.224	277.5	4.45×10^{-9}
0.531	1.30×10^{-3}	1.55×10^{-3}	0.223	277.5	4.38×10^{-9}
0.535	1.30×10^{-3}	3.05×10^{-3}	0.202	277.5	1.04×10^{-9}
0.747	1.30×10^{-3}	3.05×10^{-3}	0.210	277.5	1.45×10^{-9}
Ave. = 2.5×10^{-9}					
<u>Mono(5-methyl-1,10-phenanthroline)nickel(II) Complexes</u>					
0.531	5.35×10^{-5}	1.55×10^{-3}	0.141	310	1.88×10^{-9}
0.499	5.35×10^{-5}	1.55×10^{-3}	0.145	310	2.57×10^{-9}
0.100	5.35×10^{-5}	1.55×10^{-3}	0.148	310	1.36×10^{-9}
Ave. = 1.9×10^{-9}					
<u>Mono(5-nitro-1,10-phenanthroline)nickel(II) Complexes</u>					
0.500	2.095×10^{-3}	1.15×10^{-4}	0.236	290	2.7×10^{-8}

$$K_3 = \frac{[\text{NiPh}_2^{++}][\text{Ph}]}{[\text{NiPh}_3^{++}]} = \frac{K_2}{[\text{H}^+]} \frac{[\text{NiPh}_2^{++}][\text{NiPh}^+]}{[\text{NiPh}_3^{++}]} \quad [45]$$

$$K_3 = \frac{K_2}{[\text{H}^+]} \frac{([\text{Ni}_T - [\text{NiPh}_3^{++}])(\text{Ph}_T - 2[\text{Ni}_T - [\text{NiPh}_3^{++}])]}{[\text{NiPh}_3^{++}]} \quad [46]$$

$$[\text{NiPh}_3^{++}] = \frac{c_{\text{NiPh}} \text{Ph}_T - (2c_{\text{NiPh}} - c_{\text{NiPh}_2}) \text{Ni}_T - A_0/l}{c_{\text{NiPh}} + c_{\text{NiPh}_2} - c_{\text{NiPh}_3}} \quad [47]$$

Table 41 presents the data and calculations for the equilibrium constant, K_3 . The molar absorptivity values used for these calculations were obtained from mixing 1,10-phenanthroline and nickel(II) in neutral solutions as described in the previous section. The following values were used for these calculations:

$$c_{\text{NiPh}_2} = 2.70 \times 10^3, \text{ and } c_{\text{NiPh}_3} = 3.90 \times 10^3. \text{ An inspection of the}$$

calculations used in Tables 40 and 41 shows that very small changes in the absorbance values can greatly affect the values of the equilibrium constant. Errors inherent in the absorbance measurements can account for much of the variation in the values of the equilibrium constant.

The K_1 values for 1,10-phenanthroline are in approximate agreement with those obtained from the measurement of kinetic rates.

Thus,

$$K_1 = \frac{k_{1a}}{k_{1r}} = \frac{2.5 \times 10^{-4}}{1.0 \times 10^{-3}} = 2.5 \times 10^{-9},$$

and at any given acidity where the hydrogen ion dependence has been

$$\text{measured, } K_1 = \frac{k'_0}{k_0} :$$

Table 41. Equilibrium Constants for the
Tris(1,10-phenanthroline)nickel(II) Complex

A_{O} at 310m μ

$[H^+]$	Pa_T	Hi_T	A_{O}/l	K_3
1.02×10^{-3}	9.78×10^{-5}	3.82×10^{-6}	0.439	4.60×10^{-8}
1.02×10^{-3}	9.78×10^{-5}	7.65×10^{-6}	0.397	1.07×10^{-8}
1.02×10^{-3}	9.78×10^{-5}	1.15×10^{-5}	0.377	2.62×10^{-8}
1.02×10^{-3}	9.78×10^{-5}	1.53×10^{-5}	0.380	6.48×10^{-8}
1.29×10^{-3}	12.21×10^{-5}	1.53×10^{-5}	0.442	2.21×10^{-8}
1.29×10^{-3}	12.21×10^{-5}	2.30×10^{-5}	0.356	0.71×10^{-8}
1.26×10^{-3}	12.21×10^{-5}	3.06×10^{-5}	0.277	1.97×10^{-8}
1.29×10^{-3}	12.21×10^{-5}	3.85×10^{-5}	0.207	2.21×10^{-8}
1.29×10^{-3}	12.21×10^{-5}	4.59×10^{-5}	0.179	3.58×10^{-8}
				ave. = 2.80×10^{-8}

$$[H^+] = 0.20; \quad K_1 = \frac{2.4 \times 10^{-3}}{1.6 \times 10^6} = 1.5 \times 10^{-9}$$

$$[H^+] = 0.50; \quad K_1 = \frac{3.9 \times 10^{-3}}{1.8 \times 10^6} = 2.2 \times 10^{-9}$$

The K_1 and K_3 values are remarkably close to those values expected from statistical effects alone (5).

Thus,

$$\frac{K_{n+1}}{K_n} = \left(\frac{n+1}{n} \right) \left(\frac{H-n+1}{H-n} \right), \quad (48)$$

where n is the number of ligands and H is the total number of ligands possible.

$$\text{So that, } \frac{K_2}{K_1} = 3 \quad \text{and} \quad \frac{K_3}{K_2} = 3 \quad \text{and therefore} \quad \frac{K_3}{K_1} = 9,$$

by the statistical effect. The measured values were $\frac{K_3}{K_1} = 11$.

It was possible to calculate K_2 also by the use of successive approximation with the data from the solutions with either primarily the mono- or the tris-complex. Since the K_1 and K_3 values are not precisely known, these calculations for K_2 are not included. However, the values estimated for K_2 in this fashion are approximately, 8×10^{-9} . It is therefore possible to estimate the value of the $K_1 K_2 K_3$:

$$K = \frac{[M^{++}][F_3]^{-3}}{[MF_3^{++}]} = K_1 K_2 K_3 = 5.6 \times 10^{-25}$$

$$pK = 24.3$$

The pK value for this complex is much greater than that previously reported (13). Attention has frequently been called to the unusually high stability

of tris(1,10-phenanthroline)iron(II) ($pK = 21.3$) but it is now seen that nickel(II) forms a stronger complex with 1,10-phenanthroline than does iron(II). The values reported for the stability of the other transition metal ions with 1,10-phenanthroline indicate a much different sequence than the usual order for divalent metals, which is $Mn < Fe < Co < Ni < Cu > Zn$ (18). Copper(II) and cobalt(II) both form weaker complexes than iron(II) and nickel(II). The iron and nickel systems are distinct both in their stabilities and in their sluggish reactions.

F. Summary

The mono-, bis-, and tris(1,10-phenanthroline)nickel(II) reactions have been shown to be slow. The rates of formation and dissociation of the mono(1,10-phenanthroline)nickel(II) complex can be expressed by an acid dependent expression. Thus, the observed rate of formation constant is:

$$k_o = \frac{[H^+] + m}{n[H^+] + p}$$

and the observed rate of dissociation constant is:

$$k'_o = \frac{[H^+] + q}{r[H^+] + s}$$

where m , n , p , q , r and s are constants for each particular 1,10-phenanthroline. With 1,10-phenanthroline the following values have been determined:

$$\begin{array}{ll} m = 0.0043 & q = 0.015 \\ n = 0.435 \times 10^6 & r = 0.14 \times 10^3 \\ p = 0.0431 \times 10^6 & s = 0.060 \times 10^3 \end{array}$$

where m , n , and p are known more accurately than q , r and s .

The above kinetic expressions can be derived by assuming the reaction to consist of a hydrogen ion dependent path and a hydrogen ion independent path. There are two possible mechanisms for the hydrogen ion dependent path, one involving reaction between the phenanthrolium ion and nickel ion with subsequent loss of the proton, and the other involving an acid catalyzed displacement of the second water molecule from the nickel ion.

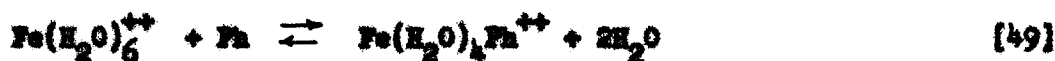
The rates of formation of the mono-complexes of substituted 1,10-phenanthrolines with nickel(II) are not very sensitive to changes in the nucleophilic character of the ring nitrogens. For a fortyfold change in the value of the acid dissociation constant of the substituted 1,10-phenanthroline, the rate of formation constant, k_{1f} , changes only threefold. It appears that the rates of formation of the bis- and tris-complexes behave similarly to the mono-complex.

An overall equilibrium constant has been calculated for tris-(1,10-phenanthroline)nickel(II), $pK = 24.2$.

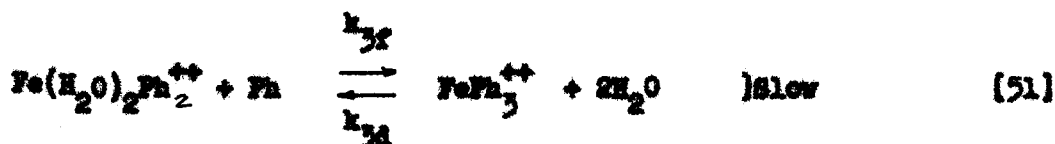
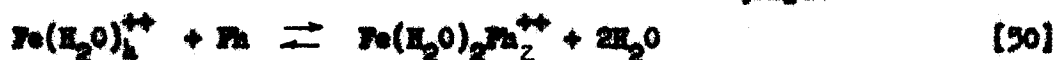
IV. IRON(II) WITH THE 1,10-PHENANTHROLINES

A. Introduction

The iron(II)-1,10-phenanthrolines and the similar 2,2'-bipyridine systems have been studied by a number of workers(15, 20, 21, 22, 23), and it has been well established that the rate of formation of tris(1,10-phenanthroline)iron(II), commonly called ferroin, consists of two rapid reactions followed by a rate determining reaction between the bis(1,10-phenanthroline)iron(II) complex and 1,10-phenanthroline. The reactions may be written:



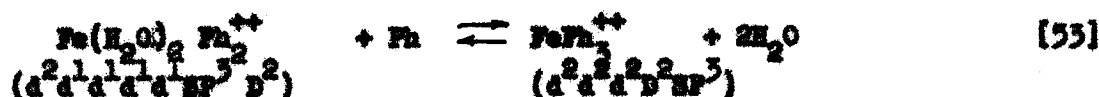
]Rapid



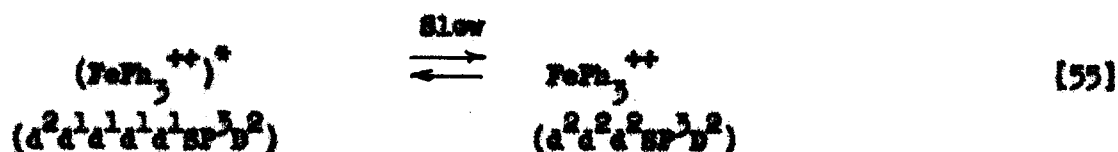
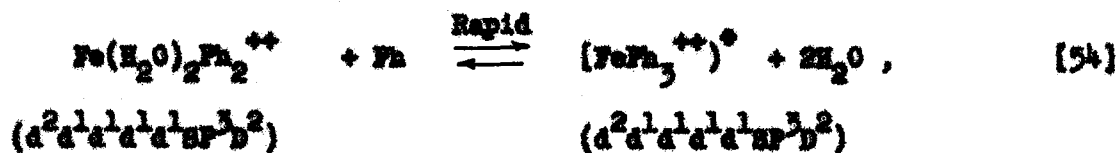
Magnetic studies indicate (1) that the last reaction involves the following change in electronic structure of the iron:



It is of interest to consider at what point in the formation of ferroin the electronic transition given in Equation [52] takes place. Two general mechanisms are possible. The transition in electronic structure may occur simultaneously with the addition of the third 1,10-phenanthroline molecule as shown in Equation [53].

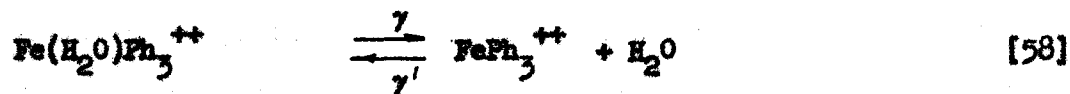
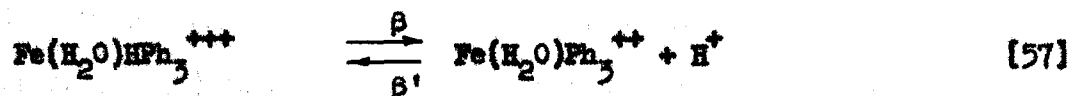
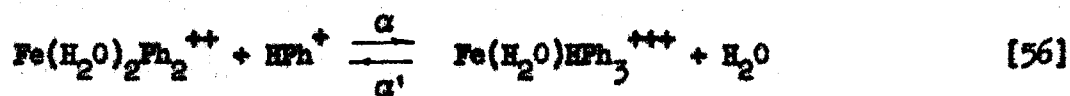


Another possible mechanism is the addition of the third 1,10-phenanthroline molecule to the iron(II) to form an unstable intermediate, with an outer orbital configuration. The intermediate then forms the stable ferroin by the pairing of the iron electrons. This is shown in Equations [54] and [55].



It might be possible to distinguish between these two mechanisms by comparing the reaction rates of substituted 1,10-phenanthrolines. If the reaction is a direct conversion of the outer orbital complex to the inner orbital complex, simultaneous with the 1,10-phenanthroline replacement of the water molecules, as in Equation [53], then the rate of reaction could be expected to vary significantly with the nucleophilic character of the incoming 1,10-phenanthroline. On the other hand, if an outer orbital intermediate is formed as in Equations [54] and [55], the reaction rate may not be very sensitive to changes in the nucleophilic character of the incoming 1,10-phenanthroline. A comparison of reaction rates of substituted 1,10-phenanthrolines with iron(II) is available from the work of Brandt and Gallstrom (8). However, before considering these data it is helpful to compare the iron(II) and nickel(II) systems with respect to the effect of hydrogen ion on the reaction rate.

Because of the rapidity of the rate of ferroin formation, these reactions, like those of 1,10-phenanthroline with nickel, have been studied in strongly acid solutions. Therefore, a hydrogen ion dependent reaction rate might be expected with iron as with nickel in Equations [19a-d] or [22a-d]. The following equations can be written without specifying the presence or absence of an outer orbital intermediate, but showing the stepwise progress which the iron system might undergo if a hydrogen ion dependence similar to one of the nickel systems were operative.



Now it can be seen that if the general mechanism of the formation of ferroin does involve an outer orbital complex, which slowly undergoes electron pairing to form the final product, then all reactions preceding the last slow step would be kinetically unimportant. Equation [53] then would be actually two steps, the last one as in Equation [55] and the rates of α and β would not be important. Therefore, the existence of a hydrogen ion dependent reaction rate would indicate the absence of a mechanism as given in Equations [54] and [55].

Past workers have stated that the dissociation of ferroin is hydrogen ion independent and that the hydrogen ion concentration affects the rate of formation only through buffering action with 1,10-phenanthroline.

However, the work of Krumholz (22) with the very similar iron(II)-bipyridine reaction indicates a definite hydrogen ion dependent reaction. His suggested mechanism has been discussed earlier in connection with the nickel(II)-1,10-phenanthroline reaction. It is simply a combination of two reactions:



and



The difficulty with this suggestion is that the observed rate constant should continue to increase with increasing acidity, whereas, actually it levels off at high acid strength(3). The tendency for the rate constant to be nearly constant at high acidity may account for the failure of previous workers to notice a hydrogen ion dependent reaction rate for the ferroin system. The following experimental work deals only with the proof that the observed rate constant for the formation of ferroin is smaller at low acidities than the values reported at high acidities. The substituent effect is discussed later.

B. Experimental

The rate of formation of ferroin was followed spectrophotometrically at 510 m μ and 25°C. and in 10⁻² molar perchloric acid solution. In 0.5 molar sulfuric acid, Kolthoff and others (8, 24) were able to use excess 1,10-phenanthroline and excess iron(II) so that the rate of formation of ferroin was zero order and easy to calculate. The reaction at 10⁻² molar perchloric acid concentration was so fast, due to the higher concen-

tration of unprotonated 1,10-phenanthroline, that it was not possible to use a large excess of either 1,10-phenanthroline or iron(II). This makes the calculation of the rate constant more difficult. The rate of reaction can be expressed as follows, where the dissociation reaction is neglected and k_o , the observed rate constant, is used in place of k_{32} . By definition, k_o may be acid dependent but k_{32} is independent of acidity.

$$\frac{d[\text{FePh}_3^{++}]}{dt} = k_o [\text{Fe}^{++}] [\text{Ph}]^3 = k_o \left(\frac{K_a}{[\text{H}^+]} \right)^3 [\text{Fe}^{++}] [\text{HPh}^+]^3, \quad [61]$$

$$\frac{d[\text{FePh}_3^{++}]}{dt} = k_o \left(\frac{K_a}{[\text{H}^+]} \right)^3 [\text{Fe}_T - (\text{FePh}_3^{++})] [\text{Ph}_T - 3(\text{FePh}_3^{++})] \quad [62]$$

It is possible to integrate this expression leading to the following equation:

$$\begin{aligned} \left(\frac{K_a}{[\text{H}^+]} \right)^3 k_o t &= \frac{3 (\text{Ph}_T - \text{Fe}_T)}{2(\text{Ph}_T - 3\text{Fe}_T)^2 \text{Ph}_T} + \frac{2.3}{(\text{Ph}_T - 3\text{Fe}_T)^3} \\ &\log \left[\frac{\text{Ph}_T - 3[\text{FePh}_3^{++}]}{\text{Fe}_T - [\text{FePh}_3^{++}]} \times \frac{\text{Fe}_T}{\text{Ph}_T} \right] - \frac{1}{2(\text{Ph}_T - 3\text{Fe}_T)(\text{Ph}_T - 3[\text{FePh}_3^{++}])^2} \\ &- \frac{1}{(\text{Ph}_T - 3\text{Fe}_T)^2 (\text{Ph}_T - 3[\text{FePh}_3^{++}])}. \end{aligned} \quad [63]$$

Since this expression cannot be conveniently graphed, it was used in order to confirm the value of k_o estimated by using a zero order plot. A good estimate of k_o was possible from a zero order plot provided only a small fraction of the progress of the reaction was followed.

$$k_o = \left(\frac{[H^+]}{K_a} \right)^3 \frac{1}{Fe_T \cdot (Ph_T)^3} \frac{[FePh_3^{++}]}{t} \quad [64]$$

The iron(II) solution was prepared and analyzed as described on page 8 . The 1,10-phenanthroline stock solution used was 2.306×10^{-3} molar. The 1,10-phenanthroline, perchloric acid and water were mixed and brought to 25°C. Five milliliters of the stock solution of iron(II) were diluted to 100 milliliters and then five milliliters of the dilute solution were added to the 1,10-phenanthroline solution, thoroughly mixed and a portion transferred to an optical cell. The aliquot for analysis of the iron(II) solution and the aliquot for the rate study were taken at the same time. The data for these rate studies are presented in Tables 42 and 43. The k_o value in Table 42 was calculated from Equation [63]. Figure 47 is typical of both of these rate studies, where the ferroin concentration is plotted against reaction time. The failure of the plot to pass through the origin was due to the initial slight yellow color of the 1,10-phenanthroline solution as well as to the approximations of Equation [64]. The incorporation of the dissociation rate expression into the zero order plot does not appreciably alter the estimated value of k_o whether k_{3d} is chosen as 0.0045 min^{-1} or one-fifth of this value. According to George (17), the oxidation of iron(II) to iron(III) during this reaction would be negligible.

C. Discussion

It is obvious that the observed rate of formation constant for ferroin does decrease with decreasing acidity. The value given in 0.5

Table 42. Spectrophotometric Data and Calculation of Reaction 5*

$[K^+]$	$= 9.25 \times 10^{-5}$	510m μ
Ph_T	$= 1.500 \times 10^{-4}$	2-cm. cell
Fe_T	$= 2.55 \times 10^{-5}$	$\epsilon_{FePh_3} = 1.157 \times 10^4$

Time (min.)	A_o	$[FePh_3^{++}] \times 10^7$
2.18	0.014	6.15
2.50	0.0165	7.25
3.50	0.022	9.56
4.50	0.0235	10.32
4.58	0.026	11.42
5.00	0.0285	12.52
6.50	0.0515	15.84
7.50	0.055	15.40
8.00	0.056	15.82
8.50	0.058	16.70

Table 43. Spectrophotometric Data and Calculation of Reaction 35

$[H^+]$	$= 9.82 \times 10^{-3}$	510m μ
Fe_T	$= 1.300 \times 10^{-4}$	5-cm. cell
Fe_T	$= 2.86 \times 10^{-5}$	$^c FeFe_3 = 1.157 \times 10^4$

Time (min.)	A_0	$[FeFe_3^{++}] \times 10^7$	k_0 (as calculated by Equation [65])
2.13	0.0345	6.07	2.95×10^{18}
2.50	0.038	6.69	2.84×10^{18}
2.85	0.0415	7.31	2.74×10^{18}
3.28	0.047	8.28	2.73×10^{18}
3.65	0.050	8.80	2.92×10^{18}
3.95	0.052	9.15	2.74×10^{18}
4.57	0.058	10.29	2.64×10^{18}
4.96	0.061	10.72	2.57×10^{18}
5.28	0.065	11.10	2.48×10^{18}
5.75	0.675	11.51	2.26×10^{18}
6.27	0.70	12.30	2.34×10^{18}
6.58	0.73	12.85	2.29×10^{18}
7.80	0.80	13.72	2.10×10^{18}
8.17	0.82	13.72	
8.65	0.85	14.96	

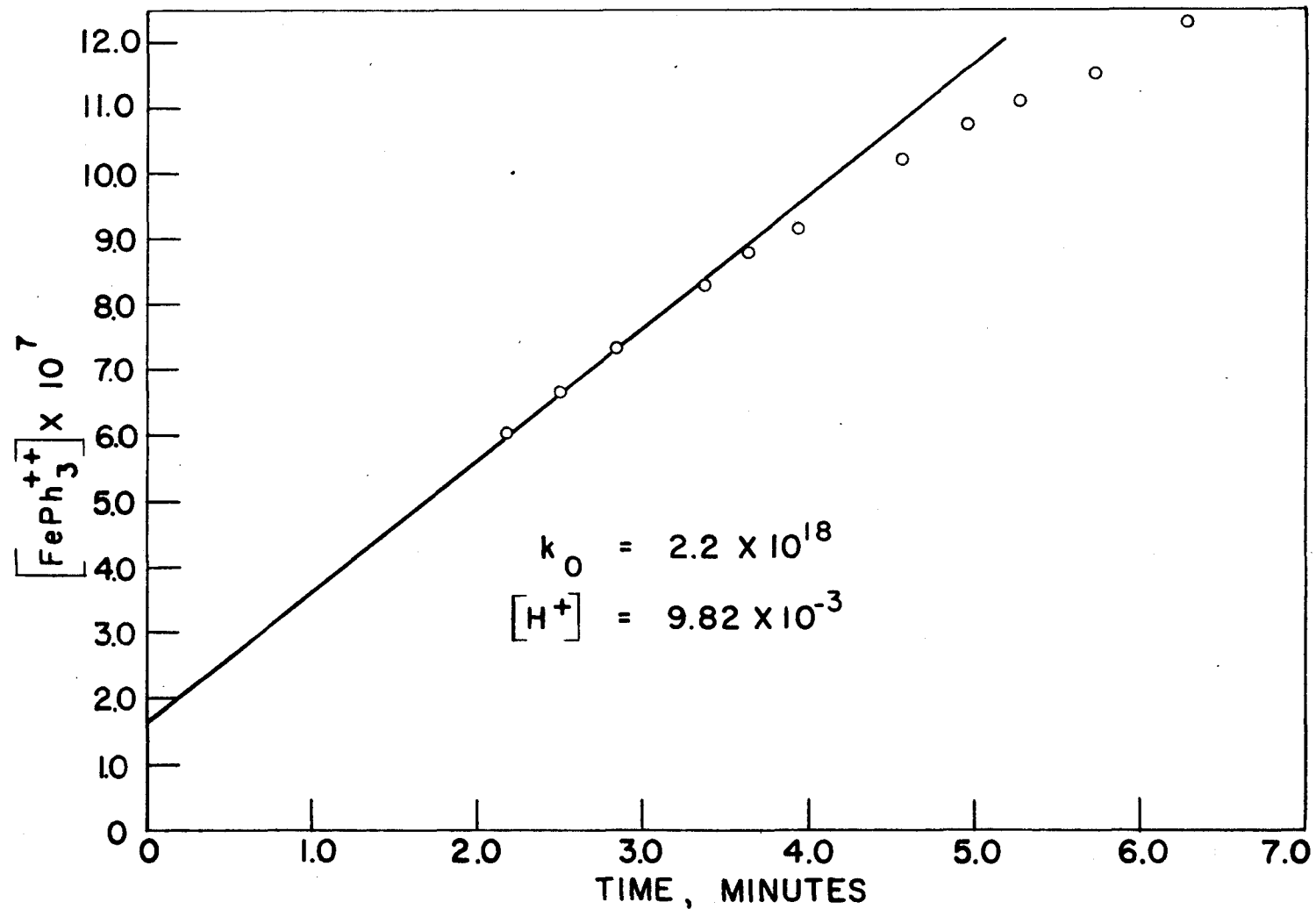


FIGURE 47, REACTION NO.35

molar sulfuric acid is $1.3 \times 10^{19} \text{ min}^{-1}$ (24) while the value in 0.01 molar perchloric acid is approximately $2.5 \times 10^{18} \text{ min}^{-1}$. It can also be seen that the degree of change of the rate constant with acidity is approximately the same as with nickel(II). This fact and the fact that the observed rate constant is nearly invariant at high acidity strongly suggests a mechanism of the type given in Equations [56, 57, and 58]. Therefore, an outer orbital intermediate of the type, $(\text{FePh}_3^{++})^*$ would not represent a kinetically significant step in the reaction process. However, an unstable intermediate of the type, $\text{Fe}(\text{H}_2\text{O})\text{Ph}_3^{++}$ is indicated.

It is now possible to examine the effect of substituents on the reaction rate from a more enlightened viewpoint. The work of Brandt and Gullstrom (8) is summarized in Figure 48 where $\log k_0$, the observed rate constant, is plotted against the $\text{p}K_a$ of the substituted 1,10-phenanthroline. At first inspection, it appears that the substituent effect is much larger for iron(II) than for nickel(II), since the rate constant changes one hundred and sixtyfold from 5-nitro-1,10-phenanthroline to 1,10-phenanthroline. However, it must be remembered that k_0 is the overall rate constant which is related to k_{3f} as follows:

$$k_0 = \frac{1}{K_1 K_2} \frac{[\text{H}^+] + n}{n[\text{H}^+] + p} \quad (65)$$

where it is assumed that the hydrogen dependence is the same as with nickel(II). In Equation [65], the values of K_1 , K_2 , n , and p are all variable for different substituted 1,10-phenanthrolines. In order to measure k_{3f} a detailed study of the hydrogen ion dependence of k_0 must

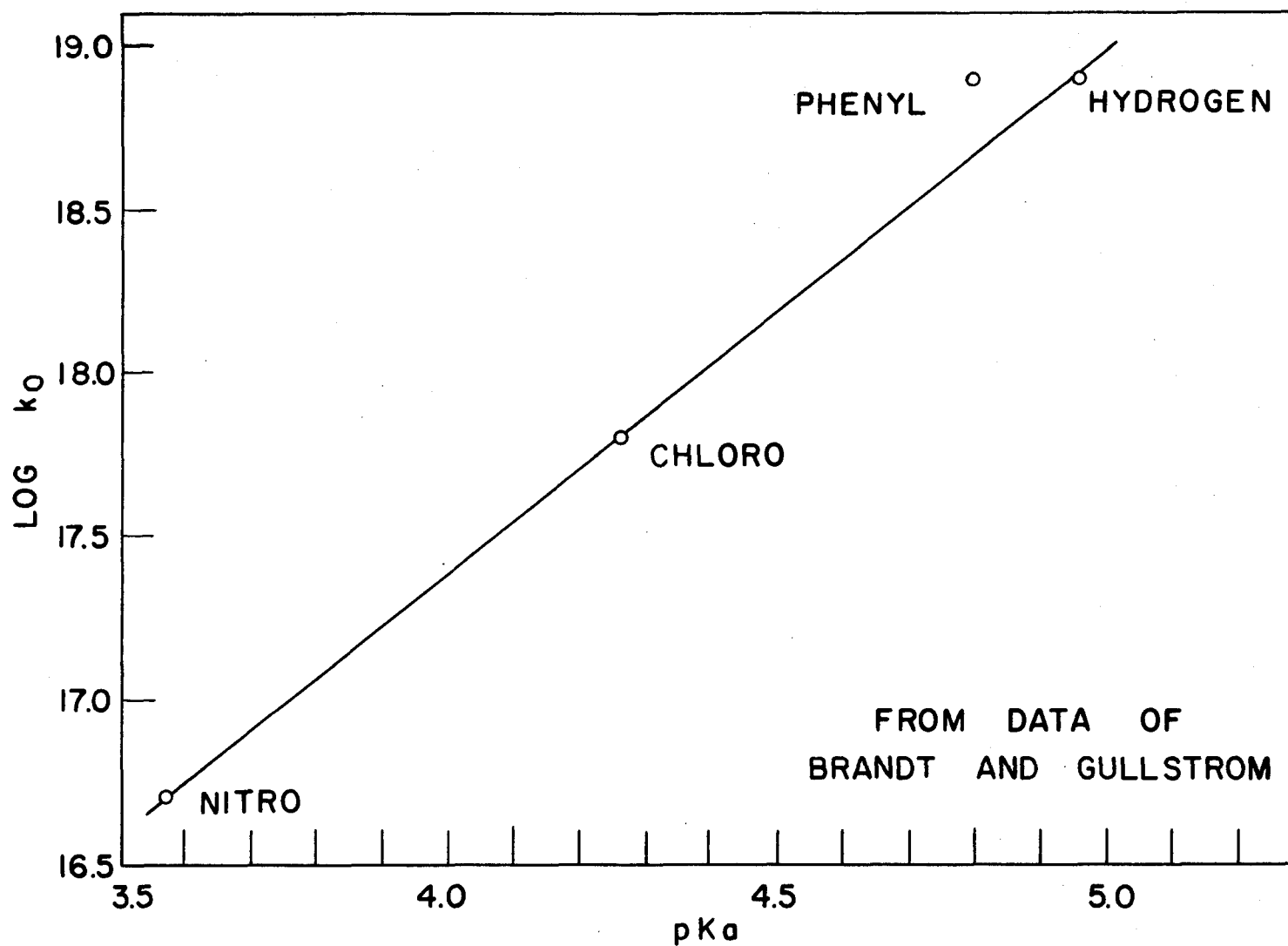


FIGURE 48, SUBSTITUENT EFFECT ON THE FORMATION RATE CONSTANT OF THE IRON(II) TRISPHEANTHROLINE COMPLEXES

be made as well as the measurement of the equilibrium constants, K_1 and K_2 , for each of the substituted 1,10-phenanthrolines. These projects are beyond the scope of the present work, but some interesting approximations can be made.

The ratio of observed rate constants of 1,10-phenanthroline to 5-nitro-1,10-phenanthroline can be simplified in terms of their respective k_{3r} values by assuming that the hydrogen ion dependence of the two 1,10-phenanthrolines to be nearly equal as shown in Equation [66].

$$\frac{k_o(\text{Ph})}{k_o(\text{NO}_2\text{Ph})} = 160 = \frac{K_1(\text{NO}_2\text{Ph})K_2(\text{NO}_2\text{Ph})}{K_1(\text{Ph})K_2(\text{Ph})} \times \frac{k_{3r}(\text{Ph})}{k_{3r}(\text{NO}_2\text{Ph})} \quad [66]$$

In order to determine the desired ratio, $k_{3r}(\text{Ph})/k_{3r}(\text{NO}_2\text{Ph})$, the values of K_1 and K_2 for each of the 1,10-phenanthrolines with iron(II) must be estimated. But only the product $K_1K_2K_3$ is known for both 5-nitro-1,10-phenanthroline and 1,10-phenanthroline with iron(II). The ratios are given in Equation [67]:

$$\frac{K_1K_2K_3 \text{ for NO}_2\text{Ph}}{K_1K_2K_3 \text{ for Ph}} = 3160 \quad [67]$$

If the differences in strength of the 5-nitro-1,10-phenanthroline complexes and 1,10-phenanthroline complexes are about the same for the mono-, bis- and tris-complexes, then

$$\frac{K_1(\text{NO}_2\text{Ph})K_2(\text{NO}_2\text{Ph})}{K_1(\text{Ph})K_2(\text{Ph})} = (3160)^{2/3} = 215 \quad [68]$$

A comparison can also be made to the equilibrium constants with the nickel(II) ion and hydrogen ion:

$$\text{with Ni(II):} \quad \frac{K_1(\text{NO}_2\text{Ph})}{K_1(\text{Ph})} = 10, \quad [69]$$

$$\text{and with H}^+: \quad \frac{K_1(\text{NO}_2\text{Ph})}{K_1(\text{Ph})} = 24.6 \quad [70]$$

All of these estimates indicate that the ratio desired is of the order of magnitude of 10^2 . If this is the case, then it can be seen from Equation [66] that the formation constant, k_{3f} , is nearly the same for 5-nitro-1,10-phenanthroline as for 1,10-phenanthroline. It appears that the value of k_{3f} is not very sensitive to changes of the nucleophilic character of the ring nitrogens. In this respect the iron(II) and nickel(II) systems are similar.

The preceding data seem contradictory with regard to distinguishing the type mechanism suggested in Equation [53] from that in Equations [54] and [55]. The hydrogen ion dependence seems to eliminate the latter mechanism, while the substituent effect seems to support this mechanism. An intermediate of the type, $\text{Fe}(\text{H}_2\text{O})\text{Ph}_3^{++}$ can be logically proposed during the stepwise formation of the 1,10-phenanthroline bonds. However, the 1,10-phenanthroline nitrogen would be expected to form a stronger bond in such an intermediate than the 5-nitro-1,10-phenanthroline nitrogen. Hence for k_{3f} to remain constant, the activation energy involved in the transition of this intermediate to ferriin must be less for 5-nitro-1,10-phenanthroline than for 1,10-phenanthroline. This seems conceivable only from the point of view that double bond formation would be easier with 5-nitro-1,10-phenanthroline than with 1,10 phenanthroline.

A great deal of work must be done in order to examine the actual effect of the nucleophilic strength of 1,10-phenanthrolines on the activation energy of the ferrous reaction. However, when K_1 , K_2 and the hydrogen ion dependence are known for this reaction, it should be possible to come to a much better understanding of the nature of slow chelate reactions.

Using the k_p value for the ferrous reaction at low acidity so that the hydrogen ion terms are not important and pK_1 value equal to 5.9 (21), it is possible to estimate that k_{2f} is equal to or greater than $4 \times 10^6 \text{ min}^{-1}$ by assuming that K_2 is equal to or greater than K_1 . In the nickel(II) system the k_{1f} value is equal to $2 \times 10^5 \text{ min}^{-1}$. The activation energy in bringing a third 1,10-phenanthroline molecule around iron(II) and in pairing the 3d electrons is seen to be less than that required to react one molecule of 1,10-phenanthroline with nickel(II).

V. VANADIUM(IV) WITH THE 1,10-PHENANTHROLINES

A. Introduction

The reaction between vanadium(IV) perchlorate and 1,10-phenanthroline proceeds at a measurable rate in acid solutions. In fact, the reaction is sufficiently slow to allow the separation of trace amounts of iron as ferroin from vanadium solutions (25). With both nickel(II) and vanadium(IV) the mono-1,10-phenanthroline complex is slow to form, while with iron(II) the tris-1,10-phenanthroline complex is the slow step.

According to Taube's correlation of reaction rates to electronic structure (35), vanadium(IV) should be labile in its reactions rather than sluggish. It might be possible to rationalize the vanadium(IV) behavior to Taube's requirements if the vanadyl ion (VO^{4+}) is considered to have a double bond between the vanadium and oxygen. However, the only slow vanadium(IV) reaction known is with 1,10-phenanthroline.

In the following work it is shown that the mono(1,10-phenanthroline)vanadium(IV) complex is the predominant species present in acid solution. The rates of reaction of 1,10-phenanthroline, 5-methyl-1,10-phenanthroline and 5-nitro-1,10-phenanthroline with vanadium(IV) are measured in 0.5 molar perchloric acid solution. These rates are compared to similar studies with nickel(II) and iron(II). These data are available through the cooperation of R. Eystroff (10) and are only summarized here.

B. Experimental

Both the ultraviolet and visible regions are suitable for the

study of the vanadium(IV)-1,10-phenanthroline complexes. Figure 49 shows the ultraviolet absorption spectra of 1,10-phenanthroline with varying amounts of vanadium(IV) in 0.01 molar perchloric acid. Absorbance measurements taken at 280 and 272m μ were used to determine the ratio of chelate to metal ion in the customary manner of continuous variations (19). The data for these plots are presented in Table 44 and in Figures 50 and 51.

The rates of formation of the mono(1,10-phenanthroline)vanadium(IV) complexes were studied in excess vanadium(IV) at 426m μ . Reactions 36, 37 and 38 are performed with vanadium(IV) and 1,10-phenanthroline, 5-methyl-1,10-phenanthroline and 5-nitro-1,10-phenanthroline, respectively. These data are presented in Tables 45, 46, and 47 and in Figure 52. Equation [11] was used for the calculation of these rates of formation:

$$\frac{d[\text{VOPh}^{++}]}{dt} = k_o [\text{VO}^{++}][\text{Ph}] \quad [71]$$

$$k_o^{\dagger} = \frac{2.3[\text{H}^+]}{K_a[\text{VO}^{++}]_T} \log \frac{\text{Ph}_T}{\text{Ph}_T - [\text{VOPh}^{++}]} \quad [72]$$

where a non-reversible first order reaction was assumed for the initial reaction progress. The observed absorbance, A_o , was corrected for absorbance due to vanadium(IV), c , so that:

$$[\text{VOPh}^{++}] = \frac{A_o - c}{c_{\text{VOPh}}^{\dagger} l} \quad [73]$$

where $c_{\text{VOPh}}^{\dagger}$ is the molar absorptivity and l is the path length. Using Equations [72] and [73] and $a = c_{\text{VOPh}}^{\dagger} l \times \text{Ph}_T$ it can be shown that:

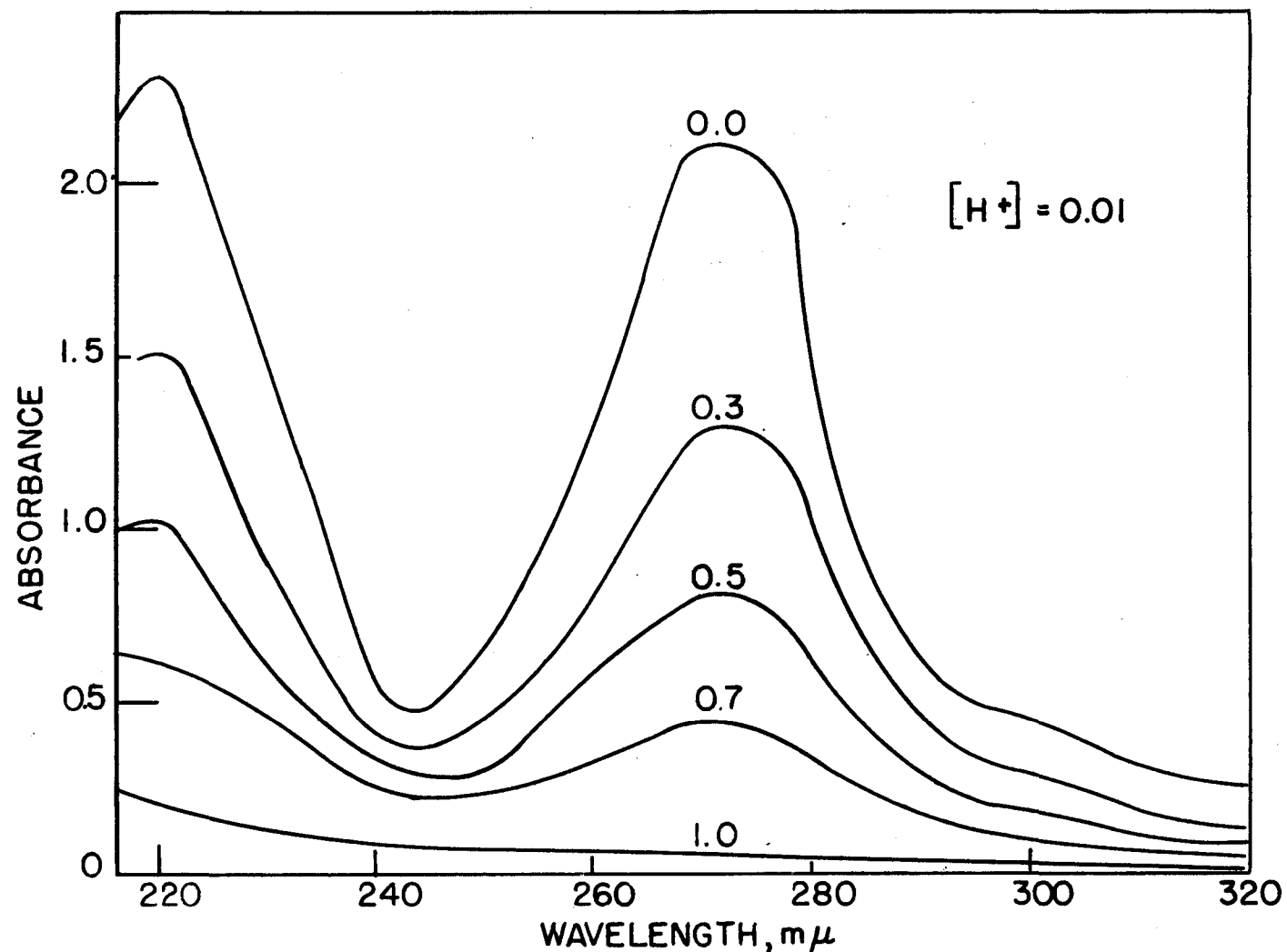


FIGURE 49, ABSORPTION SPECTRA OF PHENANTHROLINE WITH VANADIUM (IV) FOR JOB'S PLOT

Table 44. Spectrophotometric Data
for Job's Continuous Variations with
Vanadium(IV) and 1,10-Phenanthroline

$$Y = (1 - x)A_{Ph} + xA_{VO} - A_0,$$

where

A_{Ph} and A_{VO} are at $x=0$ and $x=1$, respectively.

$$x = \frac{[VO^{++}]}{[VO^{++}] + [Ph]}$$

x	Y 220m μ	Y 272m μ
0	0	0
0.1	0.117	0.085
0.2	0.170	0.159
0.3	0.1711	0.187
0.4	0.217	0.256
0.5	0.216	0.246
0.6	0.225	0.257
0.7	0.200	0.228
0.8	0.147	0.176
0.9	0.1055	0.117
1.0	0	0

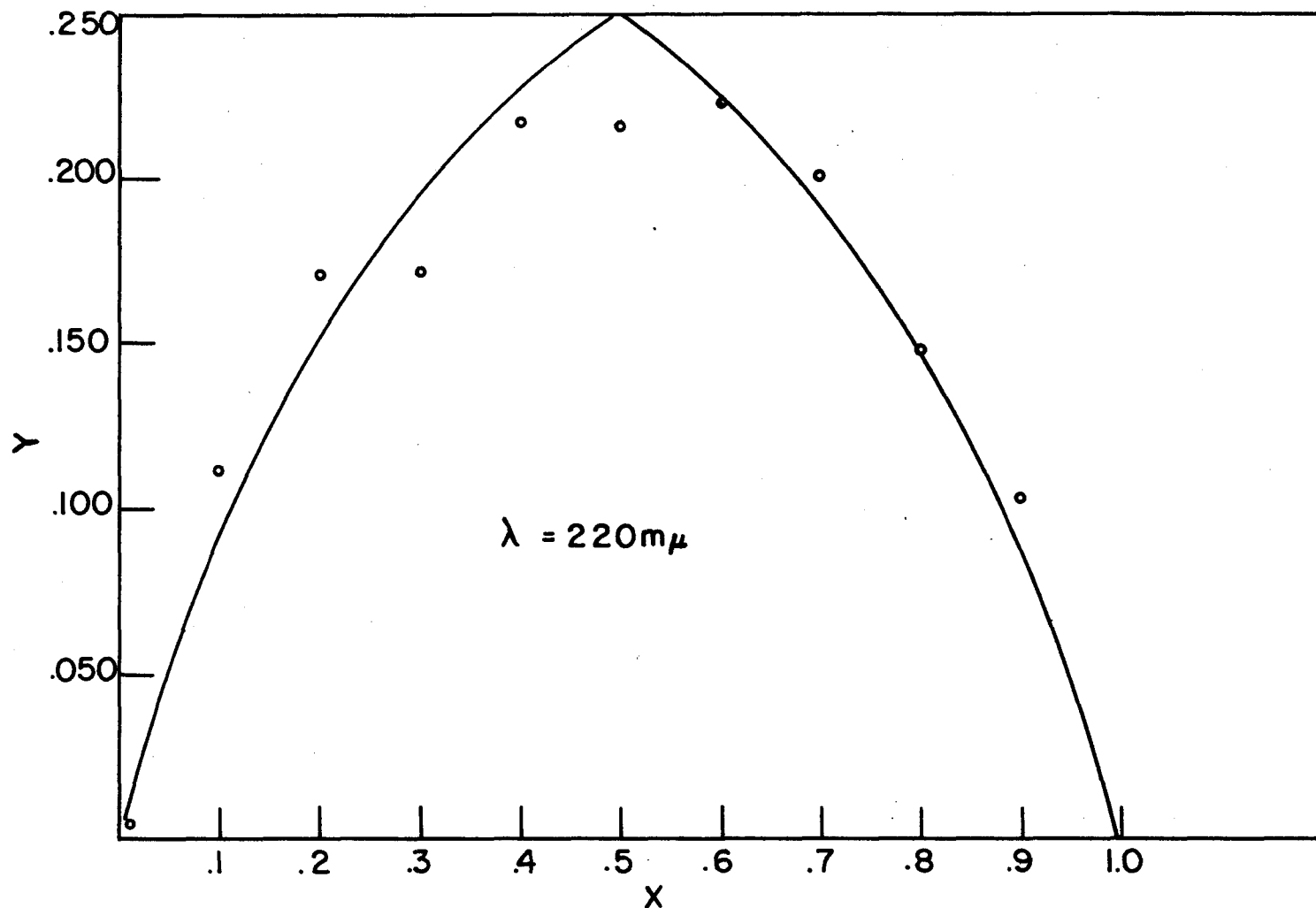


FIGURE 50, CONTINUOUS VARIATIONS FOR PHENANTHROLINE AND VANADIUM (IV)

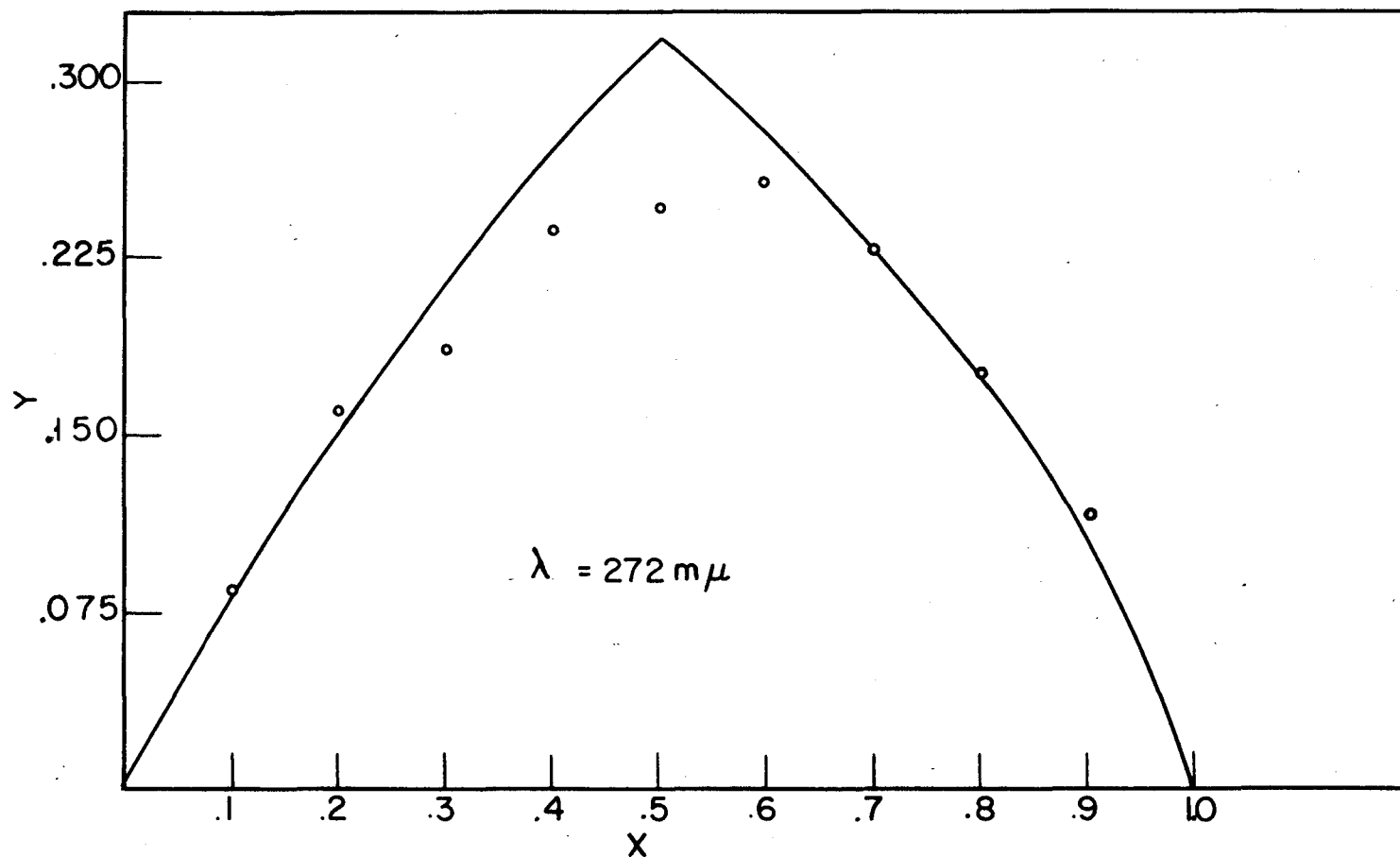


FIGURE 51, CONTINUOUS VARIATIONS
FOR PHENANTHROLINE AND VANADIUM (IV)

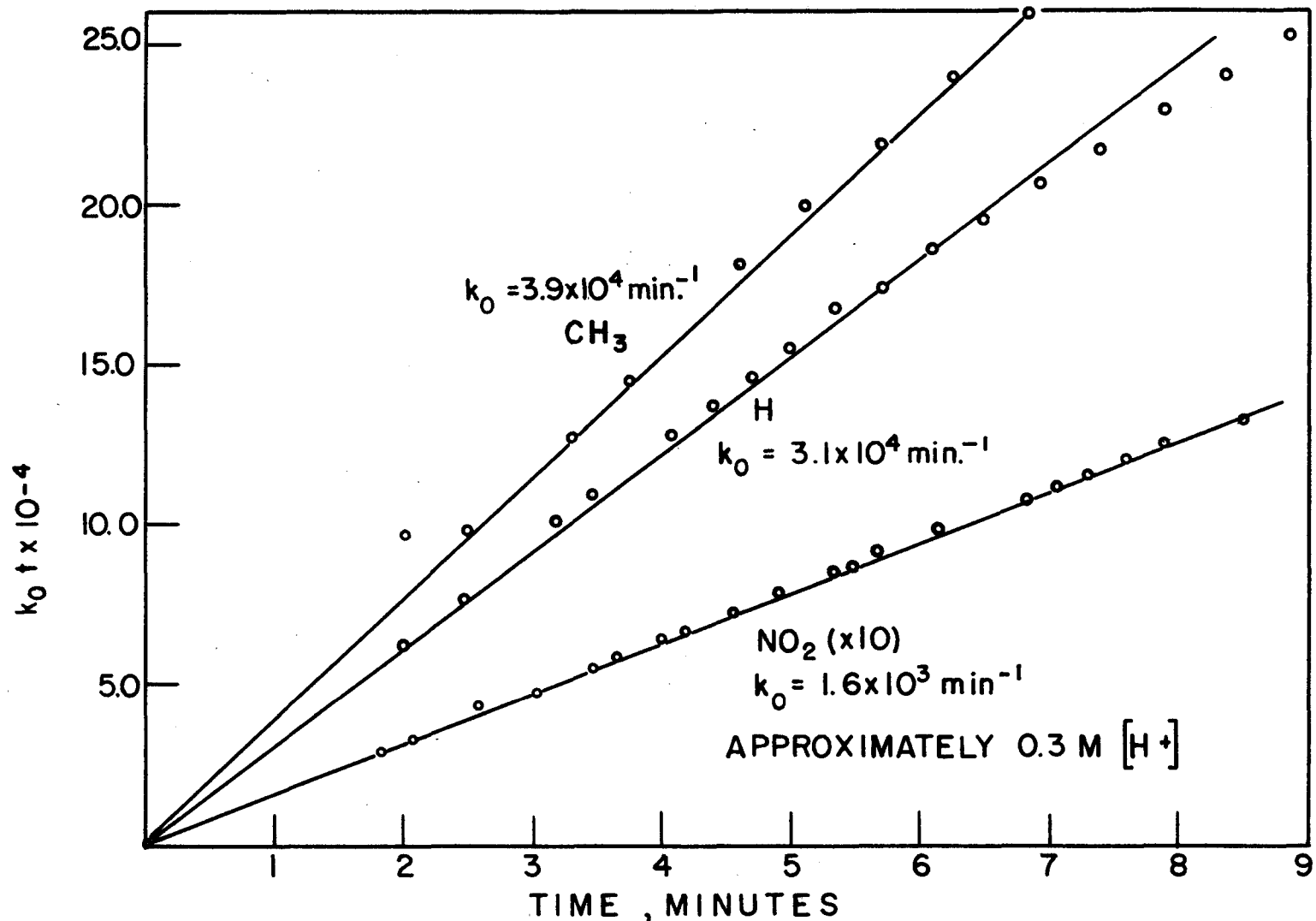


FIGURE 52, RATES OF FORMATION OF VANADIUM (IV) WITH THE PHENANTHROLINES

Table 45. Spectrophotometric Data
and Calculation of Reaction 36

426 m μ , 10-cm. cell

$$[K^+] = 0.266$$

$$[VO^{++}] = 6.47 \times 10^{-2}$$

$$[Fe]_T = 1.05 \times 10^{-3}$$

$$k_0 t = 8.60 \times 10^5 \log \frac{.297}{.315 - A_0}$$

Time (min.)	A_0	$\log \frac{.297}{.315 - A_0}$	$k_0 t$
2.00	0.065	0.072	6.2×10^4
2.47	0.075	0.090	7.7×10^4
3.18	0.090	0.118	10.1×10^4
3.45	0.095	0.127	10.9×10^4
4.05	0.105	0.148	12.7×10^4
4.58	0.110	0.158	13.6×10^4
4.68	0.115	0.170	14.5×10^4
5.00	0.120	0.180	15.5×10^4
5.33	0.125	0.194	16.7×10^4
5.70	0.130	0.203	17.4×10^4
6.08	0.135	0.215	18.5×10^4
6.47	0.140	0.227	19.5×10^4
6.92	0.145	0.239	20.6×10^4
7.40	0.150	0.252	21.7×10^4
7.90	0.155	0.266	22.9×10^4
8.35	0.160	0.279	24.0×10^4
8.88	0.165	0.294	25.3×10^4
9.45	0.170	0.308	26.5×10^4
10.05	0.175	0.324	27.8×10^4

Table 46. Spectrophotometric Data
and Calculation of Reaction 57

426m μ , 10 cm. cell

$$[H^+] = 0.285$$

$$[VO^{++}]_T = 6.47 \times 10^{-2}$$

$$[Mn^{2+}]_T = 1.069 \times 10^{-3}$$

$$k_0 t = 1.72 \times 10^6 \log \frac{.296}{.296 - A_0}$$

Time (min.)	A_0	$\log \frac{.296}{.296 - A_0}$	$k_0 t$
2.00	0.069	0.056	9.6×10^4
2.50	0.0715	0.057	9.8×10^4
3.30	0.080	0.074	12.7×10^4
3.75	0.085	0.084	14.4×10^4
4.60	0.095	0.1050	18.0×10^4
5.07	0.100	0.1160	19.9×10^4
5.70	0.105	0.1271	21.8×10^4
6.25	0.110	0.1388	23.9×10^4
6.85	0.115	0.1516	25.9×10^4
7.41	0.120	0.1627	27.9×10^4
7.98	0.125	0.1732	30.1×10^4

Table 47. Spectrophotometric Data and Calculation of Reaction 38

426m μ , 10 cm. cell

$$[H^+] = 0.280$$

$$[VO^{++}]_0 = 6.47 \times 10^{-2}$$

$$[NO_2Fe]_0 = 1.048 \times 10^{-3}$$

$$k_0 t = 3.69 \times 10^4 \log \frac{.427}{.497 - A_0}$$

Time (min.)	A_0	$\log \frac{.427}{.497 - A_0}$	$k_0 t$
1.82	0.140	0.077	2.87×10^3
2.07	0.150	0.090	3.32×10^3
2.58	0.165	0.1092	4.03×10^3
3.02	0.180	0.1293	4.77×10^3
3.47	0.195	0.1505	5.55×10^3
3.65	0.200	0.1577	5.82×10^3
4.00	0.210	0.1725	6.56×10^3
4.17	0.215	0.1801	6.65×10^3
4.55	0.225	0.1959	7.23×10^3
4.90	0.235	0.2119	7.82×10^3
5.28	0.245	0.2290	8.45×10^3
5.47	0.250	0.2377	8.77×10^3
5.68	0.255	0.2465	9.09×10^3
6.15	0.265	0.2648	9.77×10^3
6.82	0.280	0.2938	10.80×10^3
7.08	0.285	0.3041	11.20×10^3
7.31	0.290	0.3145	11.60×10^3
7.58	0.295	0.3250	12.00×10^3
7.89	0.300	0.3380	12.50×10^3
8.49	0.310	0.3586	13.20×10^3

$$k_t = \frac{2.3[X^*]}{K_0[VO^{4+}]_0} \log \frac{a}{a+c-A_0} \quad [74]$$

which is the form in which the data are presented.

C. Discussion

The Job's plots in Figures 50 and 51 indicate that mono(1,10-phenanthroline)vanadium(IV) is a stable complex and that it is the predominant complex formed between 1,10-phenanthroline and vanadium(IV) at this acidity. The lack of evidence of strong bis- or tris-complexes in these solutions seems significant. If vanadium(IV) is present as the vanadyl ion, where the oxygen is bound tightly to the vanadium, then the attraction of the metal ion for additional 1,10-phenanthroline molecules would be greatly decreased.

The rate of formation reactions is shown in Figure 52. As yet it is not known if these reaction rates have a hydrogen ion dependence such as with nickel(II) and iron(II).

The observed rate constant, k_0 , for the rate of formation of the mono-complex is much more dependent on the 1,10-phenanthroline substituents than in the reaction with nickel(II). This can be seen in Figure 53, where $\log k_0$ is plotted against pK_a . There is a twenty-fivefold difference in the value of the rate constants between 5-methyl-1,10-phenanthroline and 5-nitro-1,10-phenanthroline in 0.3 molar perchloric acid. This is approximately five times the effect of the same substituents on the rate of formation of the mono(1,10-phenanthroline)nickel(II) complex at this acidity.

The effect of the hydrogen ion concentration on the rate of formation

constants must be known before the actual substituent effect can be determined. However, the sensitivity of vanadium(IV) to the nucleophilic character of the 1,10-phenanthroline suggests a different type of reaction for vanadium(IV) than for iron(II) and nickel(II). The differences in behavior of these ions can be useful in their analytical separation.

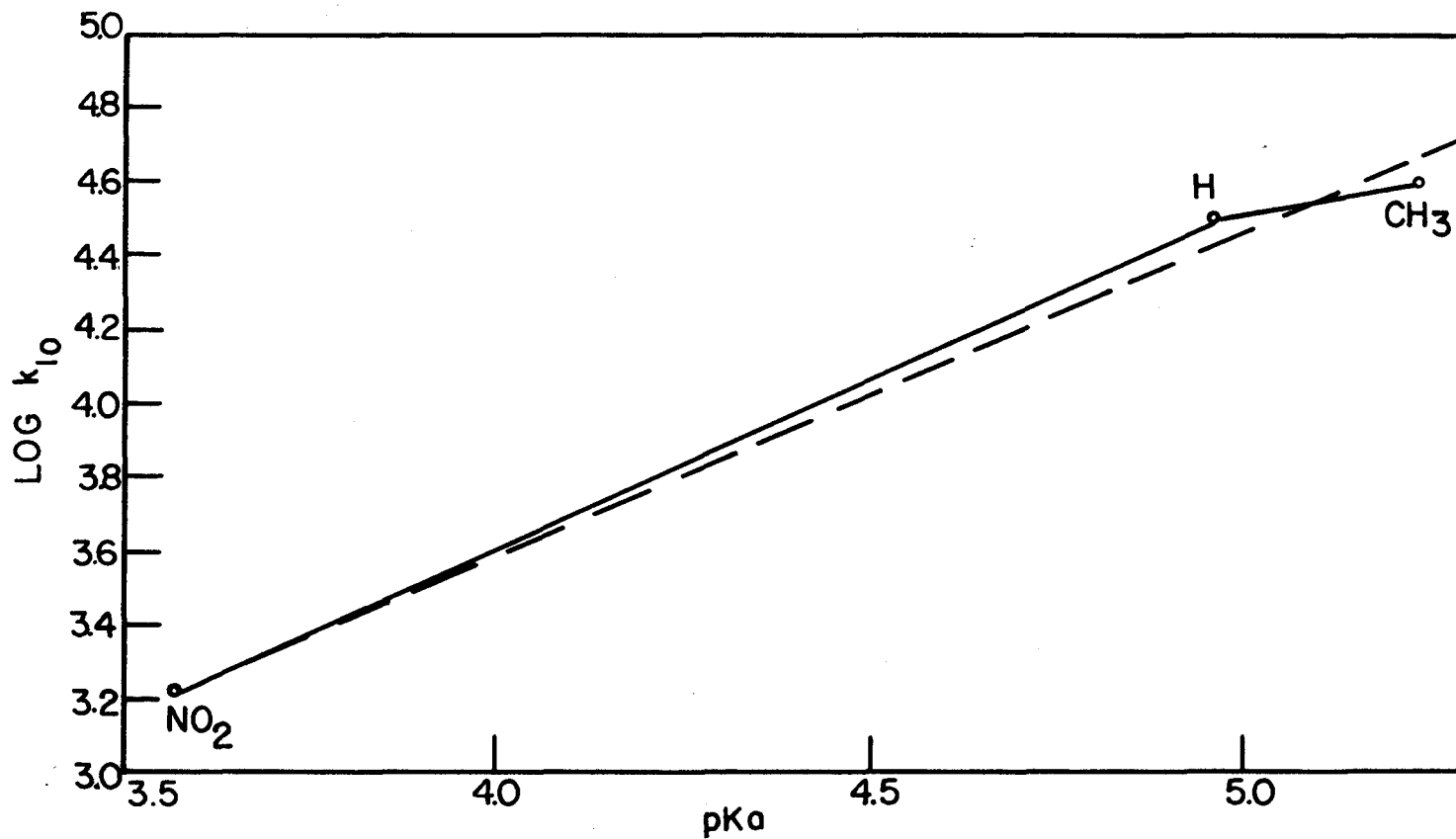


FIGURE 53, SUBSTITUENT EFFECT ON MONO(PHENANTHROLINE) VANADIUM(IV) RATE CONSTANT

VI. ANALYTICAL APPLICATION

In the preceding work the slow reactions of 1,10-phenanthroline with nichel(II), iron(II) and vanadium(IV) have been discussed at length. It is also known that the reaction of chromium(III) with 1,10-phenanthroline proceeds slowly. The copper(II) and zinc(II) reactions with 1,10-phenanthroline were investigated to confirm their reported rapid reaction rates (23). It was shown by visual and spectrophotometric tests with copper(II) and zinc(II), respectively, that the dissociation rate constant of the tris(1,10-phenanthroline)metal(II) complexes of these ions must exceed the following values:

$$\text{CuPh}_3^{2+} \quad k_M > 30 \text{ min}^{-1}$$

$$\text{ZnPh}_3^{2+} \quad k_M > 10 \text{ min}^{-1}$$

Hence the copper(II) dissociation reaction is at least 5×10^4 times as fast as the nichel(II) dissociation reaction.

The fact that the mono(1,10-phenanthroline) complexes of vanadium(IV), chromium(III), and nichel(II) are all slower to form than the tris(1,10-phenanthroline)iron(II) complex serves as the basis for the determination of iron in these metals. It is important that in each case the mono-complex forms slowly because this allows the ferroin to be formed without the use of a prohibitive amount of 1,10-phenanthroline. A short time after the addition of 1,10-phenanthroline to a solution containing vanadium(IV), chromium(III) or nichel(II) and trace amounts of iron(II), the iron(II) exists as ferroin while the other species are not appreciably changed. The analytical determination of iron then rests on the ability to take advantage of the entirely different nature of the other ions and

the iron(II) complex in a separation process before the other ions begin forming chelates. This is accomplished by an extraction of ferroin perchlorate into a nitrobenzene phase. The iron can then be determined spectrophotometrically as ferroin in the nitrobenzene. In this manner, trace quantities of iron can be separated from chromium(III), vanadium(IV) and nickel(II) solutions and analyzed with the usual accuracy of a spectrophotometric method. The procedure for these analyses is reported by Margerum and Banks (25).

Although the rate of ferroin formation is much less than the rates of reaction of 1,10-phenanthroline with nickel(II) and vanadium(IV), the latter rates are not negligible. If the nickel(II) or vanadium(IV) concentrations become too high the iron(II) is no longer quantitatively removed. It is possible to improve on these separations with the knowledge gained concerning the substituent effect in 1,10-phenanthroline chelate kinetics.

The effect of substituents on the 1,10-phenanthroline chelation rate depends upon the acidity because of the formation of the 1,10-phenanthrolium ion. If v_{Fe} , k_{Fe} and v_{Ni} , k_{Ni} are the velocities of formation and observed rate constants for ferroin and mono(1,10-phenanthroline)nickel(II), respectively, then:

$$\frac{v_{Fe}}{v_{Ni}} = \frac{k_{Fe}}{k_{Ni}} \frac{[Fe^{++}]}{[Ni^{++}]} [Ph]^2 \quad [75]$$

The initial velocities on mixing are:

$$\frac{v_{Fe}}{v_{Ni}} = \frac{k_{Fe}}{k_{Ni}} \frac{Fe_T}{Ni_T} [Ph_T]^2 \left(\frac{K_a}{[H^+] + K_a} \right)^2 \quad [76]$$

since $\text{Ph}_T = \text{HPh}^+ + \text{Ph}$ under these conditions. It can then be seen that for constant values of Fe_T , Ni_T and Ph_T , where Ph may be 1,10-phenanthroline, 5-methyl-1,10-phenanthroline or 5-nitro-1,10-phenanthroline with the corresponding K_a values,

$$\frac{v_{\text{Fe}}}{v_{\text{Ni}}} \propto \frac{k_{\text{Fe}}}{k_{\text{Ni}}} \left(\frac{K_a}{[\text{H}^+] + K_a} \right)^2 \quad [77]$$

Below pH 4 the term within the parentheses in Equation [77] becomes $K_a/[\text{H}^+]$ and above pH 6 it becomes 1. Therefore, above pH 6 the ratio of reaction velocities depends only on the ratio of the observed rate constant. Below pH 4, the ratio of reaction velocities at any given acidity depends on the square of the acid dissociation constant as well as on the rate constants. The velocities of formation of the iron(II) and nickel(II) complexes of 1,10-phenanthroline and 5-nitro-1,10-phenanthroline can be compared in strong acid. Using the values of k_{Fe} , k_{Ni} and K_a for 1,10-phenanthroline as $1.3 \times 10^{19} \text{ min}^{-1}$, $1.9 \times 10^6 \text{ min}^{-1}$ and 1.1×10^{-5} , respectively, and for 5-nitro-1,10-phenanthroline, $5.0 \times 10^{16} \text{ min}^{-1}$, $3.8 \times 10^5 \text{ min}^{-1}$ and 2.7×10^{-4} , respectively, it can be shown that:

$$\frac{\frac{v_{\text{Fe}}}{v_{\text{Ni}}} \text{ (5-nitro-1,10-phenanthroline)}}{\frac{v_{\text{Fe}}}{v_{\text{Ni}}} \text{ (1,10-phenanthroline)}} = 11 \quad [78]$$

Equation [78] means that in acid solutions the nitro derivative would give a better kinetic separation of iron(II) and nickel(II). Despite the larger rate constant for 1,10-phenanthroline as compared to 5-nitro-1,10-phenanthroline with iron(II), the smaller K_a value has the overruling

effect. If the effect of hydrogen ion concentration on the rate of formation of ferroin proves to be similar to that observed for the various 1,10-phenanthrolines with nickel(II), then Equation [78] would be true for all solutions below pH 4.

Above pH 6 the ratio v_{Fe}/v_{Ni} depends only on the ratio k_{Fe}/k_{Ni} . Unfortunately, the values of k_{Fe} are not known above pH 6 for the various 1,10-phenanthrolines. However, if these rates of reaction are assumed to be proportional to the rates in strong acid, then v_{Fe}/v_{Ni} is larger for 1,10-phenanthroline than for 5-nitro-1,10-phenanthroline by a factor of fifty. Hence, it appears that at high pH, 1,10-phenanthroline or 5-methyl-1,10-phenanthroline would give a better separation of iron(II) from nickel(II) than would 5-nitro-1,10-phenanthroline. This is the reverse of the effect at high acidity.

It can be seen from Equation [76] that, in general, the lower the acidity the greater the ratio, v_{Fe}/v_{Ni} . From this fact and the above discussion, the best separation of iron(II) and nickel(II) would be with 5-methyl-1,10-phenanthroline above pH 6. Actually this high pH is not practical due to the precipitation and oxidation of iron(II) and to the extraction of a nickel(II)nitrobenzene species (25). As long as the solution must be below pH 4 the best separation would be achieved using 5-nitro-1,10-phenanthroline in a solution as near to pH 4 as possible.

The same type of treatment can be applied to the determination of iron in vanadium. In this case if the vanadium(IV) rates can be extrapolated to higher pH values then 5-nitro-1,10-phenanthroline would be more suitable than 1,10-phenanthroline below pH 4 by a factor of 45 and

5-methyl-1,10-phenanthroline would be more suitable than 1,10-phenanthroline above pH 6.

It can now be seen that changes in the nucleophilic character of a chelate can have varying effects on the relative reaction rates of this chelate with different metal ions and that this can be put to analytical use. It should be possible to design chelates for particular kinetic separations. The 1,10-phenanthroline type chelate could be made more nucleophilic, for example, by the use of the 4,7-dimethyl derivative or much less nucleophilic by using the 4,4'-dibromo- or 4,4'-dinitro-2,2'-bipyridine molecule. The chelate 2,2',2''-terpyridine deserves investigation. It holds two protons in acid solution (9) and should have pronounced differences of rate in acid and base. The exchange rate of $\text{Co}(2,2',2''\text{-terpyridine})_2^{++}$ with Co(II) has been reported (39) to be slow, which introduces another possible kinetic separation. Compounds of entirely different nucleophilic character such as, 1,2-phenylenebisdimethylarsine offer additional areas of investigation.

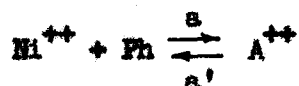
Other analytical applications of the chelate reactions, which have been studied here, are possible and should be mentioned. The ions that react very rapidly with 1,10-phenanthroline as cobalt(II), copper(II) and zinc(II) could be separated from the sluggish ones, such as, nickel(II), vanadium(IV) and chromium(III). For example, if copper(II) and iron(II) are both in a solution of vanadium(IV), the addition of 1,10-phenanthroline and perchlorate ion, followed by shaking with nitrobenzene would extract the copper(II) and iron(II) into the organic phase. The absorbance of the copper(II)-1,10-phenanthroline complex does not overlap the

ferroin absorbance so that both could be determined together. The cop-
per(II) could also be rapidly stripped from the nitrobenzene by using
strong acid solution while the ferroin dissociates so slowly that very
little iron would be removed.

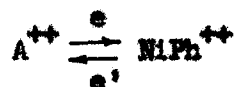
There are a great many possibilities for the analytical applica-
tion of chelate kinetics. It has been shown that relatively small
changes in the nucleophilic character of chelates can lead to rate dif-
ferences in their reaction with some metal ions. This information should
be useful in selecting other chelates for additional study.

VII. SUMMARY AND CONCLUSIONS

The mono-, bis- and tris(1,10-phenanthroline)nickel(II) reactions have been shown to be slow. To a first approximation the formation rate constant of mono(1,10-phenanthroline)nickel(II) can be expressed as first order with respect to both nickel(II) and 1,10-phenanthroline, the latter having a prior equilibrium involving its conjugate acid. With such an expression, individual reaction rates follow a very good second order plot. However, the rate constant, k_o , calculated in this manner varies approximately tenfold with acid strength between pH 0 and pH 3 while not being appreciably affected by ionic strength. The observed rates can be expressed in exact form by interpreting the system as a simultaneous reaction of 1,10-phenanthroline and of the 1,10-phenanthrolium ion with nickel(II) where unstable intermediates with a hydrogen ion equilibrium are formed or the system may be interpreted as a reaction between 1,10-phenanthroline and nickel(II) where an unstable intermediate undergoes acid catalysis to form the product. The proposed reaction mechanisms may be written:

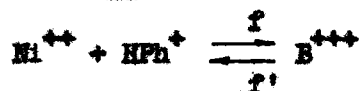


Reaction at

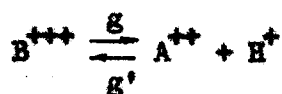


low acidity

and

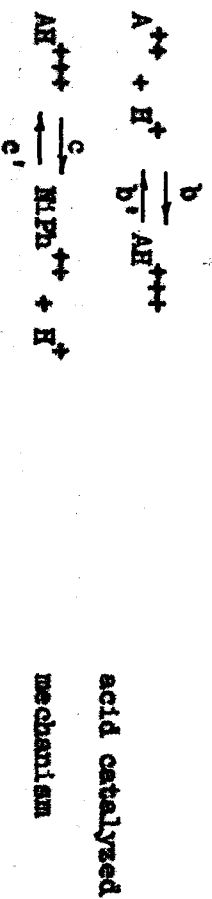


1,10-phenanthrolium



mechanism

or



where A^{++} , AH^{+++} and B^{+++} are all unstable intermediates with only one nitrogen bond between nickel(II) and the ligand.

Using appropriate approximations the observed rate constants, k_o , based on first order dependence on nickel(II) and 1,10-phenanthroline, and k'_o , based on first order dependence on mono(1,10-phenanthroline)nickel(II), can be expressed in terms of the acidity. Thus:

$$k_o = \frac{[H^+] + m}{n[H^+] + p} \quad , \quad k'_o = \frac{[H^+] + q}{r[H^+] + s} \quad ,$$

where m , n , p , q , r and s are functions of a , a' , e , e' together with either f , f' , g , g' or b , b' , c , c' .

The rates of reaction of the nickel(II)-1,10-phenanthroline complexes are not greatly affected by the presence of substituents on the 1,10-phenanthroline molecules which alter the nucleophilic character of the ring nitrogen. For a fortyfold change in the value of the acid equilibrium constant of the 5-substituted, 1,10-phenanthroline, the rate of formation constant, k_{1f} , changes only threefold. An overall equilibrium constant ($pK = 24.2$) has been calculated for tris(1,10-phenanthroline)nickel(II) which shows it to be a stronger complex than tris(1,10-phenanthroline)iron(II).

The observed rate of formation constant of tris(1,10-phenanthroline)iron(II) decreases with decreasing acidity. A hydrogen ion dependence similar to that postulated for nickel(II) is suggested. Although the observed rate of formation constant varies 160-fold with substituents, this appears to be largely due to changes in the equilibrium constants of the rapid forming mono- and bis-complexes. The actual rate of formation constant of tris(1,10-phenanthroline)iron(II) from bis(1,10-phenanthroline)iron(II) seems insensitive to changes in the nucleophilic character of the 1,10-phenanthroline nitrogens.

The rates of reaction of vanadium(IV) with 5-substituted-1,10-phenanthrolines have been measured. The existence and stability of the mono(1,10-phenanthroline)vanadium(IV) complex has been shown. The rate of formation of the mono(1,10-phenanthroline)vanadium(IV) complex is five times more sensitive to changes in the nucleophilic character of the 1,10-phenanthroline than the similar nickel(II) rate.

A comparison of the nickel(II), iron(II) and vanadium(IV)-1,10-phenanthroline systems shows that the rate constant for the rate determining step is in order of decreasing value for iron(II), nickel(II) and vanadium(IV). The substituent effect on this same rate constant appears to be in the reverse order, with vanadium(IV) showing the largest substituent effect. It seems, therefore, that with these three ions the greater the activation energy required, the larger the substituent effect.

An analytical separation of iron(II) from vanadium(IV) and nickel(II) is made by taking advantage of the different rates of reaction of these ions with 1,10-phenanthroline. It is possible to improve this

separation by utilizing the substituent effect on the equilibria and rates of reaction of the various species involved. The rate determining step with iron(II) is preceded by two equilibria, both of which are affected by 1,10-phenanthroline substituents. Hence, the overall rate constant changes more with substituents than is the case with the mono-(1,10-phenanthroline) complexes. In acid solution the rate of ferroin formation is also dependent on the cube of the acid equilibrium constant, K_a , while the mono(1,10-phenanthroline)nickel(II) or mono(1,10-phenanthroline)vanadium(IV) rates depend on K_a to the first power only. These facts permit the selection of 5-methyl-1,10-phenanthroline at high pH and 5-nitro-1,10-phenanthroline at low pH as better chelates than 1,10-phenanthroline to separate iron(II) from nickel(II) and vanadium(IV).

The ability to vary the relative rates of formation of metal chelates by changes in the nucleophilic character of the ligands and in the acidity of the solution should make possible many additional analytical separations of metal ions.

VIII. LITERATURE CITED

1. Basolo, F., and Dwyer, F. P., J. Am. Chem. Soc., 76, 1454 (1954).
2. Basolo, F., Hayes, J. C., and Neumann, H. M., J. Am. Chem. Soc., 75, 5102 (1955).
3. Baxendale, J. H., and George, P., Trans. Faraday Soc., 46, 736 (1950).
4. Blau, F., Monatsh. Chem., 19, 647 (1898).
5. Burkin, A. R., Quart. Revs., 5, 1 (1951).
6. Burstall, F. H., and Nyholm, R. S., J. Chem. Soc., 1952, 3570.
7. Brandt, W. W., Dwyer, F. P., and Gyarfás, E. C., Chem. Revs., 54, 959 (1954).
8. Brandt, W. W., and Gullstrom, D. K., J. Am. Chem. Soc., 74, 3532 (1952).
9. Brandt, W. W., and Wright, J. P., J. Am. Chem. Soc., 76, 3083 (1954).
10. Bystroff, R., Private communication, Iowa State College, 1955.
11. Cambi, L., and Cagnasso, A., Atti. Accad. Lincei, 19, 458 (1934).
12. Craig, D. P., Maccoll, A., Nyholm, R. S., Orgel, L.E., and Sutton, L. E., J. Am. Chem. Soc., 1954, 332.
13. Davis, N. R., and Dwyer, F. P., Trans. Faraday Soc., 49, 180 (1955).
14. Dwyer, F. P., and Gyarfás, E. C., J. Proc. Roy. Soc., N.S. Wales, 83, 232 (1949).

15. Dwyer, F. P., and Nyholm, R. S., J. Proc. Roy. Soc. N.S. Wales, 80, 28 (1946).
16. Gayer, K. H., and Wootner, L., J. Am. Chem. Soc., 74, 1436 (1952).
17. George, P., J. Chem. Soc., 1954, 4349.
18. Irving, H., and Williams, R.J.P., J. Chem. Soc., 1953, 3192.
19. Job, P., Ann. Chim., [10] 9, 113 (1928).
20. Kolthoff, I. M., Lee, T. S., and Leussing, D. L., Anal. Chem., 20, 985 (1948).
21. Kolthoff, I. M., Leussing, D. L., and Lee, T. S., J. Am. Chem. Soc., 72, 2173 (1950).
22. Krumholz, P., Anais. Acad. Brasil Cienc., 22, 263 (1950).
23. Lee, T. S., Kolthoff, I. M., and Leussing, D. L., J. Am. Chem. Soc., 70, 2348 (1948).
24. Lee, T. S., Kolthoff, I. M. and Leussing, D. L., J. Am. Chem. Soc., 70, 3596 (1948).
25. Margerum, D. W., and Banks, C. V., Anal. Chem., 26, 200 (1954).
26. Margerum, D. W., Sprain, W. and Banks, C. V., Anal. Chem., 25, 249 (1953).
27. Martell, A. E., and Calvin, Melvin, "Chemistry of the Metal Chelate Compounds", p. 362, New York, Prentice-Hall, 1952.
28. Nyholm, R. S., J. Chem. Soc., 1951, 3245.
29. Nyholm, R. S., Revs. Pure Applied Chem. (Aust.), 4, 32 (1954).

30. Nyholm, R. S., and Short, L. N., J. Chem. Soc., 1953, 2670.
31. Pfeiffer, P., Dominik, V., Fritzen, A., and Werdalman, B.,
Z. anorg. Chem., 260, 84 (1949).
32. Pfeiffer, P., and Tapperman, Fr., Z. anorg. Chem., 215, 273 (1933).
33. Russell, C. D., Cooper, G. R., and Vesburgh, W. C.,
J. Am. Chem. Soc., 65, 1501 (1943).
34. Smith, G. F., and McGurdy, W. H., Jr., Anal. Chem., 24, 371 (1952).
35. Taube, H., Chem. Revs., 50, 69 (1952).
36. Vesburgh, W. C., and Cooper, G. R., J. Am. Chem. Soc., 24,
457 (1941).
37. Veter, R. C., and Ranks, G. V., Anal. Chem., 21, 1320 (1949).
38. Walden, G. H., Hammett, L. P., and Chapman, R. P., J. Am. Chem. Soc.,
53, 3908 (1931).
39. West, B. O., J. Chem. Soc., 1954, 578.

IX. ACKNOWLEDGMENTS

Sincere appreciation is expressed to the many people who contributed their time and effort to this work.

Special thanks is offered to Donn Klingsman, whose superb instrumentation and able collection of data were essential to the work; to Roman Bystroff for his contributions to the vanadium section and general assistance in the problem; to Dr. George S. Hammond for his interest and criticisms; to the many persons of Analytical Group I of the Ames Laboratory who were helpful in one way or another and to Dr. Charles V. Banks whose interest and constant cooperation made this work possible.

Deep felt gratitude is expressed to my wife, Sonya, for her aid in compiling the data and for her patience and understanding.

X. APPENDIX

LIST OF ABBREVIATIONS

Ph_T	total molar concentration of all 1,10-phenanthroline species
Hi_T	total molar concentration of all nickel perchlorate species
Ph_T^+	1,10-phenanthrolium ion
$HiPh^{++}$	mono(1,10-phenanthroline)nickel(II)
$HiPh_2^{++}$	bis(1,10-phenanthroline)nickel(II)
$HiPh_3^{++}$	tris(1,10-phenanthroline)nickel(II)
$MePh$	5-methyl-1,10-phenanthroline
Ho_2Ph	5-nitro-1,10-phenanthroline
biyy	2,2'-bipyridine
A_o	observed absorbance corrected for cell blank and absorbing species other than those being measured
t	time in minutes
l	cell path in cm.
ϵ_{HiPh}	molar absorptivity of the species indicated by the subscript
K_a	instability constant of the phenanthrolium ion
K_1	instability constant of the mono complex
K_2	instability constant of the bis complex with respect to the mono complex
K_3	instability constant of the tris complex with respect to the bis complex
k_o, k_o'	observed complex rate constants as indicated
k_{1f}, k_{1d}	formation and rate dissociation constants of the mono-complex, independent of $[H^+]$

k_{2f}, k_{2d}	formation and dissociation rate constants of the bis-complex, independent of $[H^+]$
k_{3f}, k_{3d}	formation and dissociation rate constants of the tris-complex, independent of $[H^+]$
a, a', e, e'	rate constants for stepwise bonding of 1,10-phenanthroline with nickel(II)
f, f', g, g'	rate constants involving the reaction of nickel(II) with the 1,10-phenanthrolium ion
b, b', c, c'	rate constants involving the acid catalyzed reaction of 1,10-phenanthroline with nickel(II)
m, n, p	experimentally determined constants in the expression of k_0 as a function of $[H^+]$
q, r, s	experimentally determined constants in the expression of k'_0 as a function of $[H^+]$
v_{Fe}	velocity of formation of tris(1,10-phenanthroline)iron(II)
v_{Ni}	velocity of formation of mono(1,10-phenanthroline)nickel(II)